2023

Impact Of Substrate Type On Eastern Oyster (Crassostrea Virginica) Recruitment And Benthic Community Structure And Productivity In The York River

Jainita Patel
College of William and Mary - Virginia Institute of Marine Science, jpatel3131@gmail.com

Impact of Substrate Type on Eastern Oyster *(Crassostrea virginica)* Recruitment and Benthic Community Structure and Productivity in the York River

---

A Thesis

Presented to

The Faculty of the School of Marine Science

William & Mary

In Partial Fulfillment

of the Requirements for the Degree of

Master of Science

By

Jainita Patel

May 2023

APPROVAL PAGE

This thesis is submitted in partial fulfillment of

the requirements for the degree of

Master of Science

Jainita Patel

Approved by the Committee, March 2023

Rochelle D. Seitz, Ph.D.
Committee Chair / Advisor

Romuald N. Lipcius, Ph.D.

Mark Luckenbach, Ph.D.

Lisa Kellogg, Ph.D.

TABLE OF CONTENTS

ACKNOWLEDGEMENTS

The ecological health of an ecosystem relies on an array of organisms that all play unique and important roles within a community. Similarly, this project would not have been possible without all of the wonderful people who helped me physically, analytically, financially, and emotionally throughout the course of this study. I would firstly like to thank Dr. Rochelle Seitz for being my advisor and guiding me through all of the stages of this process. Thank you for taking a chance on me and helping me learn to be a better scientist. I'd also like to thank my committee members, Dr. Romuald Lipcius, Dr. Lisa Kellogg, and Dr. Mark Luckenbach, all of whom were instrumental in helping me design my study and obtaining my degree.

I would not have been able to complete this project without the support of the Community Ecology and Marine Conservation Biology labs. Thank you to Katie Knick, Gabby Saluta, Alison Smith, Mike Seebo, Natalia Schoenberg, Nihal Guennouni, Alex Schneider, and Challen Hyman. You all were the rock upon which my time at VIMS was built, and I cannot thank you enough for your help in the field, in the lab, and throughout my statistical analysis. I hope the friendships we have built along the way will last well into the future. I would not have made it this far without you. Additionally, I would like to thank Dr. Russ Burke from Christopher Newport University for providing the concrete-mix reefs for this project and Jenny Dreyer for the countless hours she spent helping me with benthic invertebrate ID. Additional thanks goes to Dr. Eric Hilton and Paul Clerkin for their help with fish ID and Sara Vahdatshoar for her help during the summer of 2022 as my REU student.

In the larger VIMS community, I would like to thank Vanessa Strohm, Aly Hall, Grace Molino, Maya Thomas, Lauren Alvaro, and Tor Mowatt-Larssen for providing me with the fuel I needed to get through this Master's program. I will never forget it. I admire all of you immensely, and I cannot wait to see how far you all will go in your own scientific and personal endeavors.

Financial support was provided by the Virginia Institute of Marine Science Office of Academic Studies and the U.S. Department of Defense's Land Restoration, Shoreline Stabilization, and Base Resilience at REPI site Naval Weapons Station Yorktown, VA grant. Additional thanks goes to the National Science Foundation for funding my REU.

Finally, I would like to thank my parents, my partner, my sister, my ba dada, my masi masa, and all my friends here at VIMS and around the world for their love and support throughout the course of this program. You keep me going. Tamārē vadē hu āyā chu ānē tāmārē līdēj hu agaḍā vadiśh.

LIST OF TABLES

LIST OF FIGURES

ABSTRACT

Restoration of eastern oyster (*Crassostrea virginica*) reefs in the Chesapeake Bay and its tributaries is important, as oyster reefs provide habitat for temperate estuarine communities and shoreline protection. Oysters that settle in crevices, such as those found on natural shell substrates, suffer low mortality, but natural shell is becoming a limited resource in the Chesapeake Bay. Finding an alternative settlement substrate that is complex like natural shell and mimics the benefits of shell substrates with less expense could be the best way to encourage oyster recruitment and survival. The two main goals of this experiment were to (1) understand which artificial substrate type (granite stone, oyster castle, diamond, c-dome, and x-reef) promotes the highest oyster recruitment and survival compared to natural shell and (2) determine the effects of reef presence on macrofaunal community structure and productivity. It was hypothesized that a new settlement substrate, oyster diamonds, given the sloping surfaces with large surface area, will be best for oyster recruitment. Additionally, it was hypothesized that oyster reef presence will substantially enhance macrofaunal community abundance and increase macrofaunal productivity compared to unstructured sediment. To address these goals, infaunal macrofauna and sediment samples were taken at three experimental sites and two control sites along the York River in June 2021. Then, two replicates of each of six reef types were deployed in a randomized block design at each of three experimental sites. The reef types included loose oyster shell, granite, oyster castles, oyster diamonds, c-domes, and x-reefs. The fall after deployment, the structures were sampled for oyster density and shell height. One year after deployment, the structures were physically sampled, removing oysters to determine oyster density and biomass, and the macrofaunal community associated with the reefs. Control sites were sampled for benthic infauna and sediment analyses. Oyster densities and biomass were extremely high and were highest on the loose shell reef (9,852 oysters/m^2 and 743 g AFDW/m^2 based on model estimates), and the x-reefs had the second-highest recruitment and biomass (3,816 oysters/m^2 and 531 g AFDW/m^2 based on model estimates). Prior to deployment of reefs, control and impact sites had similar density, biomass, and diversity of macrofauna, but one year after reef deployment, the reef impact sites had higher densities, richness, diversity, biomass, and secondary productivity of macrofaunal organisms than the control sites with the impact sites having 145 times greater secondary productivity than the controls. The diversity among reef types did not vary but the granite reefs had the highest secondary productivity overall. All reef structures showed successful oyster and macrofaunal community recruitment based on Chesapeake Bay Fisheries Goal Implementation Team metrics and densities were among the highest for alternative substrates. Based on the results of this study, researchers and managers could choose from a variety of successful alternative reef types. Based on restoration goals, the use of different reef types could lead to differences in the achievement of goals.

Impact of Substrate Type on Eastern Oyster *(Crassostrea virginica)* Recruitment and Benthic Community Structure and Productivity in the York River

All parts of this project were conducted on the homelands and in the home waters of the Cheroenhaka (Nottoway), Chickahominy, Eastern Chickahominy, Mattaponi, Monacan, Nansemond, Nottoway, Pamunkey, Patawomeck, Upper Mattaponi, and Rappahannock tribes. These indigenous communities are the current and traditional caretakers of these lands and waters. I hope this project honors them and the work they have already placed into preserving the natural ecosystems of this area.

For all that you have done and all that you continue to do, Meegwetch.

1 Introduction

Oyster reefs provide numerous ecosystem services, or "benefits to humans" (Coen et al., 2007). These services range from habitat for benthic organisms (Coen et al., 2007; Grabowski and Peterson, 2007) to erosion protection for shorelines (Peterson et al., 2003; Grabowski and Peterson, 2007; Rodriguez et al., 2014; Ridge et al., 2015, 2017). They also provide shelter and nursery habitat to enrich the macrofaunal community around them (Luckenbach et al., 2005; Beck et al., 2011; Coen and Humphries, 2017). Oysters that make up reefs also facilitate water filtration and benthic-pelagic coupling (Kellogg et al., 2016). Because oysters act as ecosystems engineers (Ruesink et al., 2005), reef presence can enhance populations of ecologically and economically important species such as the blue crab (Scyphers et al., 2011).

Oyster presence in the Chesapeake Bay and its surrounding waters have declined dramatically over the last century (Newell, 1988; Héral et al., 1990; Rothschild et al., 1994; Schulte, 2017). Since the peak of the oyster fishery in the late 1800s, overfishing and habitat destruction caused by mechanized fishing (Heinle et al., 1980; Rothschild et al., 1994), decreased water quality (Coen and Luckenbach, 2000; Wilberg et al., 2011), and disease (Mackin et al., 1950; Wood and Andrews, 1962) have led to drastic decreases in oyster populations. As oysters play an important ecological role and provide many ecosystem services, oyster reef restoration has become a major focus around the Chesapeake Bay and in other coastal areas of the eastern United States (Beck et al., 2011;

Baggett et al., 2015; La Peyre et al., 2017).

Oysters are reef-building organisms, and oyster larvae may settle with high densities on the shells of other oysters (Soniat et al., 1991; Soniat and Burton, 2005). Hard substrate is necessary for oyster settlement (Bahr and Lanier, 1981). Previous studies that utilized shell bags and loose shell have yielded promising results with high settlement rates and high macrofaunal community richness and diversity (Wall et al., 2005; Taylor and Bushek, 2008; Brumbaugh and Coen, 2009; Colden et al., 2017). Similarly, species richness is significantly correlated with the volume of interstitial space and trapped sediment in complex reef structures (Callaway, 2018). Additionally, macrofaunal density and biomass are positively related to live oyster volume (Karp et al., 2018). In particular, high-relief, complex, restored reefs provide habitat for nekton and benthic organisms and promote oyster recruitment (Nestlerode, 2004; Schulte et al., 2009; Stunz et al., 2010; Colden et al., 2017; Blomberg et al., 2018). Although oyster shell is a successful recruitment substrate, finding oyster shells for restoration is difficult and expensive (George et al., 2015; Graham et al., 2017; Mann and Powell, 2007; Goelz et al., 2020). Therefore, new methods of utilizing artificial substrates to create oyster reefs and encourage oyster settlement and growth have been developed. Additionally, as artificial reefs are functionally similar to natural oyster reefs for nekton utilization and community building (Harwell et al., 2011; George et al., 2015; Rutledge et al., 2018; Jud and Layman, 2020), they can promote development of rich and diverse benthic macrofaunal communities (Grabowski et al., 2005; Rodney and Paynter, 2006).

Because oysters prefer to settle in crevices, such as those found on natural shell substrates, to reduce predation from crabs (Michener and Kenny, 1991; Grabowski, 2004; Brumbaugh and Coen, 2009), finding a substrate that is just as complex with abundant interstitial space that can mimic the benefits of shell substrates is a viable way to encourage oyster recruitment and survival. Some studies have concluded the composition of the reef material is not as important as the amount of interstitial space and trapped sediment (Nestlerode et al., 2007; Callaway, 2018).

Oyster reefs also improve the surrounding environment through erosion protection. As a reef develops, its hard substrate can act as a barrier to mitigate coastal erosion (Scyphers et al., 2011).

Breakwater oyster reefs prevent erosion, encourage marsh expansion, and trap suspended sediment (Scyphers et al., 2011; Chowdhury et al., 2019). With proper site selection, both small, patchy, artificial intertidal reefs, and large artificial reefs can reduce marsh erosion (Stricklin et al., 2010; La Peyre et al., 2015; Wiberg et al., 2019).

Over the last 20 years, several studies have investigated which substrates are optimal alternatives to oyster shells (Goelz et al., 2020). Concrete, limestone, river rock (also known as riprap or granite), and porcelain have been explored as options for alternative substrates in oyster restoration (George et al., 2015; Graham et al., 2017; Goelz et al., 2020). Non-$CaCO_3$-based substrates, such as concrete or riprap, may resist bioeroders such as the boring sponge and promote reef health and growth (Dunn et al., 2014). Riprap mimics natural hard-bottom habitats, leading to high benthic production and vertical distribution that is similar to natural rocky intertidal habitats (Seitz et al., 2019; Sedano et al., 2020).

Artificial reef structure and composition can both influence the effectiveness of the structure. Concrete mixed with oyster shell is a cost-effective and biologically effective to encourage oyster spat settlement (Bersoza Hernández et al., 2018). Additionally, concrete can be molded to create high-rugosity environments that are vertically complex and lead to oyster densities as high as 14,000 oysters/m^2 in some high-rugosity shell treatments (Soniat and Burton, 2005; Margiotta et al., 2016; Goelz et al., 2020). Structure height is important, as low-relief reefs have increased sedimentation, and oysters with 90% of their shells covered in sediment have high rates of mortality (Colden and Lipcius, 2015; Colden et al., 2017).

Many experiments have used concrete as a primary alternative substrate to reach high oyster densities. In an experiment that used a modular concrete reef over five years in the Rappahannock River, oyster recruitment densities were 1085 oysters per m^2 river bottom, which were some of the highest ever recorded in the area for artificial reefs (Lipcius and Burke, 2018). In an experiment conducted in the Patuxent River and on the Eastern Shore of Maryland using recycled concrete aggregates, there was no significant difference between recruitment and epifaunal activity on oyster shell and concrete (Fan et al., 2020). At an intertidal site in the York River, oyster castles (a concrete

and shell mixed structure with ample surface area, interstitial space, and rugosity) were tested for their recruitment potential. It was determined that castles recruited, retained, and hosted oysters at $\sim$ 440 individuals/m^2, which was four times higher than that of unconsolidated and embedded shell, and additionally, they are cost-effective (Theuerkauf et al., 2015).

The shape of the reef is also an important factor in whether the reef maximizes surface area, vertical space, rugosity, and interstitial space to promote oyster growth (Nestlerode et al., 2007; Margiotta et al., 2016). As hydrodynamics play an important part in larval distribution and settlement (Koehl and Hadfield, 2010), reef surface angles influence larval settlement (Butler, 1954; Breitburg et al., 1995). The preferred angle for larval settlement and growth is 45-degrees (Butler, 1954).

The impact of artificial reef structures on the benthic macrofaunal community is important. One method used to measure the impact of a constructed hard substrate on community recruitment, especially when there is no ability to replicate restoration at multiple sites, is the Before-After, Control-Impact (BACI) method (Underwood, 1992; Davenport et al., 2018). This can be used to disentangle differences owing to time versus treatment. This method works by comparing control sites with impact (restoration) sites over time (before and after construction) to test the pattern of change at both types of sites (BACI). For community recruitment experiments, where conditions are variable at different sites, this method works well. The drawbacks to this method can include the inability to account for natural spatial and temporal variability; however, these can be accounted for by increasing the number of replicate impact sites and having multiple control sites (Underwood and Chapman, 2003).

If artificial substrates are placed on productive soft-sediment habitats, but they experience low recruitment, they can smoother existing macrofaunal communities and lead to low secondary productivity (Hueckel et al., 1989; Shipp, 1999; D'Itri, 2018). However, with high recruitment rates, artificial reefs can support higher secondary production than unstructured sedimentary habitats (Steimle et al., 2002; Peterson et al., 2003). High secondary production rates or accumulation of mass in an animal over a period of time (Benke and Huryn, 2006) can be linked to macrofaunal

communities with filter feeders, such as oysters (Dame, 1999). There are two main ways to indirectly measure secondary production in a community – annually or daily. One annual method involves using secondary production-to-biomass (P/B) ratios (Diaz and Schaffner, 1990), which take the biomass of a sample from a community and use established P/B ratios to find the annual secondary production of a system. One daily method is the Edgar method (Edgar, 1990), which calculates daily rates by using the equation using an empirical model ($P = 0.0049^{B}$ x 0.80^{T} x 0.89), where B is biomass (ash-free dry weight) and T is temperature at the site.

In addition to the biological effects of artificial oyster reefs, reef structures can impact the physical and chemical benthic environment adjacent them as they recruit oysters over time. Physical parameters, such as grain size and nutrient composition in the water column and the benthos, are influenced by reef presence (Kellogg et al., 2013, 2014). For grain size, even small oyster reefs promote the collection of finer sediment in the area immediately adjacent to them (Molesky, 2003; Colden et al., 2016). Oyster reefs also promote denitrification at the sediment-water interface (Kellogg et al., 2013; Humphries et al., 2016). Oysters are efficient filter feeders that capture inorganic and organic suspended material from the water around them and deposit this material in the surrounding sediment through feces and pseudofeces (Hoellein et al., 2015). Biodeposits from macrofauna that are attracted to reef structures can also increase the amount of carbon and nitrogen in the sediments surrounding reefs (Haven and Morales-Alamo, 1966; Newell et al., 2005).

In the present study, the parameters of reef type and site were examined and related to oyster density and growth and macrofaunal community density, secondary production, and composition. The goal is to use six different substrate types that combine a variety of factors that promote oyster recruitment to determine the optimal oyster reef structure to promote oyster recruitment, macrofaunal community recruitment, and secondary production in the York River. The Before-After, Control-Impact (BACI) method (Underwood, 1992; Davenport et al., 2018) will also be used to quantify changes in macrofaunal communities and secondary production before and after reef deployment at control and impact (experimental) sites.

2 Logical Framework and Hypothesis

There are two main parts of this study: Part I is to examine the hypothesis that reef type and site have an impact on oyster recruitment. Part II is to examine the hypothesis that macrofaunal community structure and secondary production are impacted by artificial reef presence.

The main objective for Part I is to compare the three metrics of oyster (1) density, (2) biomass and (3) shell height on six different artificial substrates: (1) oyster shell, (2) granite, (3) oyster castles, (4) oyster diamonds, (5) c-domes, and (6) x-reefs (described further in methods below). For this objective, hypotheses were generated with varying combinations of reef type and site for all three response variables. The two fixed factors (reef and site) that were tested against the response variables for these models were used because the main goal of this study was to understand the impact of reef type while better understanding the role that reef location played in differences. In a study with a larger sample size, the interaction effect would have also been tested between these two variables, but the sample size in this study did not allow for this. Following an Information Theoretic approach, (Chamberlin, 1890; Anderson, 2008), each hypothesis is represented by a statistical model and each model represents an alternative hypothesis (Chamberlin, 1890). For example, when looking at four models with oyster density as the response variable, model m_d4 includes both reef type and site as possible independent variables. Similar models were also created to test oyster density by surface area (m_s), oyster biomass (ash-free dry weight) by m^2 of river bottom (m_b), and oyster biomass (dry weight) by m^2 of river bottom (m_{dw}).

The main objective for Part II is to compare the control sites with the impact sites both before and one year after reef deployment to determine whether reef presence affects secondary productivity. For this objective, the interaction between reef presence and time was tested. A significant interaction between time and reef presence would show that reef presence changes an environment with time. In addition to the BACI analyses, univariate models for macrofauna will also be fit similar to the manner used in Part I for the following response variables: (1) density, (2) richness, (3) evenness, (4) diversity, (5) biomass, and (6) secondary productivity. Part II also included mul-

tivariate analyses using non-metric multidimensional scaling plots and PERMANOVA to examine how reef presence influences community structure.

The structures used in this study combine a variety of factors that can promote oyster settlement and recruitment. High settlement occurs on vertical substrates with large, continuous surfaces (Soniat et al., 2004). Additionally, 45-degree angles can encourage initial larval settlement (Butler, 1954). Finally, oyster shell can release chemicals which promote juvenile settlement (Crisp, 1967). Based on these past studies, it was hypothesized that the impact sites would have greater oyster recruitment and macrofaunal secondary productivity than the control sites. It was also postulated that the reefs that had large amounts of flat, angled space and oyster shell would have higher oyster recruitment and greater secondary productivity than the other reef structures. Specifically, the diamond was predicted to have high recruitment based on these characteristics.

3 Methods

3.1 Experimental Design

Site Selection

To determine the impact of substrate type on oyster recruitment and the macrofaunal community, field experiments were conducted at five shallow subtidal sites in the polyhaline region of the York River (Figure 1). These five study sites were selected because of ease of access and similar sediment type. The three experimental sites (two at VIMS Beach and one at Andrews Beach) were in shallow water ($\sim$ 0.45 m - 0.75 m below MLW) and were located just offshore at Gloucester Point, adjacent to the Virginia Institute of Marine Science (VIMS). The two control sites were located in shallow water ($\sim$ 0.45 m - 0.75 m below MLW) in the mainstem of the York River. The first control site (Indian Field) is 4.7 km from VIMS, on the south shore near Indian Field Creek. The second control site (Cedar Bush) is 6.2 km from VIMS, on the north shore of the York River near Cedar Bush Creek.

The sites in shallow areas of the lower York River have high wave energy and sediments largely composed of sand and shell (Gillett and Schaffner, 2009). In the lower York, the water column is much more stratified than in the upper areas of the river, as it is deeper and has weaker currents (Friedrichs, 2009); however, strong winds and mixing in shallower areas of the York cause the nearshore areas of the lower York to be well-mixed and oxygenated (Gillett and Schaffner, 2009). The tides in this area are semidiurnal with a mean tidal range of 0.8 m (Reay, 2009). Salinity varies seasonally with the lowest in the winter between 10.3 and 23.1 and the highest in the fall between 13.2 and 25.2 (Reay, 2009). Absolute temperature also varies seasonally. In the winter, temperatures range between 4.5-12.1°C and in the summer, they fall between 25.2-28.5°C (Reay, 2009). The York River has high sediment and nutrient input from tidal erosion and agricultural non-point sources (Reay, 2009).

At all three experimental sites, the twelve reef structures (two of each type) were placed in the shallow subtidal zone in two 25-m-long transects. Each reef was placed 5 m apart from the next. The placement of substrate types were along the transects in a randomized block design using a random number generator in R. At each of the VIMS Beach sites (Impact 1 and 2), there were 2 transects. The transects at Impact 1 were inside of coves and protected from wave energy by large, granite breakwaters (Figure 1). The two transects at Impact 2 were outside of the coves in that area was exposed to wave action. At Andrews Beach (Impact 3), the transects were 5 m apart from one another in two rows parallel to the shore (Figure 1).

Reef Materials

The six substrate treatments for this experiment consisted of oyster shell, granite stones, oyster castles, oyster diamonds, x-reefs, and c-domes (Table 1). For the oyster shell treatment, loose oyster shells were placed in a 0.3 m long x 0.3 m wide x 0.3 m high basket composed of plastic covering metal wire with a mesh size of $\sim$ 1 cm, and were filled to the top of the basket (Figure 2a). Similarly, for the granite stone treatment, granite (Gabion) stone with a median diameter range of 4-10 cm were placed in a 0.3 m long x 0.3 m wide x 0.15 m high basket composed of plastic

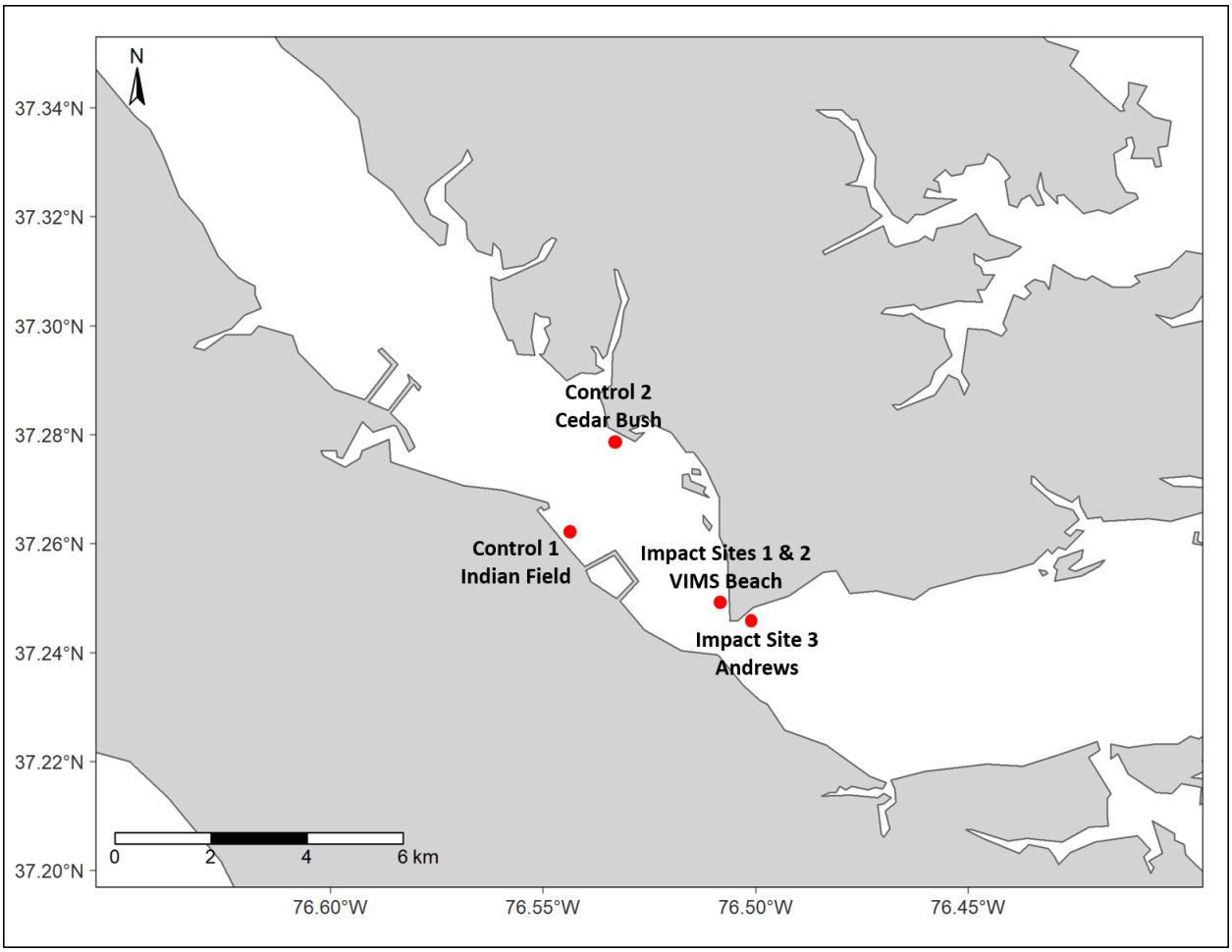

Figure 1: Map of control (Indian Field and Cedar Bush) and impact sites on Gloucester Point. Sites Impact 1 and 2 were both located at VIMS Beach and Impact 3 was located at Andrews.

covering metal wire and then stacked to reach 0.3 m tall (Figure 2b). Oyster castles (Figure 2c) are concrete structures mixed with crushed shell that have a large amount of internal and external surface area that can be connected through interlocking the modules (Theuerkauf et al., 2015). These structures are created and supplied by Allied Concrete. The castles were stacked with four modules on the bottom and one on top to create vertical space for settlement. Oyster diamonds (Figure 2d) are concrete pyramid-shaped structures that stand 0.3 m tall. Their sides are sloped at a 45-degree angle, they have surfaces that are embedded with oyster shells, and they have no internal space. C-domes (Figure 2e) are 0.3 m tall, circular, dome-shaped concrete structures that have embedded oyster shells in their surface and that are hollow from the inside with large holes that allow for internal access. X-reefs (Figure 2f) are table-like, with a cross-shape top connected to four legs, and they are 0.45 m tall. They have oyster shells embedded in their surface and internal space on the underside of the structure. Each structures was designed with different mechanisms to encourage oyster recruitment (Table 2).

Table 1: Dimensions of the reef types used for this study. Bottom area references to the true footprint of the structures without accounting for the sediment around the structure. Note that surface area for the shell structure and the granite basket were not calculated because each of the structures had shells and boulders of varying shapes and sizing, leading to inaccurate estimates of surface area. Qualitatively, the shell had the highest surface area and the granite had the second highest.

Reef Type	Reef Height (m)	Reef Width (m)	Reef Length (m)	Bottom area (m^2)	Surface Area (m^2)
Oyster Shell	0.30	0.30	0.30	0.09	NA
Granite	0.30	0.30	0.30	0.09	NA
Oyster Castle	0.61	0.61	0.61	0.37	1.78
Oyster Diamond	0.30	0.61	0.91	0.28	0.46
C-Dome	0.46	0.48	0.48	0.18	1.38
X-Reef	0.36	0.74	0.74	0.24	1.47

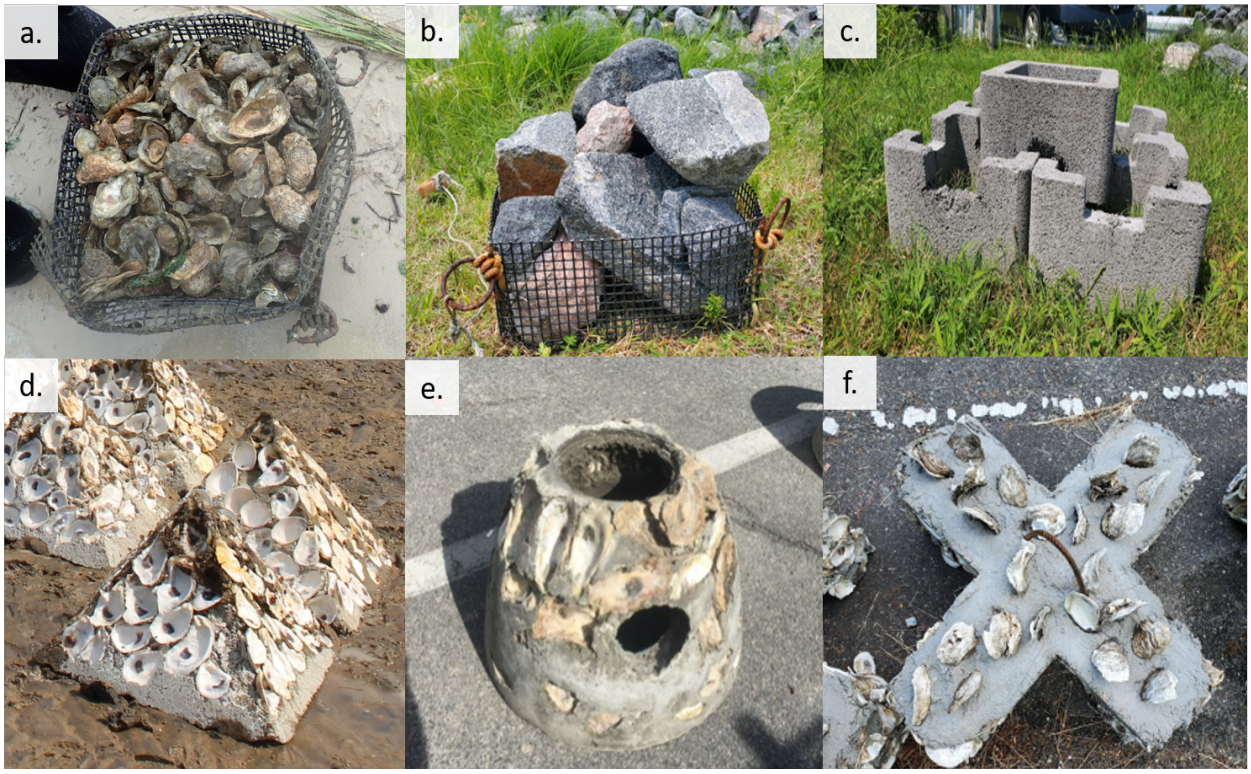

Figure 2: Reef types used for this study: (a) loose oyster shell in a mesh basket made of plastic covering metal wire, (b) loose granite in a mesh basket made of plastic covering metal wire, (c) concrete and crushed shell oyster castles stacked one on top and four on the bottom, (d) oyster diamond composed of concrete embedded with oyster shell, (e) c-dome composed of concrete embedded with oyster shell, (f) top view of an x-reef, a table-like structure composed of concrete embedded with oyster shell.

Table 2: A comparison of the features of each reef type. Internal space = large pockets of space inside of the structure that offer room for recruitment. Interstitial space = space between specific discrete particles of matter. 45-degree angle = availability of substrate that sits at a 45-degree angle. Oyster shell = availability of natural oyster shell on the structure.

Reef	Surface Area	Height	Internal Space	Interstitial Space	45-degree Angle	Oyster Shell
Shell	High	Low	Medium	High	Medium	High
Granite	High	Low	Medium	Medium	Low	Low
Castles	Medium	Medium	Medium	Low	Low	Low
Diamond	Low	Low	Low	Low	High	Medium
C-Dome	Medium	High	High	Low	Low	Medium
X-Reef	Medium	High	High	Low	Low	Medium

3.2 Measured Variables and Analyses

Physical Parameters

A YSI Pro-Plus Multiparameter instrument was used to measure temperature (°C), salinity, and dissolved oxygen (DO) (mg/L) at each site during the pre-sampling in summer 2021, fall sampling in 2021, and post-sampling in summer sampling in 2022. In summer 2021 and 2022, two sediment cores were also collected with a 2.26-cm^2 syringe to a depth of 5 cm. These were taken at one randomly selected location near the benthic sampling at each of the control and impact sites in both 2021 and 2022. One core was collected for organic carbon, hydrogen, and nitrogen (CHN). These samples were sent to the VIMS Nutrient Analysis lab for exact measurements of total organic nitrogen (TON) and total organic carbon (TOC) using an Exeter Analytical CE-440 Carbon/Nitrogen (CHN) Analyzer. The second core was used for grain-size analysis using a standard wet sieving and pipetting technique (Plumb, 1981). For 2022, two sediment cores (one for grain-size analysis and one for TOC and TON) were taken directly adjacent to each of the 36 reef structures at the experimental sites.

Dissolution rates were measured in fall of 2021 at three locations along each transect at each site (between structures) as a proxy for flow rates. A chalk block was weighed and tied to a PVC pole and 3 poles were placed 10 meters apart at each site 0.5 meter offshore of each transect. After 24 h, the blocks were retrieved, dried in for 24 h at 70°C before being weighed again. The grams lost were divided by the initial weight and multiplied by 100 to obtain the dissolution rate per block. These were then averaged by site to obtain the mean dissolution rate by site, which approximated relative amount of water flow at each site.

Part I - Oyster substrate comparison

The reefs were deployed in the shallow subtidal in June 2021 to allow for oyster settlement through the summer and early fall. Oyster recruitment was measured in the fall after summer settlement (October 2021) and one-year post-deployment (June 2022), in the following summer

after grow-out but before the next settlement period. In the fall 2021 sampling, the goal was to obtain oyster counts and shell height. Each reef was brought to shore and subsamples were taken to the nearest millimeter. Depending on the dimensions and shape of the reefs, either the entire structure was subsampled or random stratified sampling was used. The total number of subsamples varied from 6 to 14 (Table 3).

Table 3: Number of strata and subsamples taken per stratum per reef type for the fall 2021 sampling.

Reef Type	No. of Strata	Strata Description	Subsamples per Stratum	Total subsamples
Oyster Shell	1	Basket	6	6
Granite	1	Basket	6	6
Oyster Castle	1	Entire Structure	10	10
Oyster Diamond	2	Left	3	6
		Right	3	
C-Dome	2	Inside	4	8
		Outside	4	
X-Reef	3	Top	4	14
		Bottom/Inside Legs	4	
		Outside Legs	6	

As each structure varied in shape, size, and internal space, the following methods were used per structure:

1. Shell and granite baskets: a grid of 36 cells was laid over the top of the structure. Each cell was 3.68 cm x 3.68 cm. 6 cells were randomly chosen to subsample the structure. Then, any oyster that fell within those cells throughout the entire vertical column of the structure was measured and counted. The mean count of those subsamples was multiplied by 36 to obtain mean density per structure.

2. Oyster castles: a grid of 143 cells was laid over the top of the structure (i.e., a single grid cell could include either the inside or the outside of a single vertical wall of the castle). Each

cell was 3.68 cm x 3.68 cm. From each castle, 2 cells were randomly chosen for a total of 10 subsamples. To account for both the internal and external walls of the castles, when randomly chosen cells fell on bare sand in the center of the structure, the closest internal wall was chosen and the nearest vertical 3.68 cm strip of that wall was measured and counted for oysters. Similarly, if the randomly chosen cell fell on the top, flat portion of the structure, the closest vertical 3.68 strip of outer wall was measured and counted for oysters. The mean of these 10 subsamples was then multiplied by 143 to account to obtain mean density per structure. The reason the castles were not split into strata before subsampling was because the method describes here accounts for both the internal and external walls of the castle.

3. Diamonds, C-domes, and X-reefs: The structures were split into different strata based on characteristics (Table 3). Total number of 3.68 x 3.68 grid cells per strata was calculated for the structure. Each stratum was subsampled either 3, 4, or 6 times based on the size of the structure. The mean of the subsamples were then multiplied by the total number of cells in the strata to get a mean density per stratum. The mean densities by stratum were then added together to get mean density per structure.

Once mean density per structure was obtained, bottom footprint of each structure was calculated. Bottom footprint is defined as the projected area directly under the reef inclusive of any internal voids. For the oyster castles, this included the edge of the structures and any sediment underneath and internal to the castles. For the c-domes, this included the edge of the dome and any sediment underneath and inside of the domes. For the x-reef, this did not include the area between the legs, but did include the area directly underneath the flat, top portion of the reef and the legs.

The mean density per structure and the bottom footprint were the necessary numbers to run a generalized linear model with an offset. An offset is a variable used in count models to help account for known differences among observational units. This can help account for the size differences of the reef structures. For all non-count models, mean density per structure was divided by the footprint to standardize by 1 m^2 of bottom area.

In summer 2022, the goal was to obtain oyster counts, biomass, and shell height and sample the

macrofauna on the reef. In the summer, each reef was removed from the water and immediately placed in a floating tray. A quarter of each reef structure was physically sampled to obtain mean density (individuals/m^2) of both oysters and macrofauna and recruit shell height for the oysters. Each subsample was determined by placing a quadrat divided into quarters on the structure, and a random numbers generator selected which cell to sample. All organisms within the cell including oysters and all macrofauna, were scraped off, bagged, and stored on ice. In the laboratory, oysters were rinsed in freshwater to remove macrofaunal organisms and counted. The height of each oyster was measured to the nearest millimeter.

To obtain biomass, the oysters were subsampled by ordering each of the oysters from 36 reefs by size and taking 30 oysters spread across varying size classes per reef. These subsampled oysters were then shucked and dried for 48 h at 70°C to obtain dry weight. Then, the oyster flesh was combusted in a muffle furnace for 4 h at 550°C to obtain weight of ash (e.g. ingested sediment), which was subtracted from dry weight to obtain grams of ash-free dry weight (AFDW). The subsampled oyster biomass from each sample was then used to calculate biomass for the remaining oysters on the specific structures they were sampled from with the following power regression (Luckenbach and Ross, 2003), where shell height is the measurement from umbo to the farthest point of the shell: $ln(afdw) = \beta_0 + \beta_1 ln(height)$. This value was then was multiplied by four to determine the total oyster biomass per structure then divided by the area of footprint of the structure to determine oyster biomass per m^2. Then, secondary productivity (g C/m^2/yr) for the standardized oyster biomass was found using a P/B ratio of 2.9 (Diaz and Schaffner, 1990).

After the data were collected, models were fit in R (version 4.1.3) for (1) fall 2021 oyster densities, (2) summer 2022 oyster densities, and (3) summer 2022 oyster biomass both by ash-free dry weight and by dry weight alone. Based on the distribution of the data, a negative binomial generalized linear model was fit for the fall 2021 and summer 2022 density data. To standardize density to 1 m^2 of river bottom, the models were run on the non-standardized raw oyster counts and offset with the footprint (bottom area) of each reef (Table 1). For the both the ash-free dry weight and the dry weight for oyster biomass, a linear model was used based on the distribution and the

response variable was standardized to 1 m^2 of river bottom before running the models. The reason for this discrepancy is because an offset is more accurately used for count data in generalized linear models (glm) than linear models (lm) such as the one used for the distribution of biomass. For all response variables, the model with the best fit (lowest AICc) was further examined to determine the impact of the parameters on the response variables. The estimated marginal means (least-squares means) were found using the "emmeans" package in R. These means were of the response variable per levels of the tested independent variables for the model with the best fit (Lenth, 2022). For all response variables, pairwise comparisons were run on the model-estimated means to understand the differences between the variables for the levels of each factor.

For the concrete-mix structures only, oyster densities from summer 2022 were also examined by surface area of the individual structure. Surface area models did not include the oyster shell and granite reef structures because of difficulty in obtaining accurate surface area measurements, given their inconsistent and irregular shapes (multiple shells or stones of different sizes). For surface area, a similar approach to standardization by m^2 was taken; however, oyster densities were standardized based on 1 m^2 of surface area for each of the concrete-mix structures instead of by footprint (Table 1).

Part II - Macrofaunal production before and after reef deployment

To perform the "before" part of the BACI method, we conducted pre-sampling in May and June of 2021 at all five sites (both control and impact prior to reef deployment). At eight sampling points per site, a benthic suction sampler was used to collect larger, deep-dwelling, infaunal organisms from the shallow subtidal (Eggleston et al., 1992). For the suction sampling, a 0.11-m^2 core was inserted to a depth of 40 cm, and the contents were collected, sieved through a 3-mm mesh bag, and frozen. This sampling method targets large bivalves, such as *Macoma balthica*, and larger polychaetes, such as *Glycera dibranchiata* and *Alitta succinea*.

The macrofaunal samples were rinsed in cool water before being sorted twice in the lab without a microscope to pull out any organisms that were alive at the time of sampling including

crustaceans, amphipods, isopods, sponges, polychaetes, phoronids, bivalves, crabs, fish, tunicates, anemones, and algae (though not "macrofauna", algae provides important macrofaunal habitat and is important to the community). Barnacles were not included. The collected infauna was then stored in 70% ethanol until the organisms were identified and enumerated. Organisms were identified to the lowest practical taxon (except some polychaetes, such as Capitellidae and Spionidae, and amphipods from the Caprellidae, Gammaridae, and *Corophium* taxanomic groups, which were sorted to family). Bivalves were measured to obtain shell height (mm). All samples were placed separated into lowest taxanomic group and dried for 48 h at 70°C to obtain dry weight to the nearest 0.0001 g. Then, the organisms were combusted in a muffle furnace for 4 h at 550°C to obtain the weight of ash, which was also weighed to the nearest 0.0001 g and subtracted from dry weight to obtain grams of AFDW. These weights were then converted to productivity using P/B ratios ((Diaz and Schaffner, 1990); crustaceans: 5.7; polychaetes: 4.9; nemerteans: 4.3; bivalves: 2.9) to obtain secondary production for each sampling point. Phoronids, sponges, and anemones made up a very small part of the macrofauna and were not included in secondary productivity measures.

One year after reef deployment, the same methodology was used to take suction samples at the control sites. At the experimental sites, the quarter of each reef that was randomly physically sampled for oysters was also used to collect macrofauna. To ensure accurate measurements of the macrofaunal community, the oysters from Part I were also scraped and cleaned of macrofauna to account for the organisms that lived on, between, and inside of individual oysters including crustaceans, amphipods, isopods, sponges, polychaetes, phoronids, bivalves, crabs, fish, tunicates, anemones, and algae. During the sampling, if any mobile fauna fell into the floating collection tray, they were individually collected and counted as 1/4 an organism for density and their biomass was also divided by four. The macrofauna in the sample were then counted, identified, measured, dried, and weighed using the same methodology as listed above.

For this part of the experiment, community density is defined as the number of macrofaunal organisms within 1 m^2 of river bottom (counting only organisms with heads). Richness is defined as the number of species. Evenness is defined as the relative abundance of organisms by species.

Diversity is estimated using the Shannon diversity index:

$$H' = -\Sigma(\pi * log(\pi)) \tag{1}$$

The higher the number, the more diverse the community. Macrofaunal community biomass is defined as macrofaunal grams of AFDW/m^2 of river bottom (excluding oyster biomass and including pieces of organisms without heads). Macrofaunal secondary productivity is defined as grams of carbon produced by the total number of organisms residing in 1 m^2 of the benthos per year.

Before-After, Control-Impact (BACI) analyses consisted of fitting an ANOVA, linear regression, or a generalized linear model based on the distribution of the response, including the interaction between time and site (control or impact) as the fixed response variable in R (version 4.1.3). Response variables consisted of macrofaunal density, richness, evenness, diversity, biomass, macrofaunal secondary productivity, and combined macrofaunal and oyster secondary productivity. Significant BACI interactions indicate a significant effect of the treatment over time.

To test the differences among treatments (reef types and impact sites) using the community data and univariate analyses in 2022, several models were fit in R (version 4.1.3) with reef and site as the fixed variables (Table 4). Both of these variables were analyzed for their effect on density, richness, evenness, Shannon diversity, and biomass. For secondary productivity, only the reef variable was further explored as the model that included site was not the best fit (Table 4). The models with the lowest AICc and highest weighted probability were tested against the second best model using an ANOVA to determine if there was a significant difference. For most response variables, either the u_3, including only site as a variable, or the u_4 model, including both reef type and site, had the best fit. Because the goal of this project was to determine the impact of alternative reef structures, all further analyses were run on the u_4 models to take into account reef type.

For the density models, a generalized linear negative binomial model was used for the response variable of abundance. These models had an offset of reef footprint (bottom area; Table 1) to standardize densities by 1 m^2 of river bottom. For linear models, the appropriate transformations (i.e.,

Table 4: Models and parameters for linear models and generalized linear bionomial models compared with AICc for univariates across reef types and impact sites for 2022. β represents inclusion of the parameter in the model. k = the number of parameters for the model. β_0 represents the intercept of the model which is the mean of the shell reef and the Andrews site. Note that community density are negative binomial models that are offset by the footprint of each reef type (Table 1). R = reef; S = site.

Model	k	Intercept	R	S
u_1 (null)	2	β_0		
u_2	7	β_0	β_{1-5}	
u_3	4	β_0		β_{6-7}
u_4	9	β_0	β_{1-5}	β_{6-7}

square-root or log) were applied to normalize the distribution of data. For biomass and secondary productivity, the response variable was standardized by 1 m^2 of river bottom before running the models. As with part I, emmeans and pairwise comparisons were run to determine differences between the means of the models with the best fit.

To look at differences in community assemblages, multivariate analyses were run in Primer-E v 7. Non-metric multi-dimensional scaling (nMDS) was used on square-root transformed data to visually represent community structure for abundance and biomass. The distance between individual points on the nMDS indicated the scale of differences between assemblages and a Pearson correlation > 0.75 was used to obtain a general overview of the major drivers of community differences amongst reef types. To test differences in macrofaunal assemblages by reef and site variables, a Type III distance-based permutational multivariate analysis of variance (PERMANOVA) was run for both density and biomass (McArdle and Anderson, 2001; Anderson, 2001). Note that for multivariate analyses, mobile fauna including fish and crabs were included in the analyses. Macroalgae was also included in the multivariate biomass analysis because it provides habitat for organisms including amphiphods (Fredette and Diaz, 1986; McCain, 1968) and can inform differences between community assemblage between the structures.

4 Results

4.1 Part I - Oyster substrate comparison

Analysis of Impact Sites

The three impact sites were examined to determine whether environmental conditions had an impact on the measured response variables. Because sediment is one indicator of biological and physical differences among sites, a linear regression was fit for a response variable that combined the combined percent of very-fine sand to gravel with phi < 4 (Wentworth, 1922). This variable was titled "hard". The means by site ranged from 96.80 - 98.50 (Table 5). Protected sites tended to have a lower percent hard sediment than the other sites. In pairwise site comparisons, there were no significant differences between hard sediment composition among sites (Table 6).

Total organic carbon in summer 2022 at the impact sites was $<0.170\%$ adjacent to all reef structures and total organic nitrogen was $<0.014\%$. This tended to be consistent with the pre-sampling data in summer 2021, though statistics were not run. Temperature ranged from 24.1 to 26.6°C salinity ranged between 16.97 and 18.8 at the impact sites in summer 2022. DO ranged from 6.0 to 6.9 mg/L.

Andrews and the exposed site tended to have higher wave exposure than the protected site. Andrews had a mean dissolution rate of 32.12 g lost/24 h. The exposed site had a mean dissolution rate of 32.01 g lost/24 h, and the protected site had a mean dissolution rate of 17.78 g lost/24 h.

Table 5: Mean percent hard sediment by site for impact sites. SE = Standard error; CL = confidence level; df = degrees of freedom.

Site	Mean	SE	df	lower.CL	upper.CL
andrews	98.50	0.52	33	97.44	99.56
exposed	97.51	0.52	33	96.45	98.57
protected	96.80	0.52	33	95.74	97.86

Confidence level used: 0.95

Table 6: Pairwise comparisons among impact sites with site as a fixed variable and percent of hard sediment as the response. Mean percent hard sediment by site for impact sites. SE = Standard error; df = degrees of freedom.

Contrast	Estimate	SE	df	t.ratio	p.value
exposed - andrews	-0.99	0.74	33	-1.34	0.38
protected - andrews	-1.70	0.74	33	-2.31	0.07
protected - exposed	-0.71	0.74	33	-0.97	0.60

Oyster Density

During the first round of sampling (fall 2021), all structures showed substantial oyster recruitment. Of the several models fit to determine the factors with the greatest influence on density (Table 7), m_f4, which included reef type and site as variables, had the best fit. Based on the model estimates, mean oyster densities on the reef structures ranged from 825 to 16,721 oysters/m^2 (Table S1) with shell reefs at the top of that range and diamonds at the bottom. Based on the parameter estimates for m_f4, shell reefs had significantly higher densities ($p < 0.01$) than other structures (Table 8; Figure 3). The pairwise comparisons conducted on the model-estimated means reflected the parameter estimates and also showed that the diamond reefs had significantly less densities than all other reefs except castle (Table S2). By site, the protected site had a model-estimated mean of 6,204 oysters/m^2 while the exposed site had 2,465 oysters/m^2 and the Andrews site had 3,946 oysters/m^2. According to pairwise comparisons conducted on model-estimated means, the protected site had significantly higher ($p < 0.01$) densities than the exposed sites (Table S3).

For analysis of the 12-month sampling (summer 2022), of the models, m_d4, including reef type and site, had the best fit with an AICc of 480.72 (Table 9). Based on the parameter estimates for m_d4, all of the artificial reefs had significantly lower oyster ($p < 0.01$) densities than the shell reefs (Table 10; Figure 4). Based on model estimates, oyster densities ranged from 716 to 9,853 oysters/m^2 with the shell being the highest of that range and diamonds the lowest (Table S4). After the shell reef, the c-dome and x-reef structures had the next highest densities and had, on average,

Table 7: AIC analysis for generalized linear negative binomial models for oyster density from reef alternative substrates in fall 2021. Models were offset by footprint of reef type (Table 1) to standardize to 1 m^2 of river bottom R = reef; S = site; (F) = log of the offset footprint of individual reef structures

Model	Variables	k	AIC	AICc	dAICc	wts
m_f1	null + (F)	2	582.46	578.46	46.51	<0.01
m_f2	R + (F)	7	555.90	541.90	9.95	0.01
m_f3	S + (F)	4	585.23	577.23	45.27	<0.01
m_f4	R + S + (F)	9	549.95	531.95	0.00	0.99

Table 8: Parameter estimates from the generalized linear negative binomial model, m_f4, for oyster recruitment density in fall 2021. Note that the intercept is a sum of the Andrews site and the oyster shell reef type.

Parameter	Variable	Estimated Mean	SE	t.value	Pr(>|t|)
β_0	intercept	9.73	0.29	33.38	<0.01
β_1	granite	-1.84	0.36	-5.13	<0.01
β_2	castle	-2.45	0.36	-6.86	<0.01
β_3	diamond	-3.01	0.36	-8.41	<0.01
β_4	c-dome	-0.94	0.36	-2.64	0.01
β_5	x-reef	-0.46	0.36	-1.30	0.20
β_6	exposed	-0.47	0.25	-1.86	0.06
β_7	protected	0.45	0.25	1.79	0.07

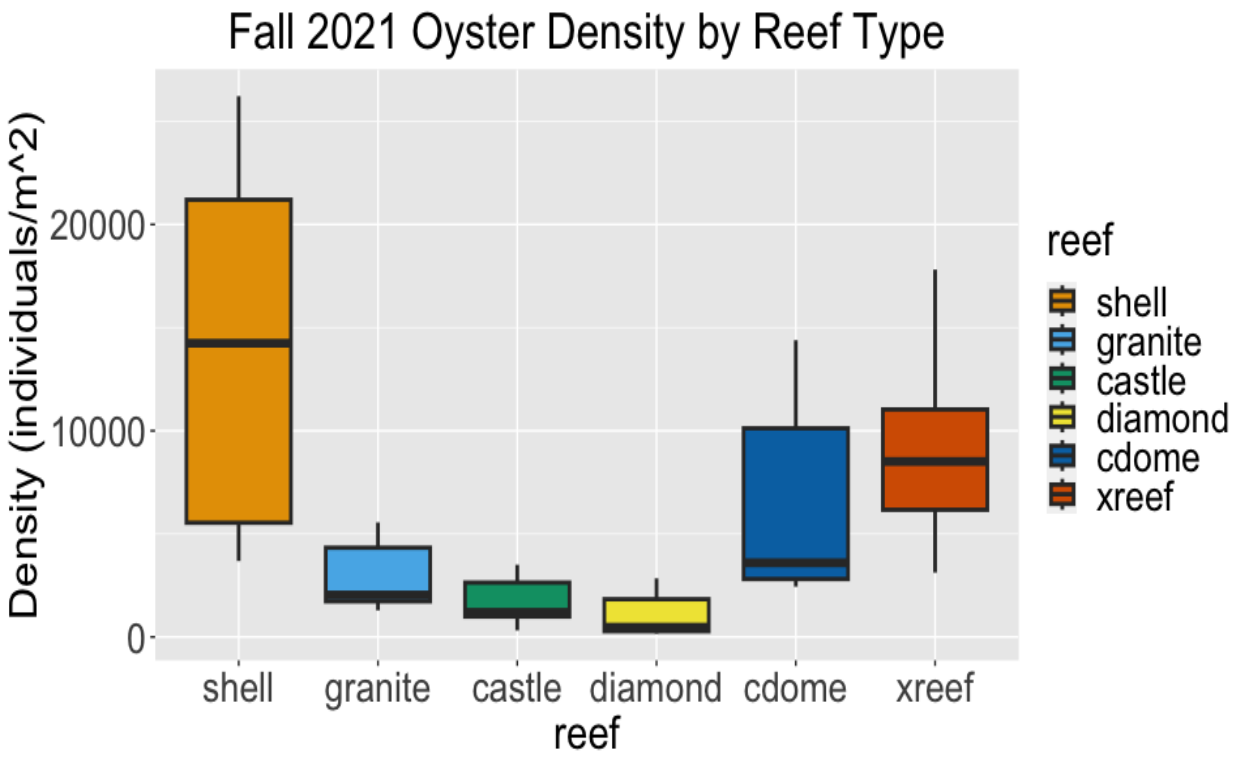

Figure 3: Oyster density by reef type in fall of 2021. Densities were standardized to 1 m^2 of river bottom. The box represents the first and third quartile of the data while the central line represents the median. The vertical lines represent the full range of the data.

oyster densities similar to each other after a year of growth, with means of 3,202.30 and 3,816.67 oysters/m^2 respectively (Table S4). In pairwise comparisons based on these means, shell had significantly higher densities than the other structures ($p < 0.01$) and diamonds had significantly lower densities (($p < 0.01$; Table S5). For differences between sites, mean oyster density means based on model estimated means ranged between 1,743.77 - 4,110.42 oysters/m^2 (Table S6; Figure 5). For pairwise comparisons based on these means, exposed site had significantly lower densities than the Andrews and protected sites ($p < 0.01$), but there was high variability (Table S7).

Table 9: AIC analysis for generalized linear negative binomial models for oyster density from reef alternative substrates in summer 2022. Models were offset by footprint of reef type (Table 1) to standardize to 1 m^2 of river bottom. R = reef; S = site; (F) = log of the offset footprint of individual reef structures.

Model	Variables	k	AIC	AICc	dAICc	wts
m_d1	null + (F)	2	549.41	549.77	62.13	<0.01
m_d2	R + (F)	7	509.09	513.09	25.45	<0.01
m_d3	S + (F)	4	546.03	547.32	59.68	<0.01
m_d4	R + S + (F)	9	480.72	487.64	0.00	0.99

Table 10: Parameter estimates from the generalized linear model m_d4 for oyster recruitment density in summer 2022. Note that the intercept is a sum of the Andrews site and the oyster shell reef type.

Parameter	Variable	Estimated Mean	SE	z value	Pr(>|z|)
β_0	intercept	9.32	0.14	68.80	<0.01
β_1	granite	-1.25	0.17	-7.46	<0.01
β_2	castle	-1.49	0.17	-8.99	<0.01
β_3	diamond	-2.62	0.17	-15.62	<0.01
β_4	c-dome	-1.12	0.17	-6.77	<0.01
β_5	x-reef	-0.95	0.17	-5.72	<0.01
β_6	exposed	-0.62	0.12	-5.25	<0.01
β_7	protected	0.24	0.12	2.01	0.04

For density by surface area, several generalized linear regression negative binomial models

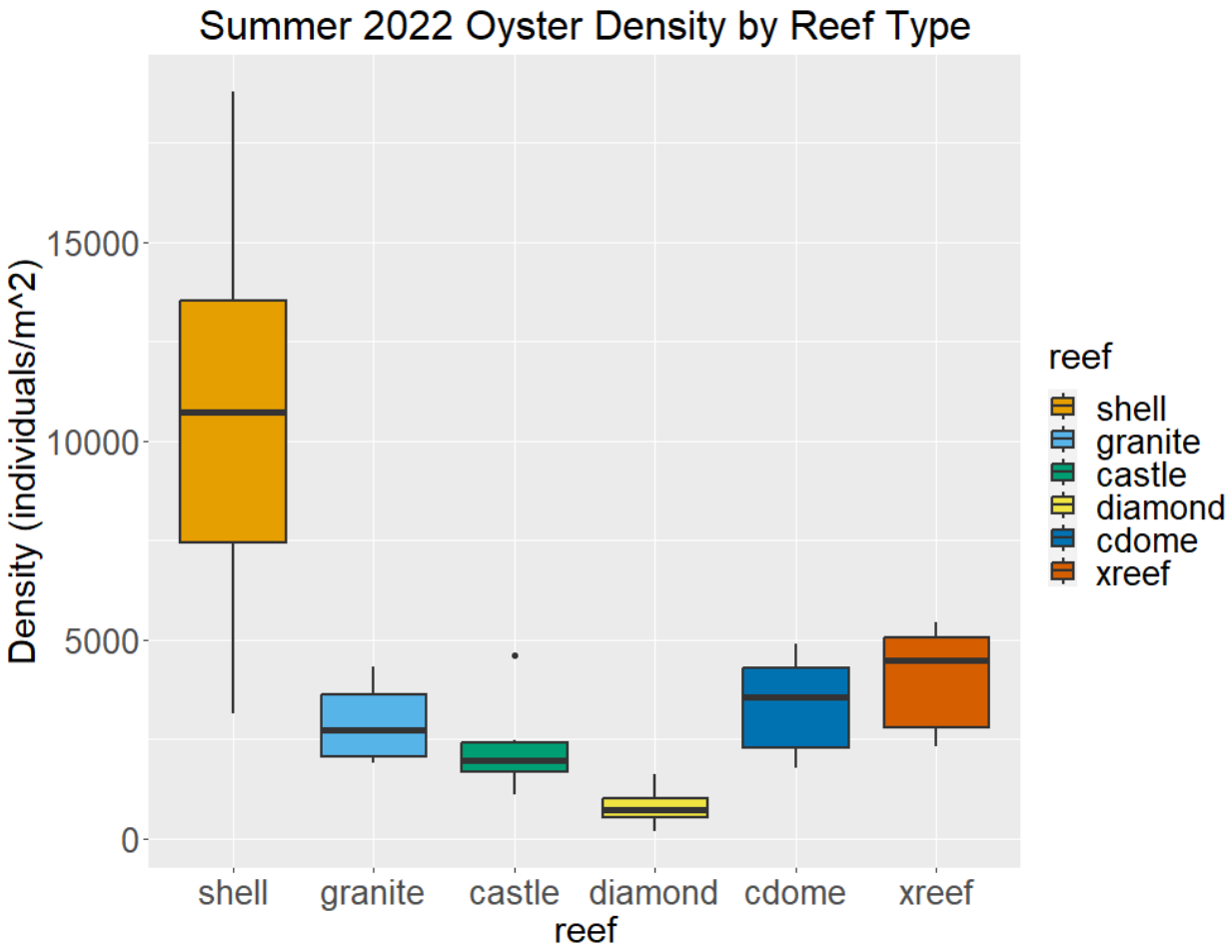

Figure 4: Oyster density by reef type in summer of 2022. Densities were standardized to 1 m^2 of river bottom. The box represents the first and third quartile of the data while the central line represents the median. The vertical lines represent the full range of the data without outliers while dots represent outliers.

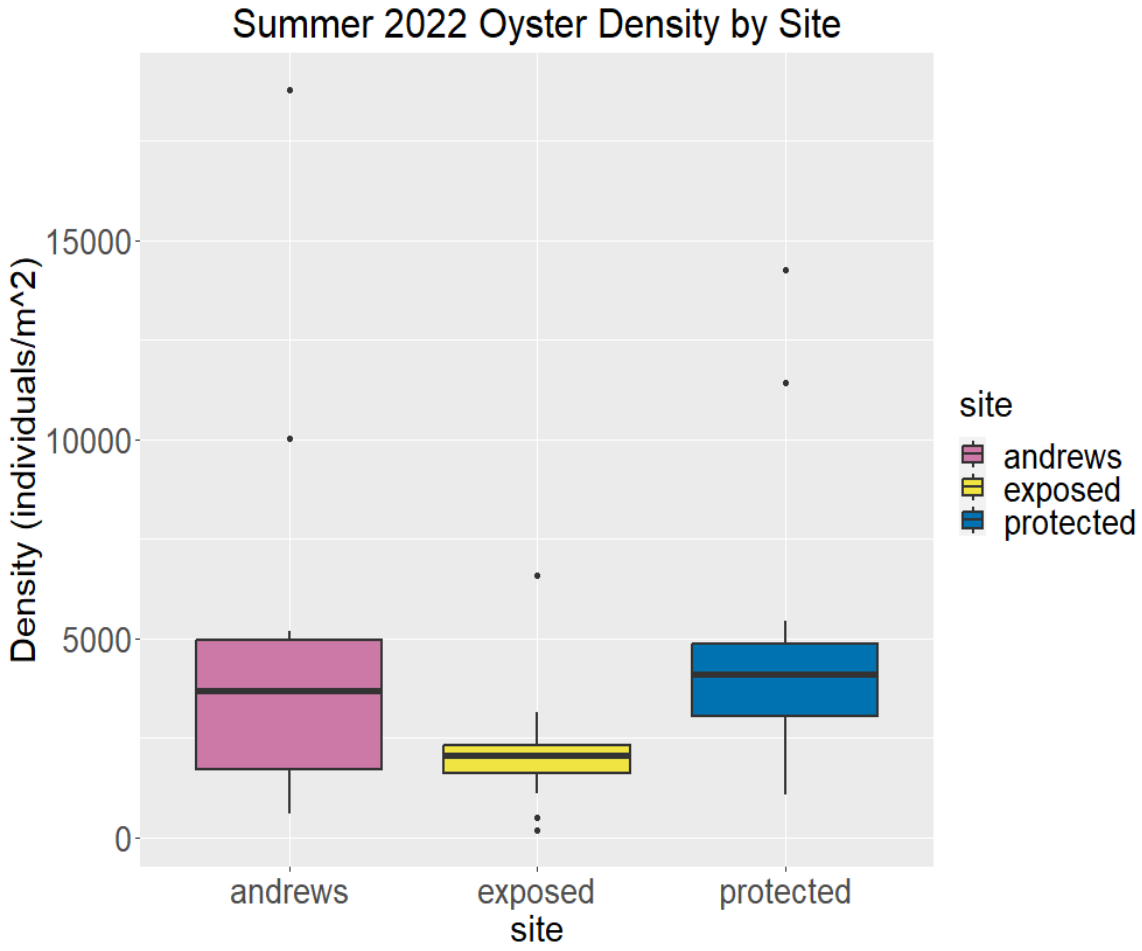

Figure 5: Oyster density by site in summer of 2022. Densities were standardized to 1 m^2 of river bottom. The box represents the first and third quartile of the data while the central line represents the median. The vertical lines represent the full range of the data without outliers while dots represent outliers.

were fit (Table 11) and the model with the best fit, m_s4 included both reef type and site. Based on the parameter estimates, all structures had significantly lower oysters densities than the castles ($p < 0.01$) except the x-reef (Table 12). Based on model estimates, mean oyster densities for the concrete mix structures by surface area (s.a.) ranged from 23.09 to 478.56 oysters/m^2 s.a., with the x-reef at the top of that range and the diamond at the bottom (Table S8). In the pairwise comparisons based on the model estimated means, all structures were significantly different from one another except the x-reefs and the oyster castles (Table S9). By model estimates for site, the exposed site had 118.45 oysters/m^2 s.a., whereas the protected site had 289.57 oysters/m^2 s.a. (Table S10). The exposed site also had significantly lower model estimated mean oyster density than the Andrews ($p < 0.01$) and the protected sites ($p < 0.01$; Table S11).

Table 11: AIC analysis for generalized linear negative binomial models for oyster density from reef alternative substrates in summer 2022. Models were offset by surface area of reef type (Table 1) to standardize to 1 m^2 of surface area. R = reef; S = site; (SA) = log of the offset surface area of individual reef structures.

Model	Variables	k	AIC	AICc	dAICc	wts
m_s1	null + (SA)	2	376.43	377.00	46.63	<0.01
m_s2	R + (SA)	5	342.67	346.00	15.64	<0.01
m_s3	S + (SA)	4	377.65	379.76	49.39	<0.01
m_s4	R + S + (SA)	7	323.36	330.36	0.00	0.99

Oyster Biomass

Of the models tested for oyster biomass m_b4, including both reef substrate and site, had the best fit (Table 13). Based on parameter estimates for this model (Table 14), all reef types had significantly lower oyster biomass than shell reefs ($p < 0.01$; Figure 6) and the exposed site had significantly lower biomass than the Andrews site ($p < 0.01$; Figure 7). When examining model-estimated means of oyster biomass of the reef types, means ranged between 117.48 and 743.90 g AFDW (Table S12). The castle, c-dome, and x-reef structures all had mean oyster biomass that was greater than the granite and diamond structures, with diamonds at the bottom of that range. The

Table 12: Parameter estimates from the generalized linear model m_s4 for oyster density per unit surface area for concrete-mix structures in summer 2022. Note that the intercept is a sum of the Andrews site and the oyster castle structure and that all numbers are standardized to 1 m^2 of surface area.

Parameter	Variable	Estimated Mean	SE	t.value	Pr(>|t|)
β_0	intercept	7.40	0.14	52.65	<0.01
β_1	diamond	-2.77	0.16	-16.84	<0.01
β_2	c-dome	-0.60	0.16	-3.67	<0.01
β_3	x-reef	-0.06	0.16	-0.34	0.73
β_4	exposed	-0.62	0.14	-4.34	<0.01
β_5	protected	00.28	0.14	1.97	0.05

exposed site had a mean of 267.83 g AFDW, whereas the protected and Andrews sites had a mean of >450 grams (Table S13). In pairwise comparisons by reef type based on the model-estimated means, shell had significantly higher biomass than all other structures with the exception of the x-reefs, which had similar biomass (Table S14). C-domes also had significantly higher biomass than diamonds (p = 0.03). For pairwise comparisons between sites based on the model-estimated means, the exposed site had significantly less biomass than the protected site and the Andrews site (Table S15).

Table 13: AIC analysis for linear models for oyster biomass from reef alternative substrates in 2022. All numbers were standardized to m^2 of river bottom. R = reef, S = site.

Model	Variables	k	AIC	AICc	dAICc	wts
m_b1	null	2	506.97	507.32	24.09	<0.01
m_b2	R	7	486.85	490.85	7.51	<0.01
m_b3	S	4	505.37	506.66	23.42	<0.01
m_b4	R + S	9	476.31	483.24	0.00	0.99

An analysis was also run on oyster dry weight as this is the standard unit of measurement for oyster restoration practices in the Chesapeake Bay (Sustainable Fisheries, 2011). Model $m_{dw}4$, which included both reef type and site, had the lowest AICc for oyster dry weight (Table 15). As

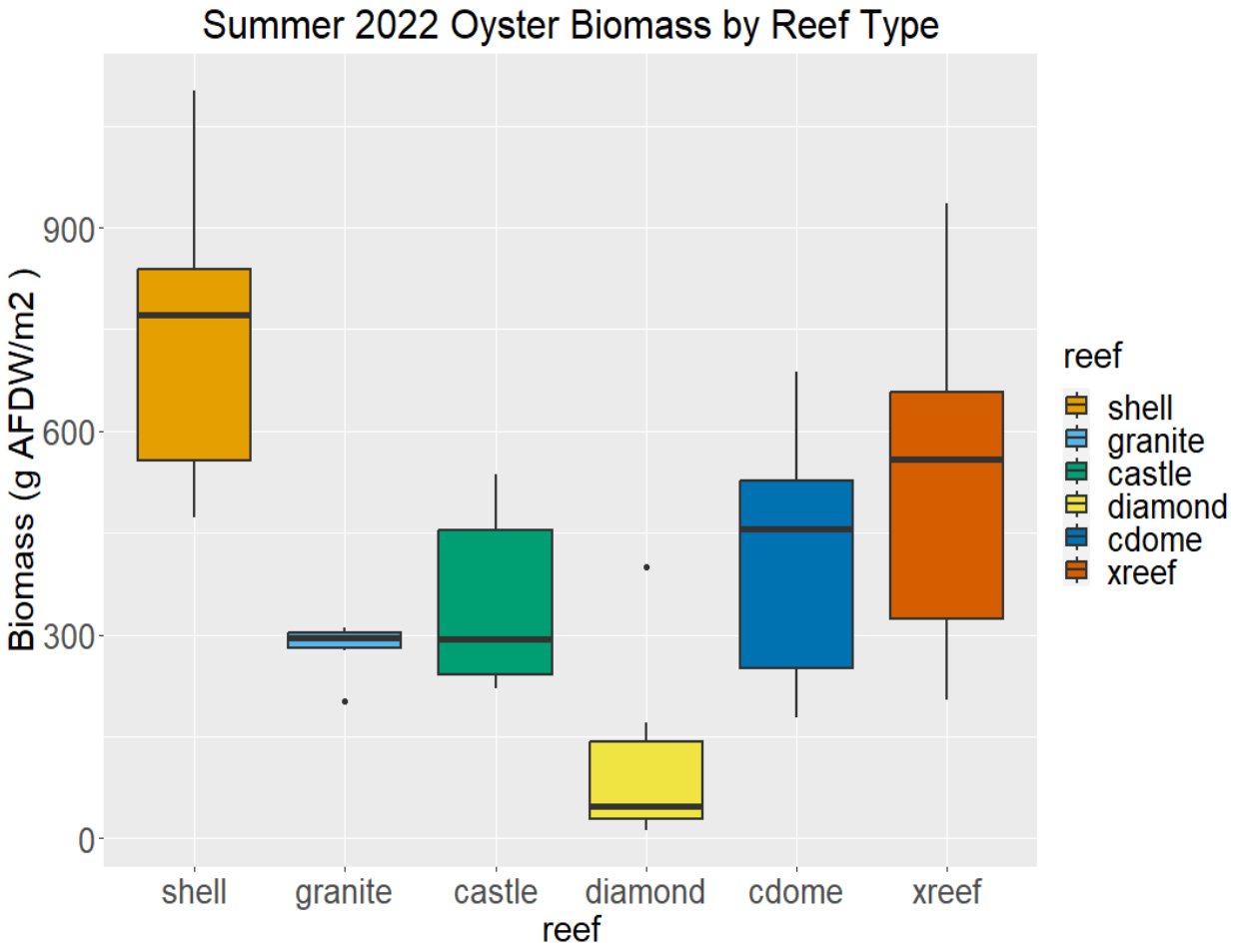

Figure 6: Oyster AFDW by reef type in summer of 2022 standardized to 1 m^2 of river bottom. Biomass was derived from from oyster shell heights using shell height to ash-free dry weight regressions developed as part of this project. The box represents the first and third quartile of the data while the central line represents the median. The vertical lines represent the full range of the data without outliers while dots represent outliers.

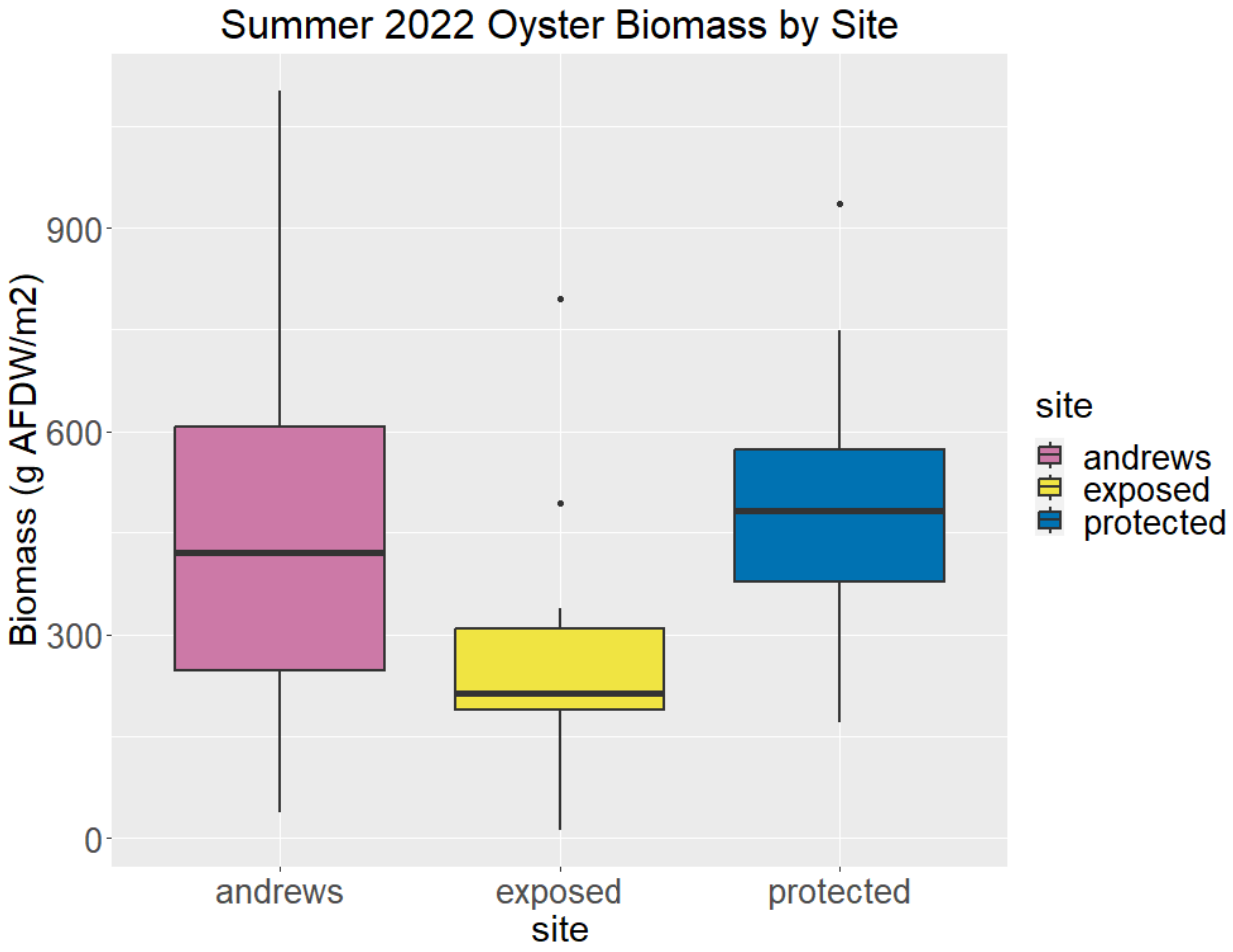

Figure 7: Oyster AFDW by site type in summer of 2022 standardized to 1 m^2 of river bottom. Biomass was derived from from oyster shell heights using shell height to ash-free dry weight regressions developed as part of this project. The box represents the first and third quartile of the data while the central line represents the median. The vertical lines represent the full range of the data without outliers while dots represent outliers.

Table 14: Parameter estimates from the generalized linear model m_b4 for oyster biomass in summer 2022. Note that the intercept is a sum of the Andrews site and the oyster shell reef type.

Parameter	Variable	Estimated Mean	SE	t.value	Pr(>|t|)
β_0	intercept	793.74	75.20	10.56	<0.01
β_1	granite	-463.06	92.10	-5.03	<0.01
β_2	castle	-397.97	92.10	-4.32	<0.01
β_3	diamond	-626.42	92.10	-6.80	<0.01
β_4	c-dome	-325.56	92.10	-3.53	<0.01
β_5	x-reef	-212.15	92.10	-2.30	0.03
β_6	exposed	-188.39	65.12	-2.89	<0.01
β_7	protected	38.86	65.12	0.60	0.56

with m_b4, $m_{dw}4$ also demonstrates that shell had the biomass that was significantly higher ($p < 0.01$) than the rest of the structures (Table 16). Additionally, according to the model, the exposed site had significantly lower dry weight than the Andrews site (Table 16). Based on the model-estimated means, dry weight biomass was high for all substrate types and ranged from 147.12 and 895.03 g DW/m^2 with diamonds being the structure with the lowest means in that range (Table S16). In pairwise comparisons by reef conducted on the model-estimated means, diamond had significantly lower oyster dry weight than all reefs aside from castle (Table S17). Based on $m_{dw}4$, the protected site had the highest mean dry weight at 553.92 g while the exposed site had the lowest at 308.09 g (Table S18). In pairwise comparisons by site conducted on the model-estimated means, trends were similar to the AFDW analysis, with the exposed site having significantly lower oyster dry weight after a year than the protected ($p < 0.01$) and the Andrews sites ($p < 0.01$; Table S19).

Oyster Shell Height

Trends in oyster shell height show the presence of recruitment by multiple cohorts, visible as multiple peaks in individual histograms by reef type and site (Figure 8). Across sites, the shell reef had the most small, newly settled oysters (e.g., note the high peak at 15 mm for Andrews shell reefs). All structures supported many small oysters, as seen by peaks in the data at small size

Table 15: AIC analysis for linear models for oyster dry weight biomass from reef alternative substrates in summer 2022. All numbers were standardized to m^2 of river bottom. R = reef, S = site.

Model	Variables	k	AIC	AICc	dAICc	wts
$m_{dw}1$	null	2	520.72	521.08	26.44	<0.01
$m_{dw}2$	R	7	501.79	505.79	11.15	<0.01
$m_{dw}3$	S	4	517.72	519.01	24.37	<0.01
$m_{dw}4$	R + S	9	487.72	494.64	0.00	0.99

Table 16: Parameter estimates from the generalized linear model $m_{dw}4$ for oyster dry weight in summer 2022. Note that the intercept is a sum of the Andrews site and the oyster shell reef type.

Parameter	Variable	Estimated Mean	SE	t.value	Pr(>|t|)
β_0	intercept	956.14	88.10	10.85	<0.01
β_1	granite	-546.32	107.90	-5.06	<0.01
β_2	castle	-476.44	107.90	-4.42	<0.01
β_3	diamond	-747.91	107.90	-6.93	<0.01
β_4	c-dome	-397.35	107.90	-3.68	<0.01
β_5	x-reef	-245.27	107.90	-2.27	0.03
β_6	exposed	-245.83	76.30	-3.22	<0.01
β_7	protected	62.50	76.30	0.82	0.42

classes, and a few larger oysters. The diamond reef had low oyster counts regardless of size, seen especially in the diamonds at the Andrews and the exposed sites. Overall, the shell, castle, c-dome, and x-reef structures had abundant, newly settled oysters. The the protected sizes, the castles and the x-reefs had higher numbers of larger, older oysters than other structures, as seen by the tail-end of the data that stretches past 100 mm for the castles at some sites and up to 75 mm for the x-reefs.

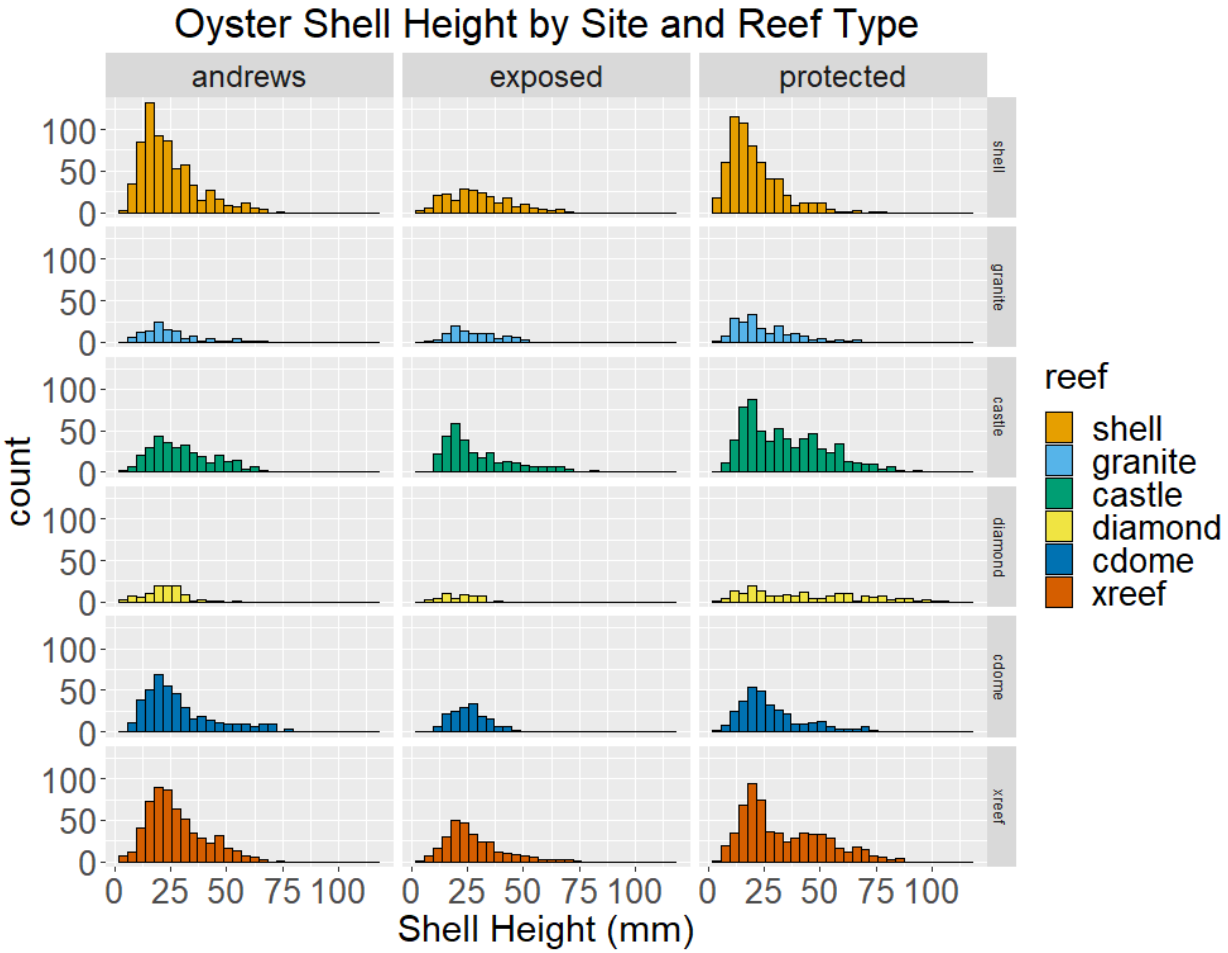

Figure 8: Frequency (counts) of different oyster shell height by reef type and site for summer 2022. Note that this is the raw data for shell height and counts across reef types. A total of 36 reefs were sampled with n = 6 per reef type and n = 12 per site. Each histogram represents 2 reefs.

4.2 Part II - Macrofaunal production before and after reef deployment

Before-After, Control-Impact macrofaunal community comparisons

Macrofaunal density, richness, evenness, Shannon diversity, biomass, and secondary productivity varied significantly by year. At the impact sites, macrofaunal density was 200 times greater than at the bare sediment control sites (Figure 9), and the BACI interaction was significant (glm, $p = 0.03$). Macrofaunal richness was 3.7 times greater at the impact sites than at the control sites after a year (Figure 9), and the BACI interaction was significant (ANOVA, $p < 0.01$). Macrofaunal evenness was lower at the impact sites than at the control sites after a year (Figure 9), and the BACI interaction was not significant (ANOVA, $p = 0.1$). Macrofaunal Shannon diversity was 1.4 times greater at the impact sites than at the control sites after a year (Figure 9), and the BACI interaction was significant (ANOVA, $p = 0.01$). For macrofaunal community biomass, the impact site had 21 times greater biomass than the control site after a year (Figure 10), and the interaction was significant (glm, $p < 0.01$). Benthic macrofaunal community secondary productivity at the impact sites was 450 g C/m^2/yr and 40 times greater than at the control sites (Figure 10). For secondary productivity, the BACI interaction was significant (glm, $p < 0.01$).

A BACI analysis was also run on total secondary productivity that included macrofuanal community and oyster biomass. With oyster AFDW accounted for, the impact site had a mean secondary productivity of 1631 g C/m^2/yr, which is over 145 times greater than the bare sediment control site at 11.2 g C/m^2/yr (Figure 10). Mean oyster secondary productivity at the impact site after a year based on the raw data and the BACI analysis was $\sim$ 1,178 g C/m^2/yr and mean macrofaunal secondary productivity based on the BACI analysis and the raw data was $\sim$ 452 g C/m^2/yr. For total secondary productivity, the interaction (glm, $p < 0.01$) between site and time was significant.

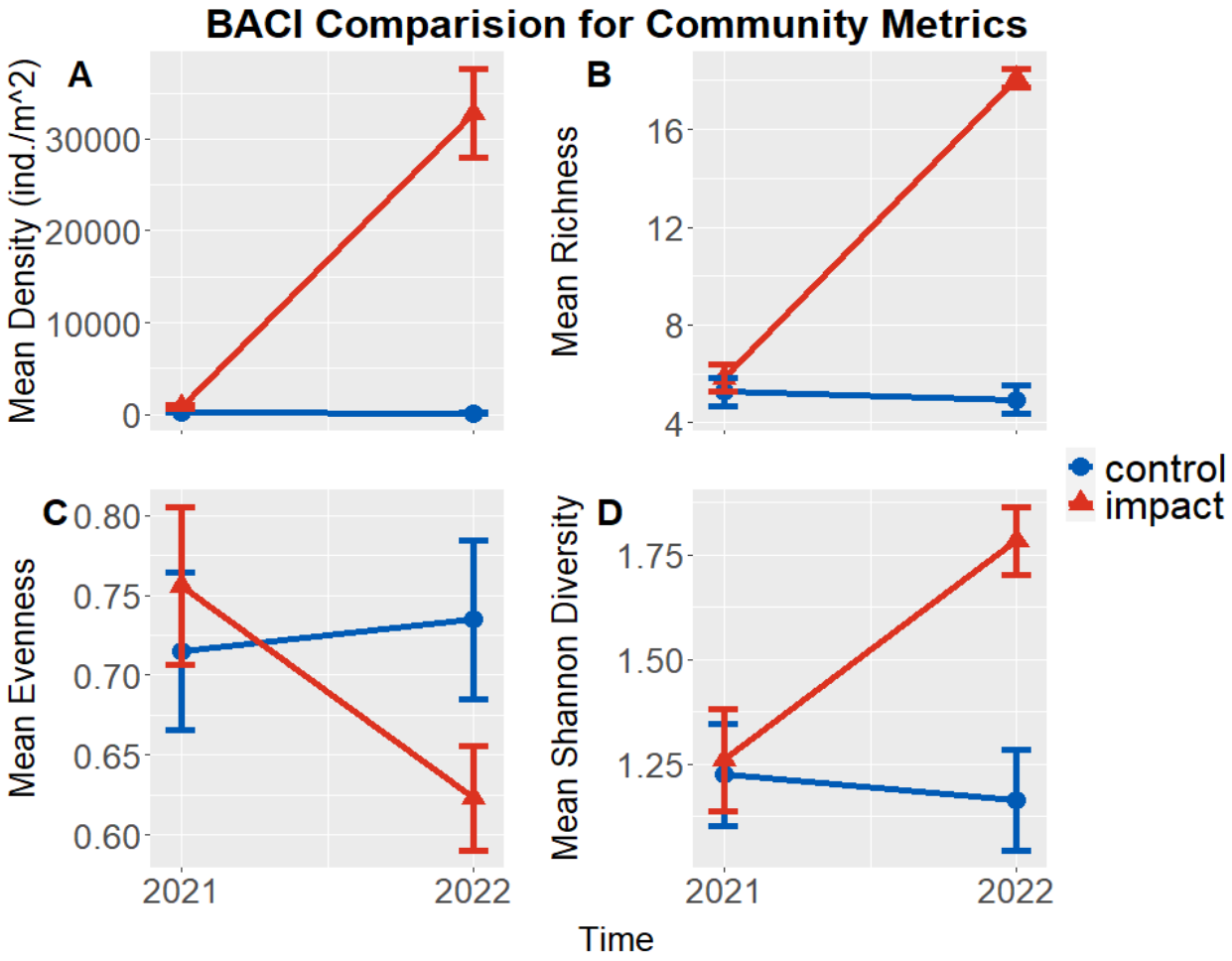

Figure 9: Benthic marcofaunal (A) density, (B) richness, (C) evenness, and (D) Shannon diversity from summer 2021 to summer 2022 for the bare sediment control and the reef impact sites. Error bars indicate standard error.

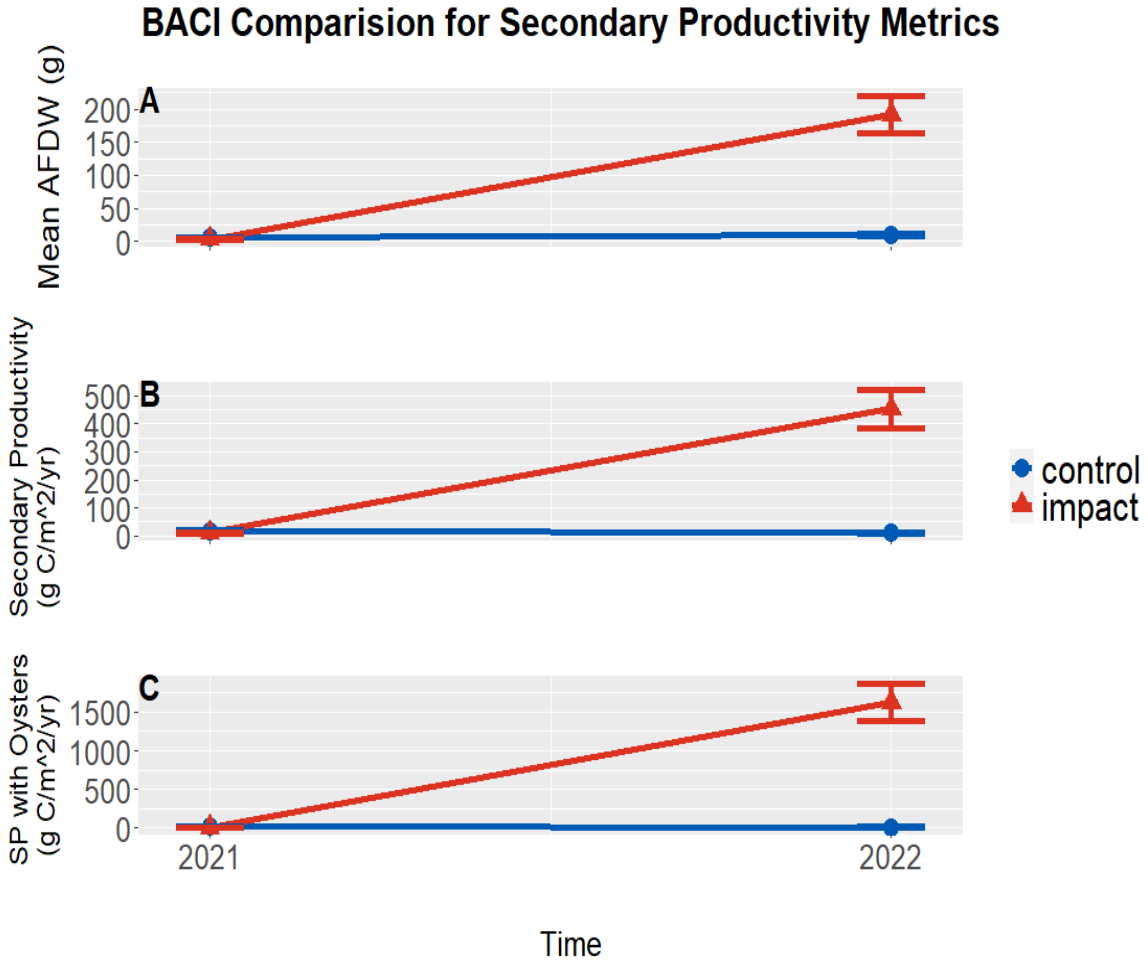

Figure 10: Benthic marcofaunal (A) biomass (AFDW) and (B) secondary productivity as well as (C) secondary productivity that included oyster biomass from summer 2021 to summer 2022 for the bare sediment control and the reef impact sites. SP = secondary productivity. Error bars indicate standard error.

Analyses of Univariate data

All AICc values for the tested models for univariate data can be found in Table 17. All parameter estimates for the model with the best fit can be found in Table 18 and the means based on those models can be found in Table S20.

For community density, generalized linear negative binomial models were fit, and the model with the best fit, u_4, included both reef and site. The granite had significantly higher ($p < 0.01$) and diamond reefs had significantly lower community density ($p < 0.01$) than the shell reefs (Figure 11). In pairwise comparisons run on model-estimated means, the diamond had significantly lower community density than all other structures and granite had significantly higher community density than all structures except castles and c-domes (Table S21). As with oyster density alone, based on the model u_4, the protected ($p < 0.01$) and exposed ($p < 0.01$) sites had significantly lower organism density than the Andrews site (Figure 12). In pairwise comparisons run on model-estimated means for sites, all sites significantly differed from one another (Table S22).

For richness, the linear model with the best fit, u_4, also included both reef and site. The granite ($p = 0.05$), castle ($p < 0.01$), and x-reef ($p = 0.02$) had significantly higher community richness than the shell reefs (Figure 13). Based on pairwise comparisons between model-estimated means, as with community density, the diamond reef tended to under-perform for richness (Table S23). Pairwise comparisons also revealed that the exposed sites also had significantly lower community richness $p < 0.01$) than the Andrews site (Table S24; Figure 14).

For evenness, the model with the best fit, u_3, included only site. There was no significant difference between u_3 and u_4 so u_4 was further examined (ANOVA; Table S25). All of the reefs performed equally for community evenness (Figure 15). In pairwise comparisons based on model-estimated means, there were no significant differences between reef type (Table S26). However, those same comparisons for site showed that the protected and exposed sites had significantly greater ($p < 0.01$ for both) organism evenness than the Andrews site (Table S27; Figure 16).

Similar to the evenness models, for the Shannon diversity models, the model with the best fit, u_3, included only site. There was no significant difference between u_3 and u_4, so u_4 was further

examined (Table S25). The diamond reef had significantly lower Shannon diversity (p = 0.03) than the other structures (Figure 17); however, pairwise comparisons based on model-estimated means showed that there were no major differences for community diversity between reef types (Table S28). Based on pairwise comparisons from the model-estimated means, the exposed and the protected site had significantly higher (p = 0.03 and $p < 0.01$ respectively) diversity than the Andrews site despite having a lower density of organisms (Table S29; Figure 18).

For biomass, the model with the best fit, u_4, included both reef type and site as variables. Granite had significantly higher biomass than the shell ($p < 0.01$) and greater biomass than the most of the concrete-mix structures as well (Figure 19). According to pairwise comparisons run on model-estimated means, the diamond reef had significantly lower biomass than other structures (Table S30). The Andrews site had higher overall biomass than the other two sites and, based on pairwise comparisons from the model-estimated means, had significantly higher biomass than the exposed site (p = 0.01; Table S31; Figure 20).

For secondary productivity, the model with the best fit, u_2, included only reef type as a variable. All of the concrete-mix structures showed significantly lower secondary productivity than the shell structure (castle: p = 0.2; diamond: $p < 0.01$; c-dome: p = 0.04; x-reef: $p < 0.01$; Table 18). The granite reef had no significant difference from the shell reef (Figure 21), as both had high secondary production. According to pairwise comparisons of model-estimated means, the diamond structure had significantly lower secondary productivity than most of the structures and the granite had significantly higher secondary productivity than any other structure type (Table S32).

The main species that were the drivers of these differences, and differences among structures, are depicted in Figure 22. Amphipod species including those of the Caprellidae and Gammaridae families and the *Corophium* genus had the highest densities across all structures with amphipod on the granite structure reaching over 120,000 individuals per m^2 of river bottom. Polychaetes such as *Alitta succinea, Potamilla neglecta* and *Parasabella microphthalma* were also seen in high densities across reef types. The crustacean taxonomic group which included species like *Panopeus herbstii, Eurypanopeus depressus*, and *Dyspanoepus sayi* had overall high biomass with crustacean

biomass on the granite structure reaching over 150 g AFDW/m^2. The miscellaneous category included tunicates, sponges, and anemones. This also had a high biomass reaching over 150 g AFDW/m^2 on the cdome structured and over 125 g AFDW/m^2 on the xreef.

Table 17: AIC results for all models of response variables for univariate community data, ordered by increasing AICc weight (wts). Models with the lowest AICc are in bold. All models that are departures from linear model that use normal distributions are listed in parenthesis below the response variable. k = number of model parameters.

Response	Model	k	AIC	AICc	dAICc	wts
Community	u_1	2	700.72	696.72	54.52	<0.01
Density	u_2	7	698.49	684.49	42.29	<0.01
(Neg. Bin.)	u_3	4	678.70	670.70	28.50	<0.01
	u_4	**9**	**660.20**	**642.20**	**0.00**	**0.99**
	u_1	2	177.99	178.36	16.97	<0.01
Richness	u_3	4	173.24	174.53	13.14	<0.01
	u_2	7	167.66	171.66	10.28	<0.01
	u_4	**9**	**154.46**	**161.38**	**0.00**	**0.99**
	u_2	7	-20.33	-16.33	27.00	<0.01
Evenness	u_1	2	-27.30	-26.93	16.40	<0.01
	u_4	9	-40.31	-33.39	9.94	0.01
	u_3	**4**	**-44.62**	**-43.33**	**0.00**	**0.99**
Shannon	u_2	7	52.94	56.94	21.64	<0.01
Diversity	u_1	2	47.81	48.18	12.88	<0.01
	u_4	9	35.63	42.55	7.25	0.03
	u_3	**4**	**34.01**	**35.30**	**0.00**	**0.97**
Community	u_1	2	451.13	451.49	19.36	<0.01
Biomass	u_3	4	450.05	451.34	19.21	<0.01
	u_2	7	433.28	437.28	5.15	0.07
	u_4	**9**	**425.21**	**432.13**	**0.00**	**0.93**
Secondary	u_3	4	250.34	251.63	30.54	<0.01
Productivity*	u_1	2	247.68	248.05	26.95	<0.01
	u_4	9	216.76	223.69	2.60	0.21
	u_2	**7**	**217.09**	**221.09**	**0.00**	**0.79**

* Linear model with a square root transformation.

Table 18: Parameter estimates for univariate community data from 2022. Estimates were derivated from the models supported with wts > 0.1 as listed in Table 17. Significant parameters ($\alpha = 0.05$) are in bold and SE is included with the $\pm$ indicator. Xs are parameters not included in the selected models. Abbreviations for models as in Table 4. β_0 is the intercept and a mean of the oyster shell reef and Andrews site parameters. The family of model used per response variable is listed in parenthesis beneath that response variable. LM = general linear model. Note that models that only found site as a significant parameter were compared using an ANOVA to models that included both site and reef, and no significant differences were found. In the case where only site was found to be significant, this table presents the model that include both site and reef as factors to better examine the effect of alternative reefs on the univariate response variables.

Response	Model	β_0 Intercept	β_1 Granite	β_2 Castle	β_3 Diamond	β_4 C-dome	β_5 X-reef	β_6 Exposed	β_7 Protected
Density*	u_4	**10.87** $\pm$	**0.82**$\pm$	0.05$\pm$	**-0.81**$\pm$	0.22$\pm$	0.09$\pm$	**-0.93**$\pm$	**-1.55**$\pm$
(Neg. Bin.)		**0.20**	**0.25**	0.25	**0.25**	0.25	0.25	**0.17**	**0.17**
Richness	u_4	**18.42** $\pm$	**2.17**$\pm$	**3.50**$\pm$	-1.83$\pm$	1.00$\pm$	**2.67**$\pm$	**-3.08**$\pm$	**-1.67**$\pm$
(LM)		**0.86**	**1.05**	**1.05**	1.05	1.05	**1.05**	**0.75**	**0.75**
Evenness	u_4	**0.55** $\pm$	-0.10$\pm$	-0.08$\pm$	-0.12$\pm$	-0.01$\pm$	-0.08$\pm$	**0.17**$\pm$	**0.25**$\pm$
(LM)		**0.06**	0.07	0.07	0.07	0.07	0.07	**0.05**	**0.05**
Diversity	u_4	**1.58** $\pm$	-0.20$\pm$	-0.11$\pm$	**-0.46**$\pm$	0.02$\pm$	-0.13$\pm$	**0.39**$\pm$	**0.68**$\pm$
(LM)		**0.17**	0.20	0.20	**0.20**	0.20	0.20	**0.14**	**0.14**
Biomass	u_4	**245.08** $\pm$	**144.84**$\pm$	-48.17$\pm$	**-145.04**$\pm$	23.01$\pm$	45.60$\pm$	**-106.29**$\pm$	-63.65$\pm$
(LM)		**36.98**	**45.29**	45.29	**45.29**	45.29	45.29	**32.02**	32.02
Secondary	u_2	**644.50** $\pm$	8.47$\pm$	**-39.25**$\pm$	**-241.18**$\pm$	**-30.50**$\pm$	**-58.91**$\pm$	X	X
Production		**3.30**	6.60	**6.60**	**6.60**	**6.60**	**6.60**		
(LM*)									

* Parameters back-transformed by squaring.

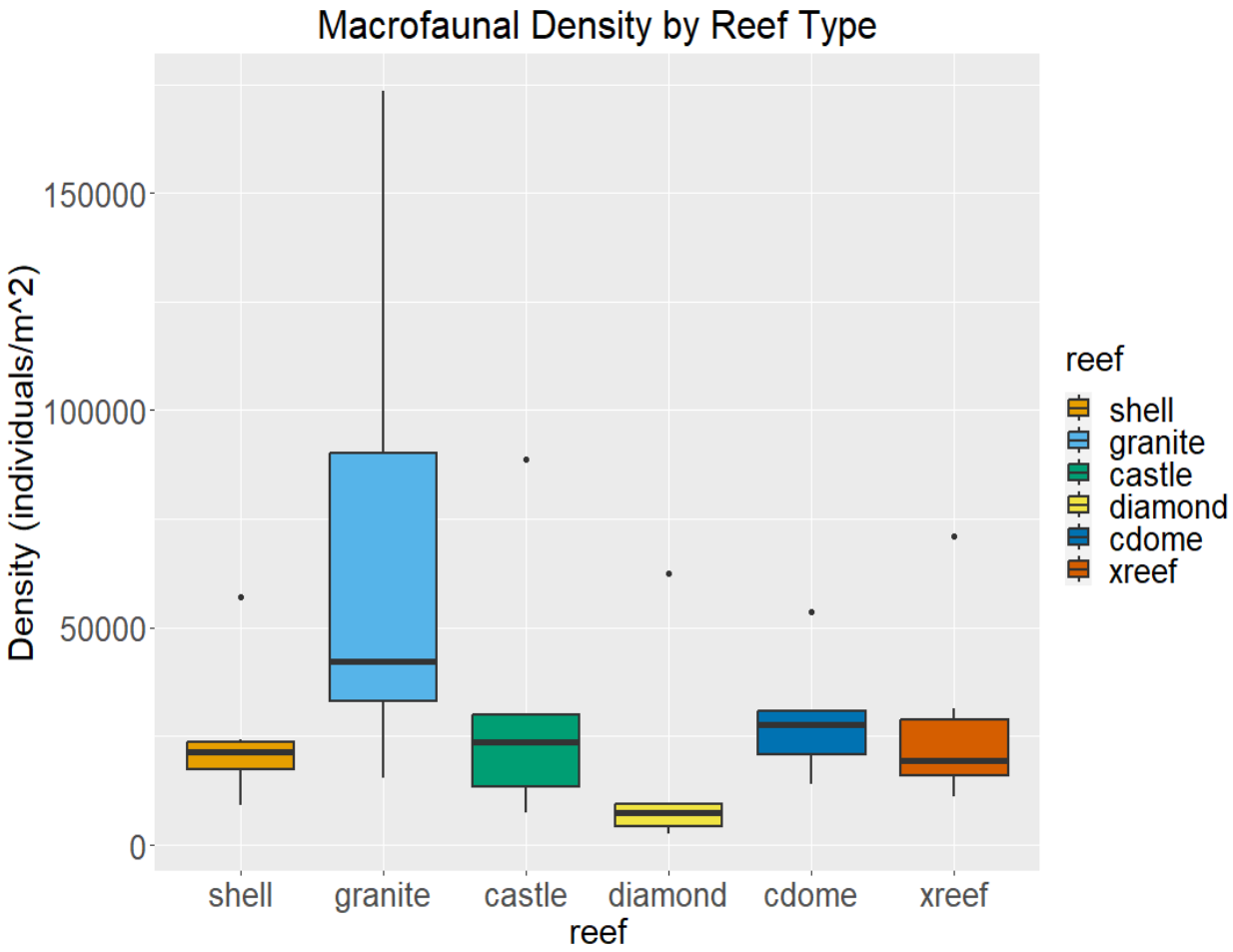

Figure 11: Macrofaunal community density by reef type at the impact sites in summer 2022. All numbers standardized to 1 m^2 of river bottom. The box represents the first and third quartile of the data while the central line represents the median. The vertical lines represent the full range of the data without outliers while dots represent outliers. Note that algae and oysters were not included.

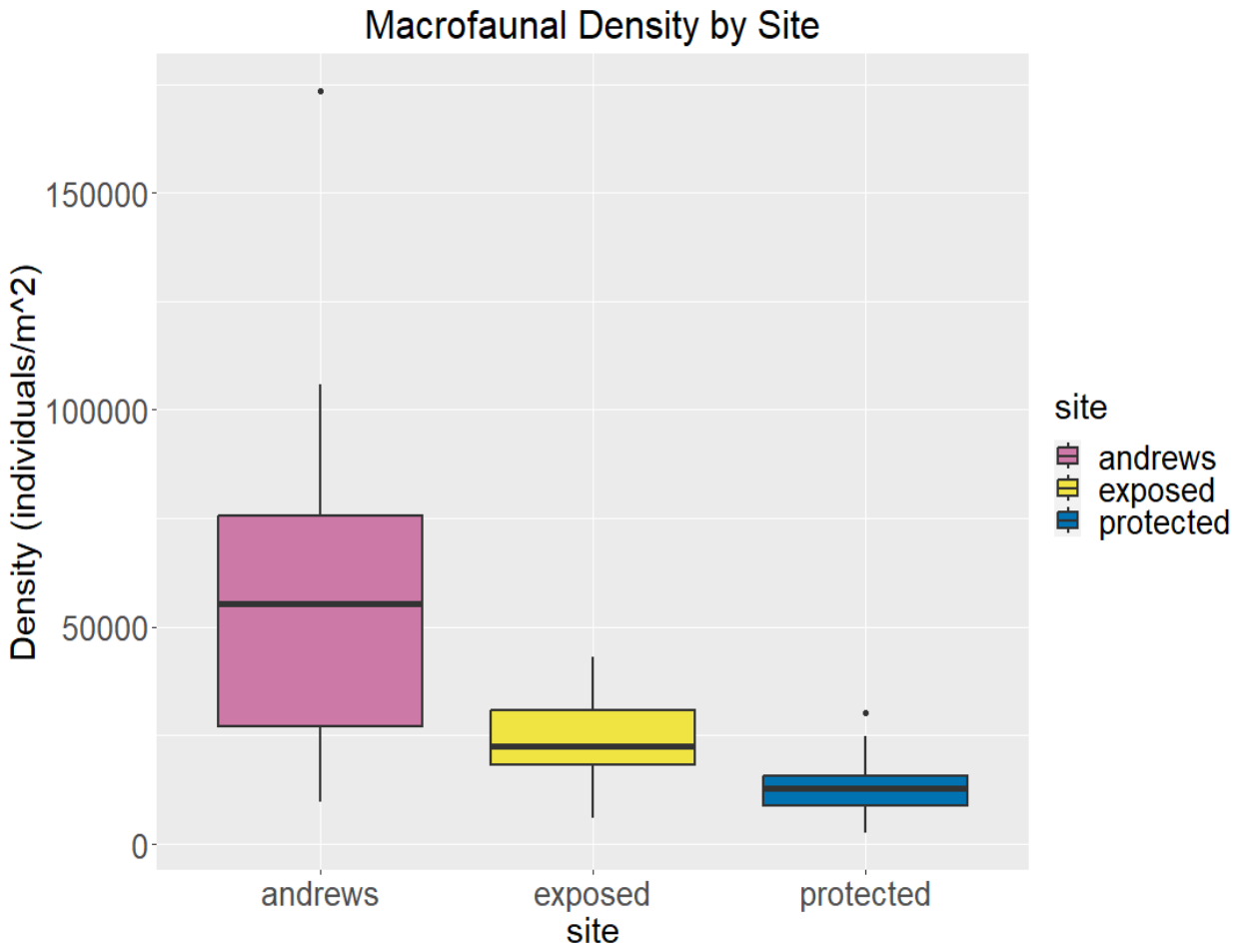

Figure 12: Macrofaunal community density by impact site in summer 2022. All numbers standardized to 1 m^2 of river bottom. The box represents the first and third quartile of the data while the central line represents the median. The vertical lines represent the full range of the data without outliers while dots represent outliers. Note that algae and oysters were not included.

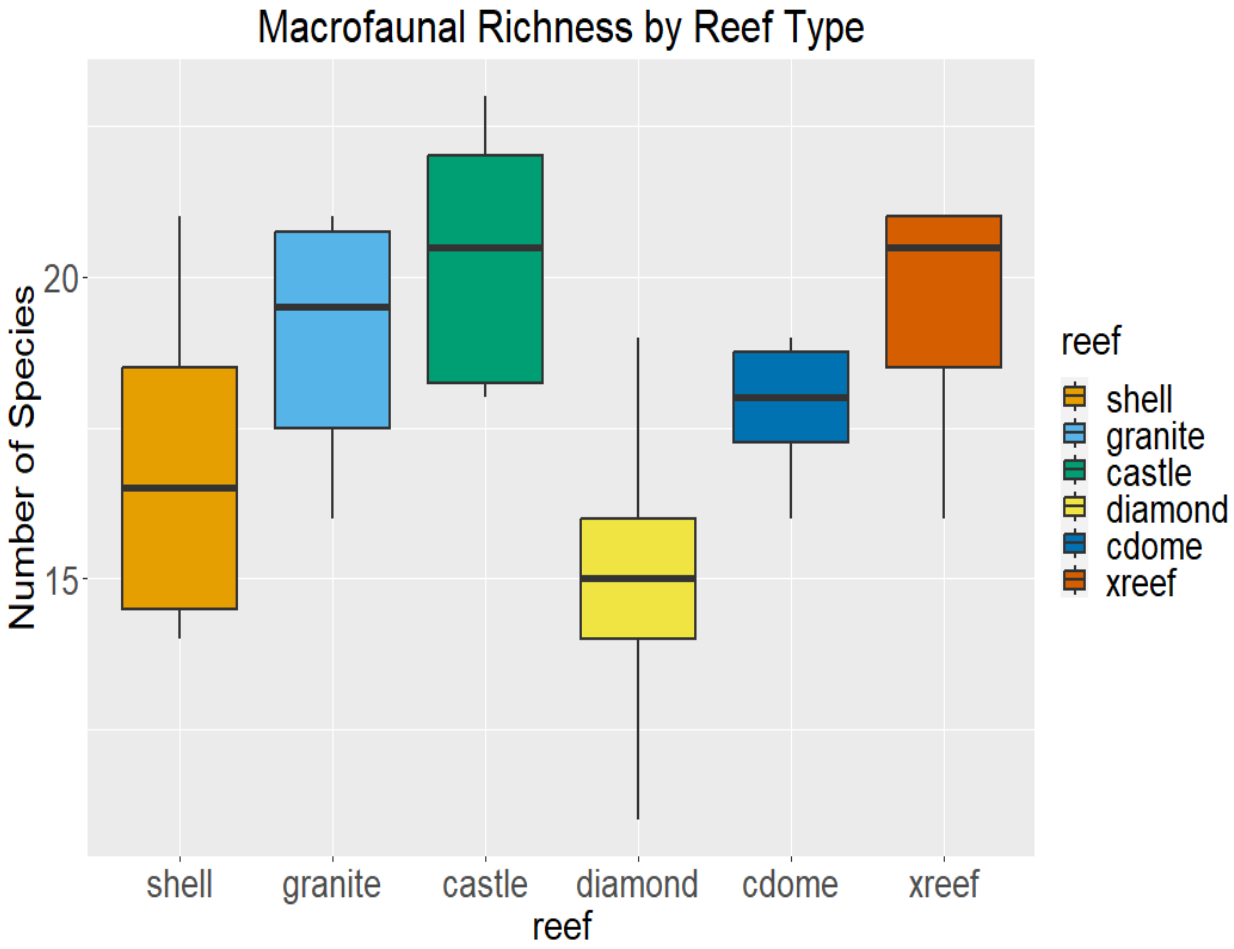

Figure 13: Macrofaunal community richness by reef type at the impact sites in summer 2022. The box represents the first and third quartile of the data while the central line represents the median. The vertical lines represent the full range of the data. Note that algae and oysters were not included.

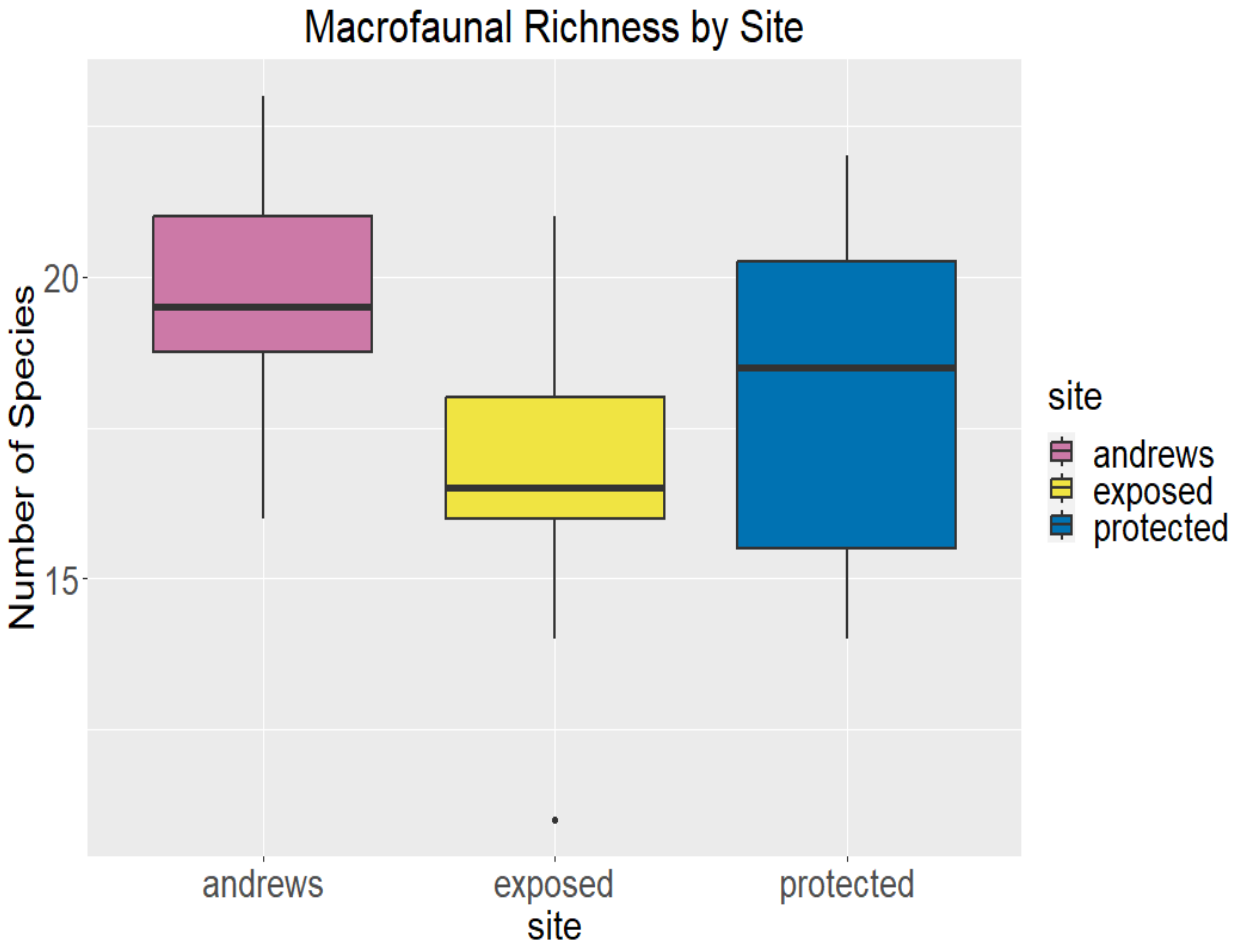

Figure 14: Macrofaunal community richness by impact site in summer 2022. The box represents the first and third quartile of the data while the central line represents the median. The vertical lines represent the full range of the data without outliers while dots represent outliers. Note that algae and oysters were not included.

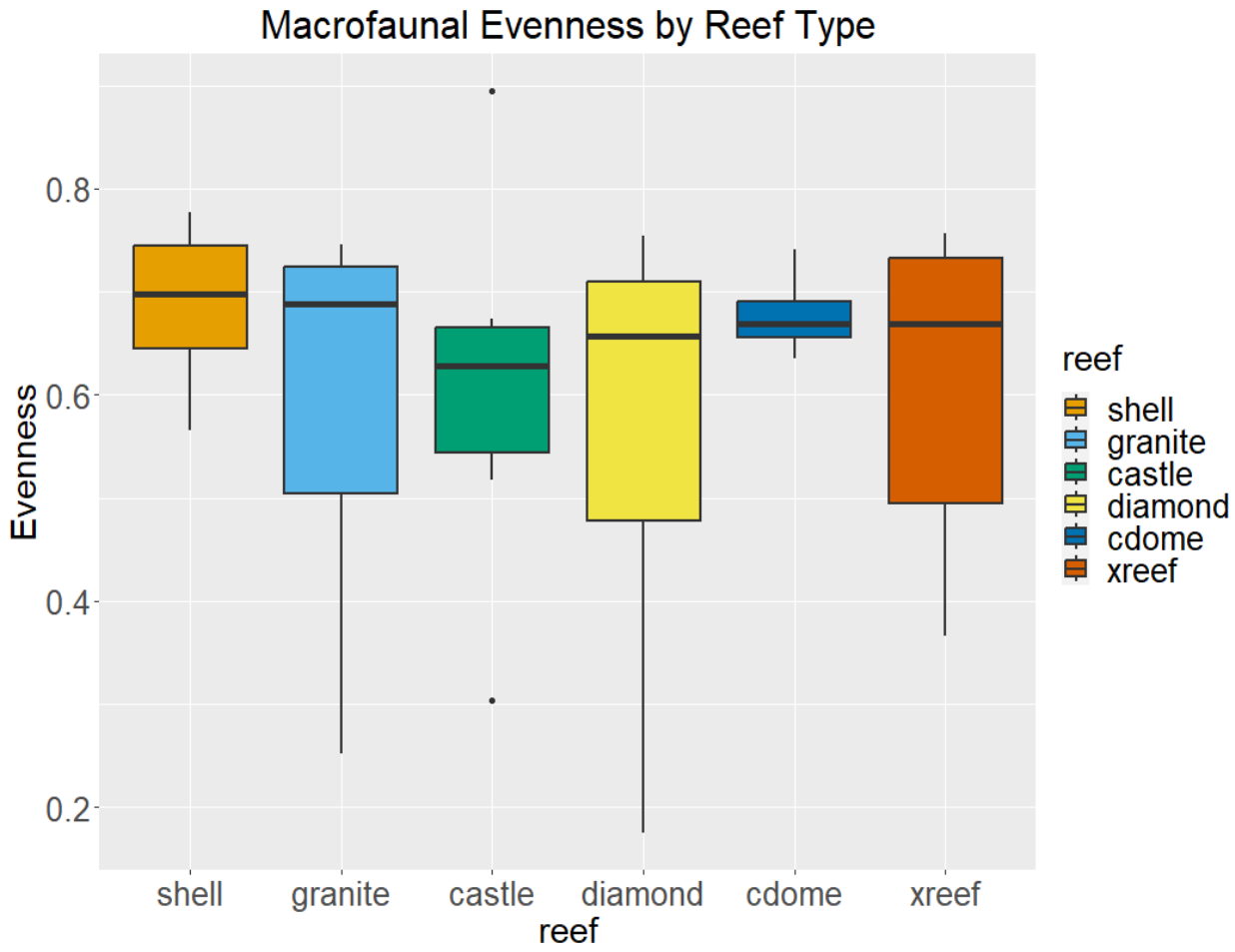

Figure 15: Macrofaunal community evenness by reef type at the impact sites in summer 2022. The box represents the first and third quartile of the data while the central line represents the median. The vertical lines represent the full range of the data without outliers while dots represent outliers. Note that algae and oysters were not included.

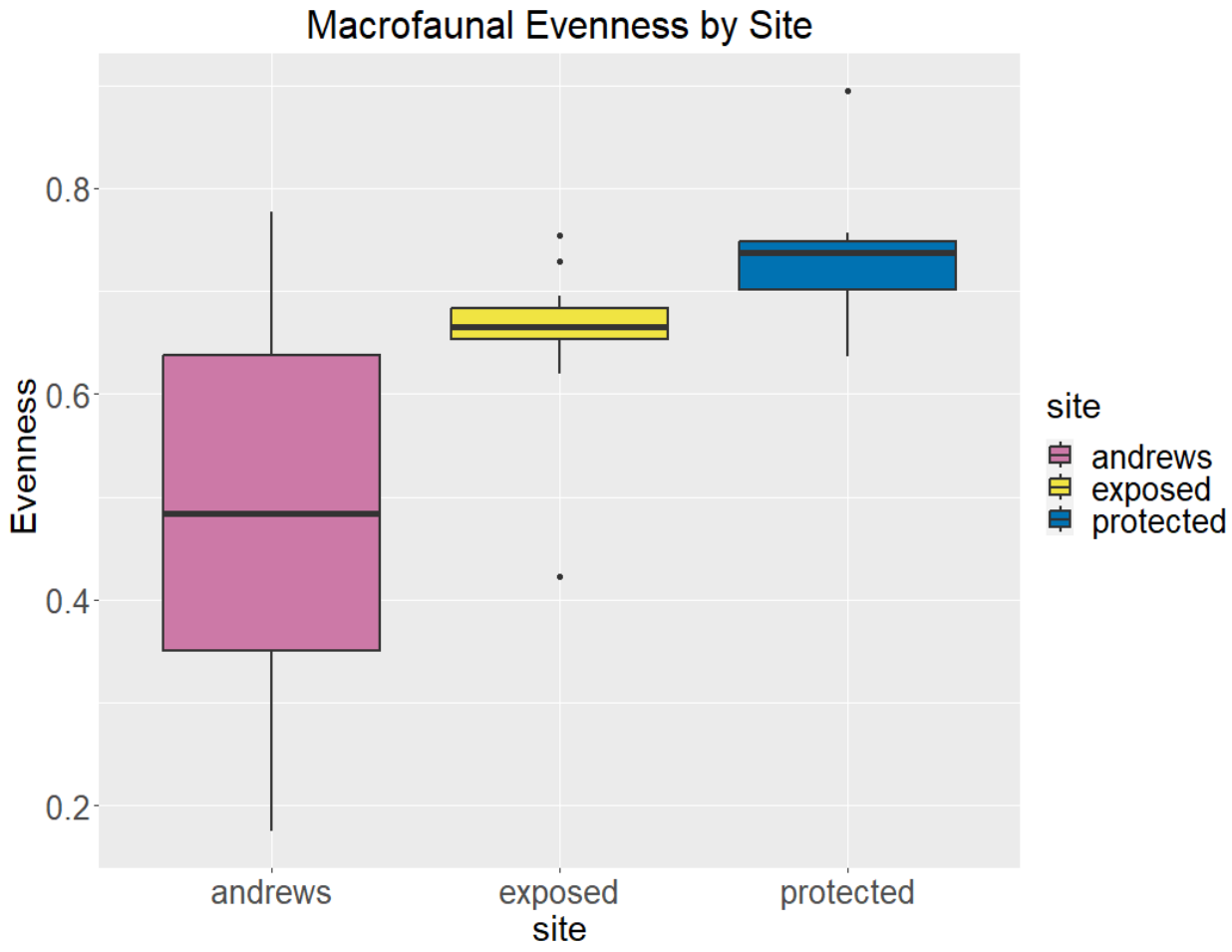

Figure 16: Macrofaunal community evenness by impact site in summer 2022. The box represents the first and third quartile of the data while the central line represents the median. The vertical lines represent the full range of the data without outliers while dots represent outliers. Note that algae and oysters were not included.

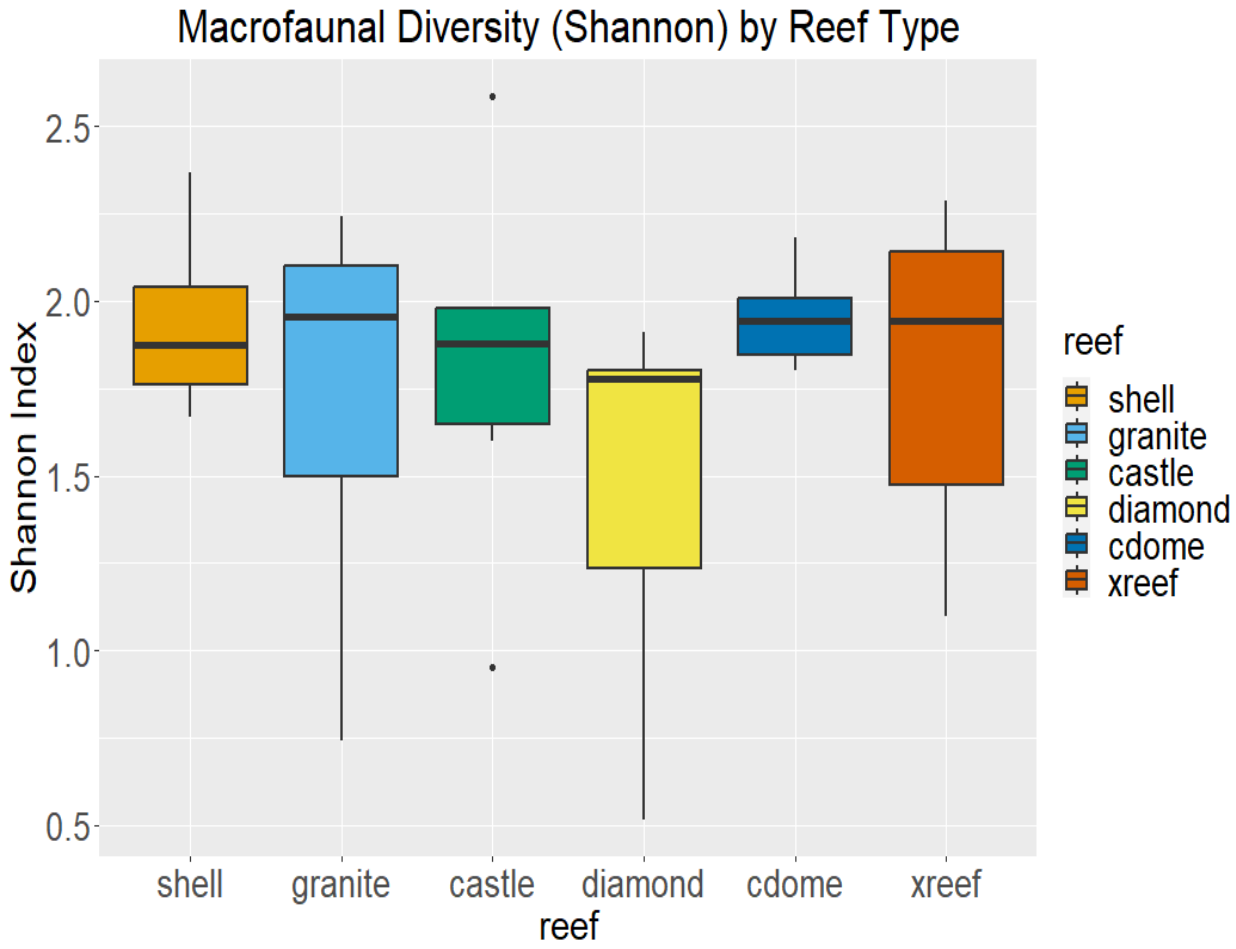

Figure 17: Macrofaunal community Shannon diversity by reef type at the impact sites in summer 2022. The box represents the first and third quartile of the data while the central line represents the median. The vertical lines represent the full range of the data without outliers while dots represent outliers. Note that algae and oysters were not included.

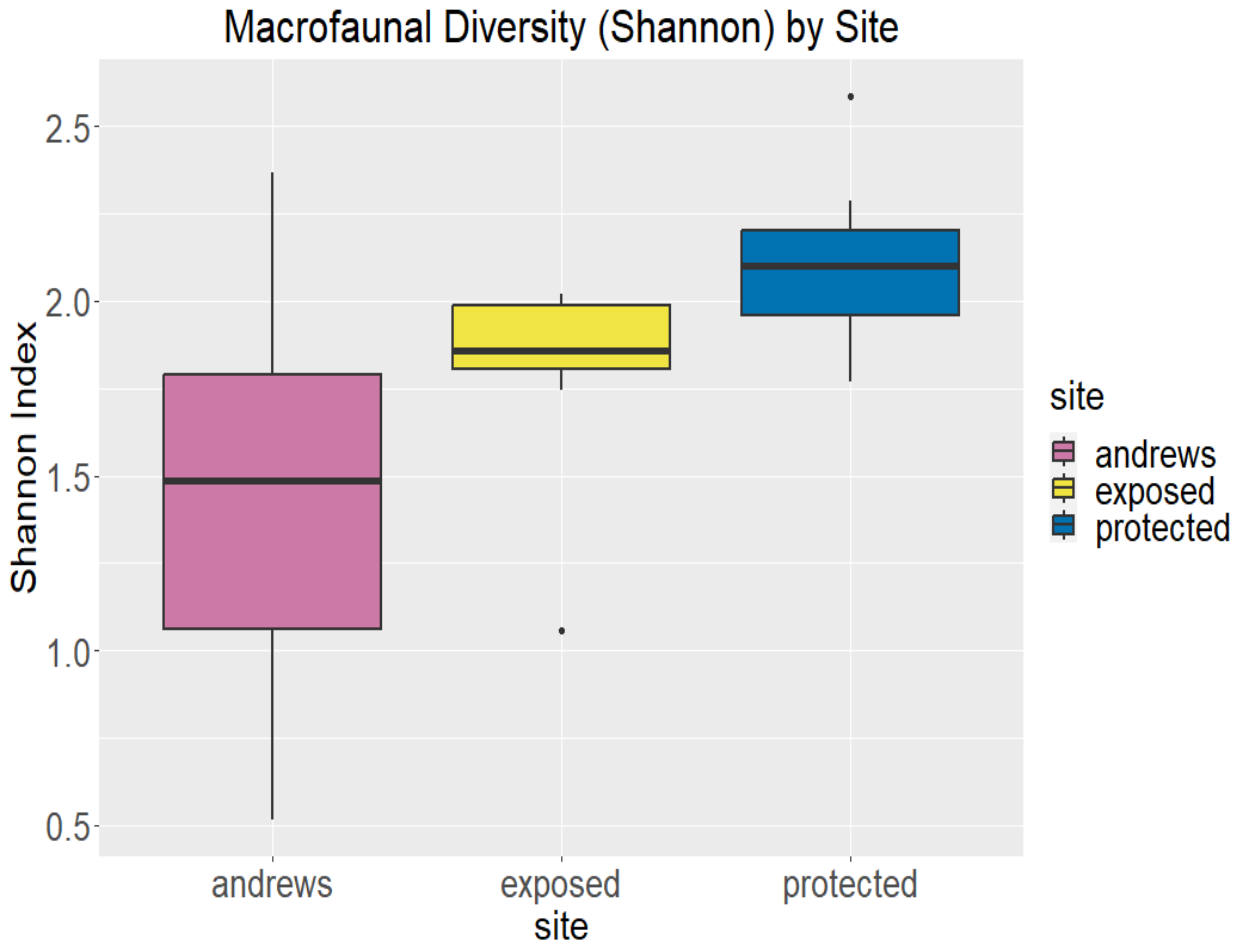

Figure 18: Macrofaunal community Shannon diversity by impact site in summer 2022. The box represents the first and third quartile of the data while the central line represents the median. The vertical lines represent the full range of the data without outliers while dots represent outliers. Note that algae and oysters were not included.

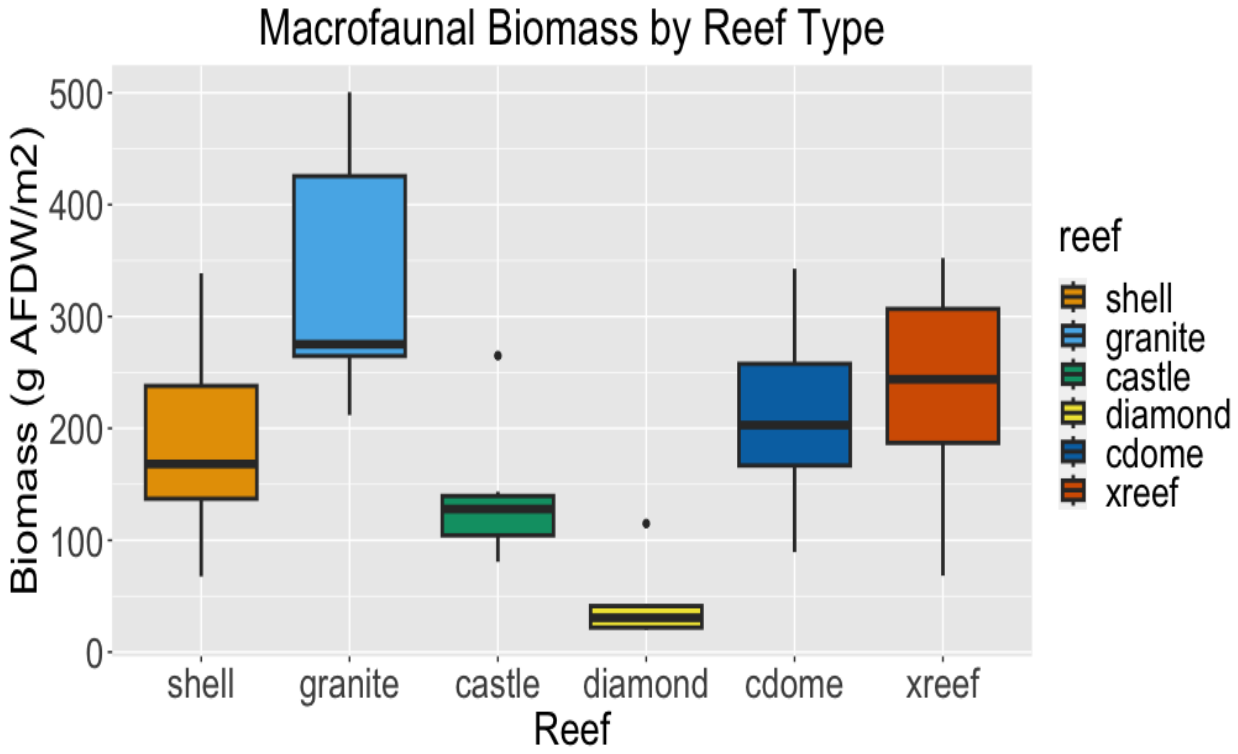

Figure 19: Macrofaunal community biomass (g AFDW) by reef type at the impact sites in summer 2022. All numbers standardized to 1 m^2 of river bottom. The box represents the first and third quartile of the data while the central line represents the median. The vertical lines represent the full range of the data without outliers while dots represent outliers. Note that oysters were not included.

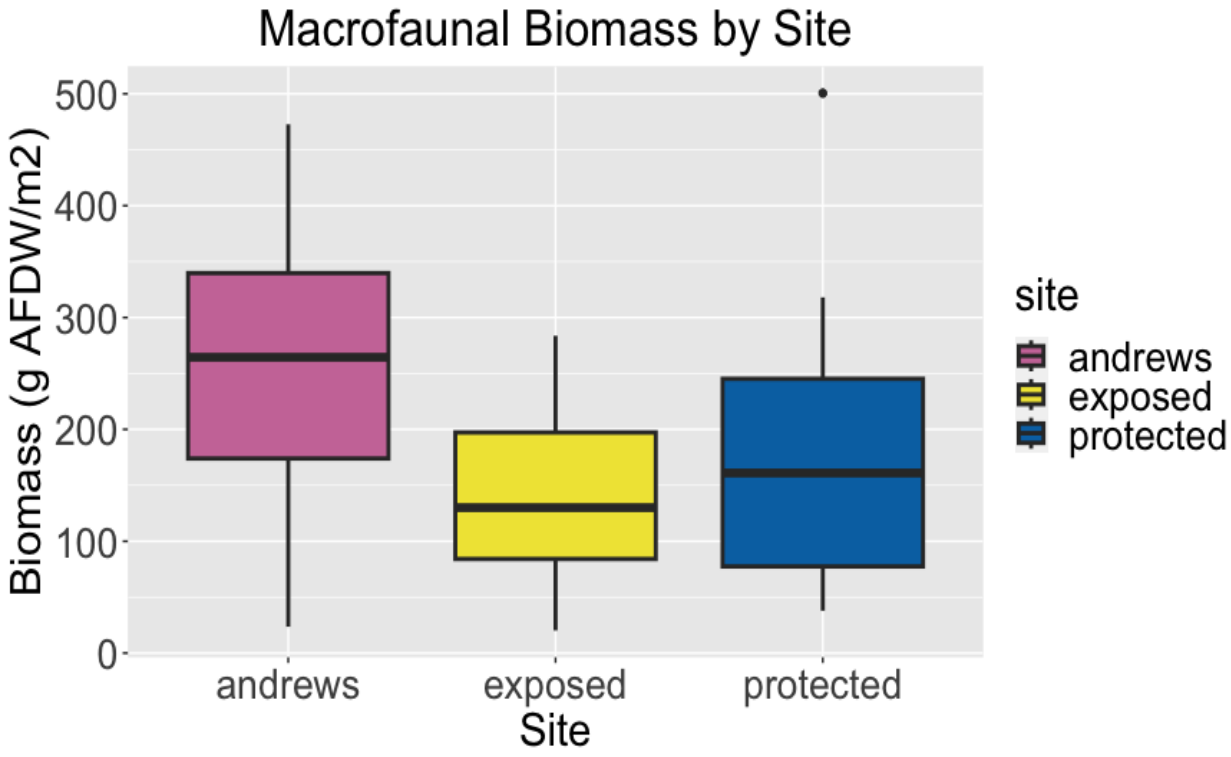

Figure 20: Macrofaunal community biomass (g AFDW) by impact site in summer 2022. All numbers standardized to 1 m^2 of river bottom. The box represents the first and third quartile of the data while the central line represents the median. The vertical lines represent the full range of the data without outliers while dots represent outliers. Note that all numbers are the square root of the actual values. Note that algae and oysters were not included.

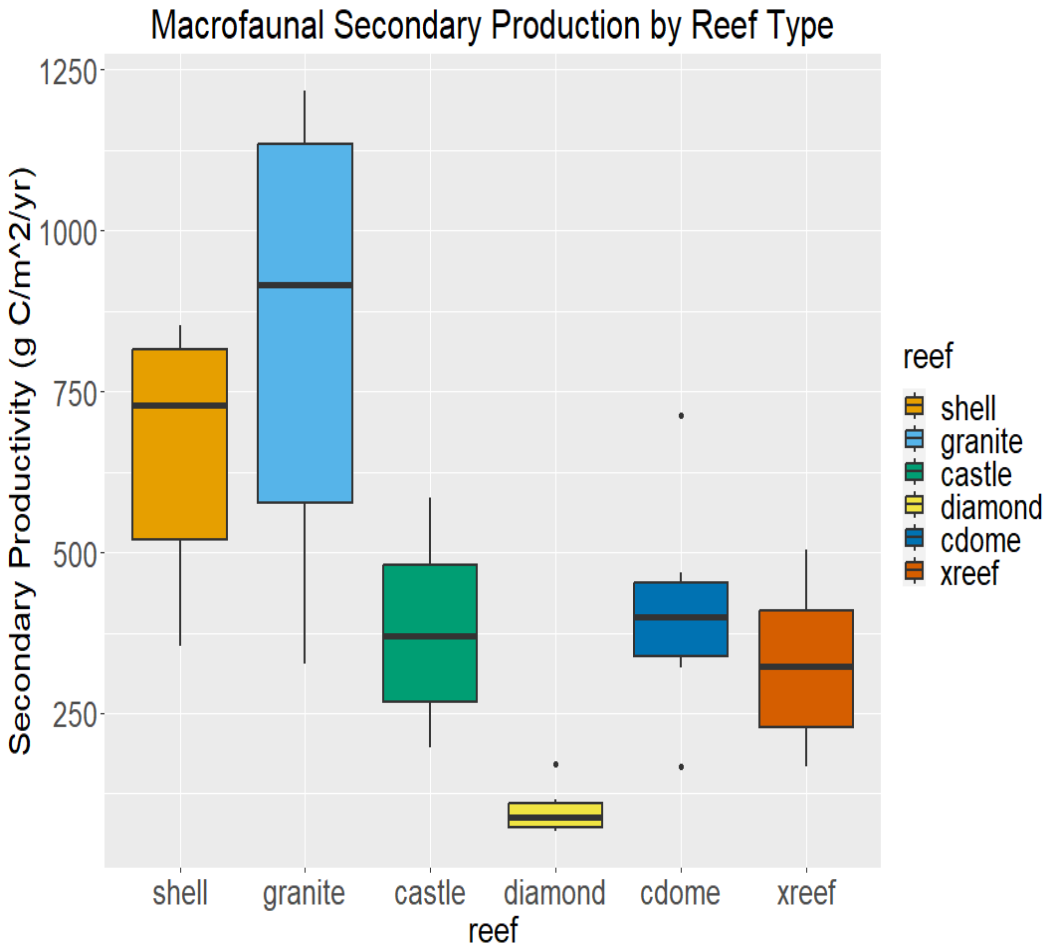

Figure 21: Macrofaunal community secondary productivity (g C/m^2/yr) by reef type at the impact sites in summer 2022. All numbers standardized to 1 m^2 of river bottom. The box represents the first and third quartile of the data while the central line represents the median. The vertical lines represent the full range of the data without outliers while dots represent outliers. Note that all numbers are the square root of the actual values and that algae and oysters were not included.

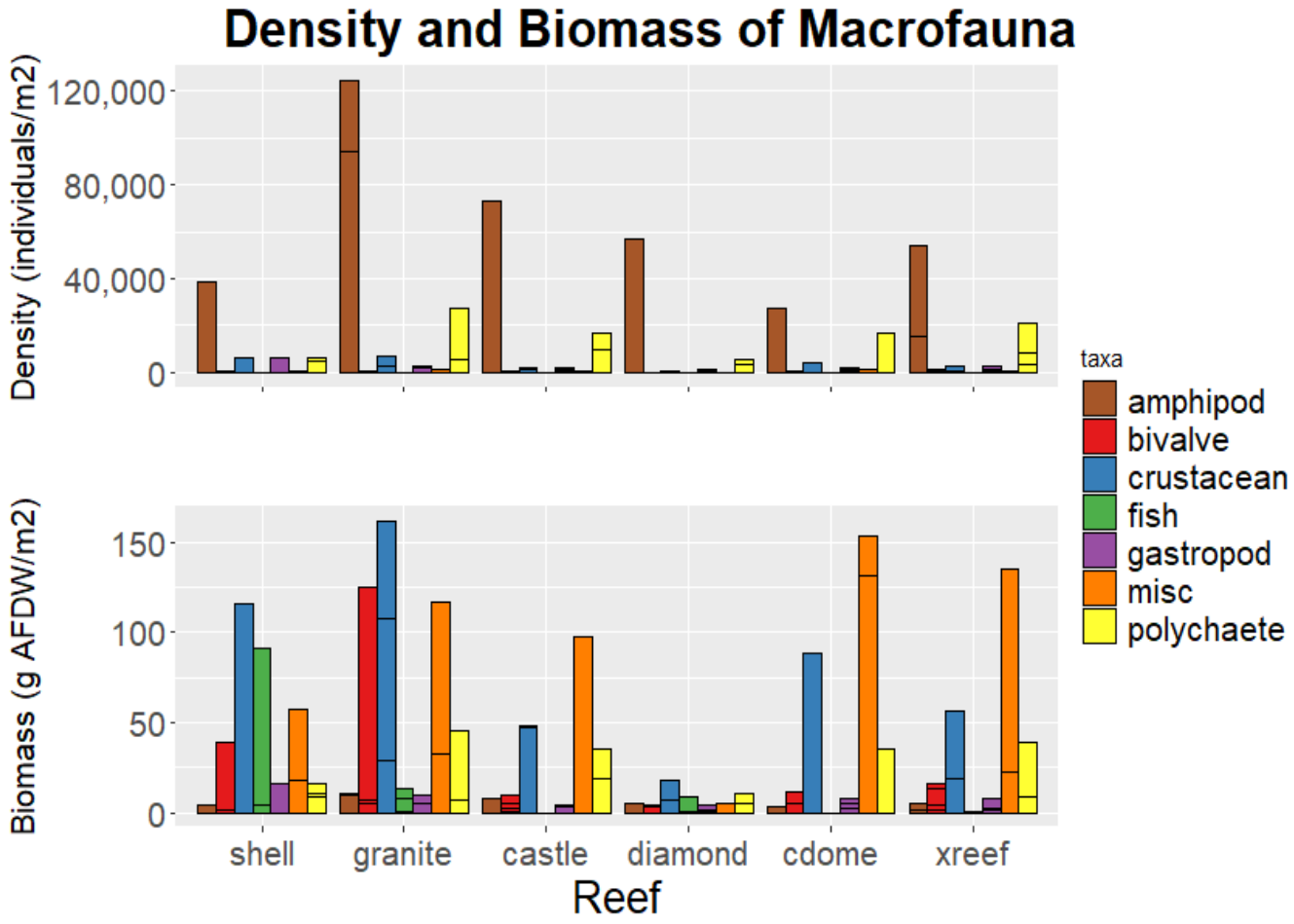

Figure 22: Density and biomass by species and reef type. The line breaks within each bar represent species within that taxonomic group. These are the raw densities and biomass numbers from the data standardized over 1 m^2. Note that these numbers do not include algae or oysters.

Multivariate Analyses

Looking at non-metric multidimensional scaling (nMDS) plots for community density (stress: 0.14), community composition tended to differ by reef type. The shell and granite reefs had a community composition that was more similar to each other than to any of the concrete-mix structures. Diamond reefs were generally different from other structures (Figure 23). Amphipods of the family Caprellidae drove differences in community density among the concrete-mix versus shell and granite structures (Figure 23), with high densities of amphipods on shell and granite reefs and low densities on the diamond reefs. Larger crustaceans, such as *Eurypanopeus depressus*, and tunicates (*Molgula manhattensis*) also had higher densities on the shell and granite reefs than on the concrete-mix structures. List of all of the species found and their proportions for density can be found in the appendix (Table S33; Figure S1).

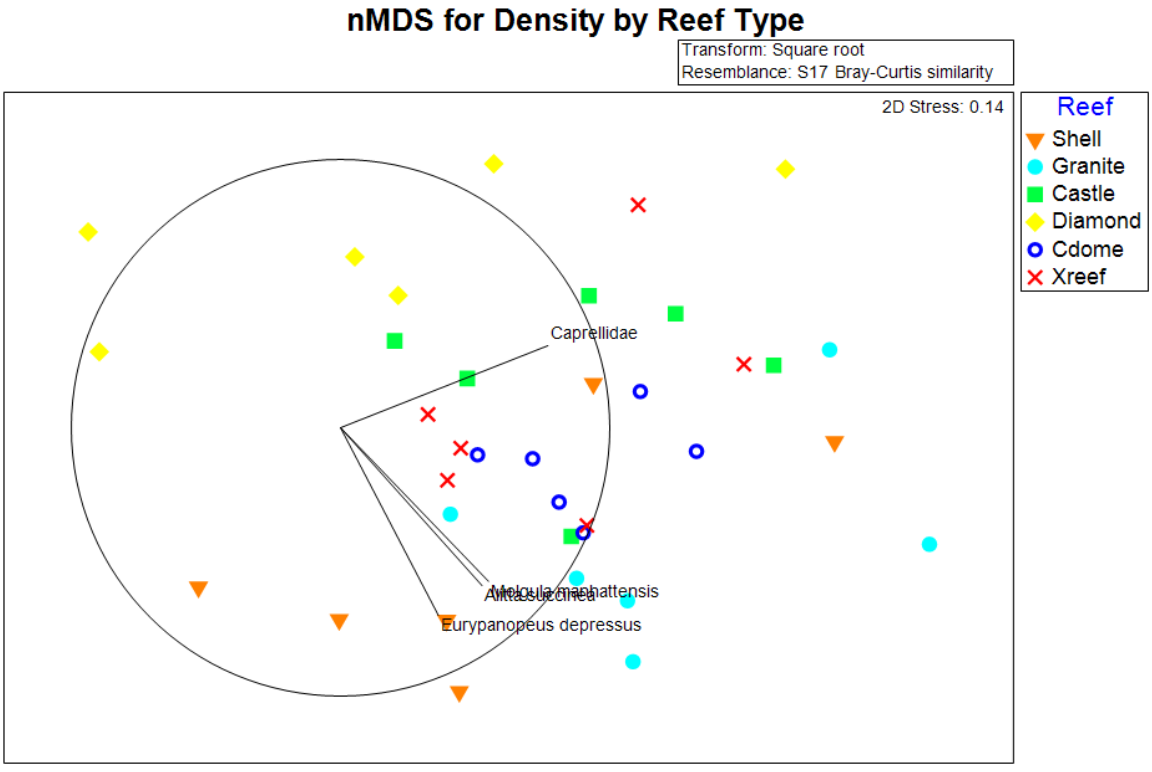

Figure 23: nMDS of square-root transformed community density in 2022 across all impact sites overlaid with the top four species driving community change based on a Pearson coefficient of 0.75.

In terms of biomass, the diamond reefs displayed different macrofaunal community structure than the other structures, as evidenced by a high degree of separation between these structures and any others (Figure 24; stress = 0.19). Amphipods of the family Caprellidae and gastropods, such as *Astyris lunata*, drove reef differences for biomass between the diamond structures and the other concrete-mix structures (Figure 24). Larger crustaceans, such as *Callinectus sapidus*, which have a high biomass on average, preferred the shell and granite reefs over the other structures. Full community composition proportions by biomass can be found in the appendix (Figure S2).

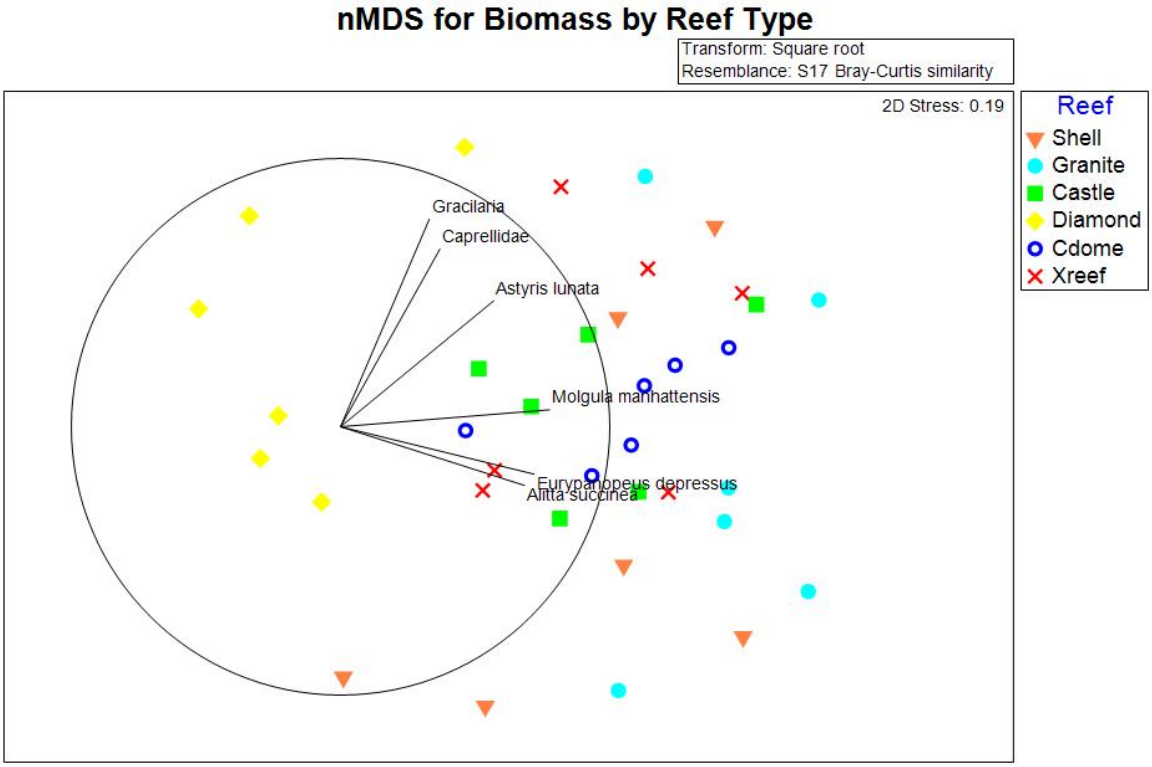

Figure 24: nMDS of square-root transformed community biomass in 2022 across all impact sites overlaid with the top 6 species driving community change based on a Pearson coefficient of 0.75. Note that algae was included in this analysis.

PERMANOVA revealed that both reef type and site had significant impacts on community assemblages for both density and biomass (Table 19). Looking closer at differences between community assemblages on reef types (Table 20), shell had significantly different community density assemblages to all other reef types. Diamond also significantly differed in community density assemblages from other reef types. For community assemblage by biomass, the shell significantly differed from all other structures except granite and diamond differed significantly from all structures. For both density and biomass, the c-dome and x-reef structures did not differ when it came to community structure.

Table 19: Summary of PERMANOVA results for community density and biomass across reef type and site. Significant results are in bold.

Source of Variation	df	SS	MS	Pseudo-F	P(perm)
Density					
Reef	5	11314	2262	6.659	**0.001**
Site	2	9946	4973	14.634	**0.001**
Reef x Site	10	3080	308	0.906	0.644
Residuals	18	6116	339		
Biomass					
Reef	5	14047	2810	4.251	**0.001**
Site	2	9643	4822	7.296	**0.001**
Reef x Site	10	6817	681	1.032	0.419
Residuals	18	11896	660		

Table 20: Summary of PERMANOVA pairwise comparisons for community density and biomass across reef type. Significant results are in bold. Note that numbers are square-root transformaed and use a Bray-Curtis similarity resemblance.

Groups	t	P(perm)	Unique perms
Density			
Shell, Granite	2.6533	**0.002**	989
Shell, Castle	2.7259	**0.004**	992
Shell, Diamond	3.1336	**0.002**	989
Shell, Cdome	3.0355	**0.001**	996
Shell, Xreef	2.6989	**0.004**	993
Granite, Castle	2.2279	**0.011**	994
Granite, Diamond	3.7243	**0.004**	996
Granite, Cdome	2.0217	**0.022**	995
Granite, Xreef	2.254	**0.02**	991
Castle, Diamond	2.3512	**0.005**	993
Castle, Cdome	1.2651	0.188	991
Castle, Xreef	0.7958	0.691	993
Diamond, Cdome	3.3585	**0.004**	991
Diamond, Xreef	2.5269	**0.012**	993
Cdome, Xreef	1.2196	0.215	995
Biomass			
Shell, Granite	1.4433	0.069	997
Shell, Castle	2.191	**0.007**	996
Shell, Diamond	2.7086	**0.005**	992
Shell, Cdome	2.2118	**0.004**	994
Shell, Xreef	1.9509	**0.005**	994
Granite, Castle	1.4915	0.075	994
Granite, Diamond	2.7893	**0.002**	993
Granite, Cdome	1.486	0.07	990
Granite, Xreef	1.406	0.102	993
Castle, Diamond	2.5519	**0.002**	994
Castle, Cdome	1.1502	0.3	990
Castle, Xreef	1.0618	0.382	994
Diamond, Cdome	2.966	**0.002**	995
Diamond, Xreef	2.3447	**0.008**	992
Cdome, Xreef	1.1213	0.324	991

5 Discussion

Key findings of this study include: (1) All reefs performed well for density and biomass at this subtidal area of the lower York River; (2) x-reefs performed just as well as shell reefs initially, but after a year, shell reefs had higher oyster densities and biomass than all structures; (3) after a year, granite had higher community biomass and secondary productivity than all other structures; and (4) after a year, all reefs had greater macrofaunal density, richness, diversity, biomass, and secondary productivity than bare sediment. Although shell reefs had the highest oyster density and biomass (9,852 oysters/m^2 and 743 g AFDW based on model estimates),the x-reefs performed very well both after a year, with oyster model-estimated densities of 3,816 oysters/m^2 river bottom.

Results suggest that the placement of hard substrate on a soft-sediment bottom in the York River can lead to denser, more diverse macrofaunal assemblages. The granite reefs had the highest secondary productivity overall, which should factor into future reef selection for this area if secondary productivity is a key goal.

5.1 Trends in Oyster Recruitment

Post-settlement survival is enhanced by factors such as vertical relief (Soniat et al., 2004), interstitial space to facilitate protection from predation and reduce competition (Lavan, 2019; Nestlerode et al., 2007), and the accessibility of oyster shell. For this reason, after one year, the shell reefs had overall higher densities of oysters than the granite and concrete-mix structures both after the fall 2021 sampling and after summer 2022 sampling. This is consistent with literature that shows that oyster shell is the preferred settlement substrate for spat (Nestlerode et al., 2007; Brumbaugh and Coen, 2009; Goelz et al., 2020). Although this structure was lacking in height at only 0.3 m off the bottom, it still exceeded the minimum height threshold to encourage oyster settlement (Colden et al., 2017). The x-reefs had the second highest oyster density because it combines several factors that can promote oyster settlement through extra space for settlement, internal space for protection from predation, and oyster shell (Table 2). Although most of the other

substrates had good oyster recruitment (mean oyster densities per unit river bottom) as well, the diamond substrate, with its sloping sides, did not have densities as high as the other substrates. This was likely because the shape of the structure encouraged sedimentation and sinking, decreasing the amount of substrate protruding into the water column and available for settlement, and suffocating already settled spat (Colden and Lipcius, 2015; Colden et al., 2017). In addition, the diamond reefs were generally shorter structures with less overall surface area leading to lower density per unit river bottom.

When examining recruitment by surface area (s.a.) on the concrete-mix substrates, the diamond structures only had a model-estimated 92.32 oysters/m^2 s.a. The diamond's drastic difference from the other structures when examined by both surface area of the structure and river bottom lends further support to the idea that the diamond's oyster settlement can be attributed to sedimentation through sinking (Colden and Lipcius, 2015; Colden et al., 2017). In future studies, structures that have sloped sides and hollow bottoms like the diamonds would likely perform better if they have support under the structure to prevent sinking. Materials such as geotextile cloth are sometimes used in oyster restoration, which generally prevents sinking of the restoration materials into the sediment (Stokes et al., 2012).

By surface area, other concrete-mix structures had between 808.21 individuals/m^2 s.a and 1,466.58 individuals/m^2 s.a with castles at the top of that range and c-domes at the bottom. The x-reefs had similar densities to the castles. Although the c-domes were constructed in a similar manner to the x-reef, with oyster shell embedded inside of concrete, and with vertical height and internal space, results indicate that the complexity design of castles and x-reefs provided to greater settlement area. The x-reefs had a large, open internal area that was partially sheltered by the legs and top, but allowed for good water flow and increased protection from predation. This could have led to optimal hydrodynamics through the structure, and allowed spat a place to settle and room to grow, unlike the c-domes (Nestlerode et al., 2007; Wheeler et al., 2015). The oyster castles, similarly were laid out in a way that had several small niches to enhance survival, because the structure had solid walls on all four sides, it also likely had decreased predation inside of the structures. The

structures that had higher complexity and most avaliable surface area for settlement could have also reduced the competition for space and access to resources and increased recruitment (Stachowicz and Byrnes, 2006). Surface area available on an oyster-restoration structure can impact oyster densities, thus, on structures where surface area can be easily measured, it could be used as a metric to measure oyster restoration success, in addition to the standard oysters per m^2 of river bottom (Sustainable Fisheries, 2011).

Oyster biomass was highest on both the shell substrate and the x-reef (743 g AFDW and 531 g AFDW respectively based on model estimates). The protected internal area of the x-reef likely allowed oysters to grow large without risk of mortality from predation, as occurred in previous studies that used artificial oyster settlement substrates, with intertidal castles accumulating up to 440 individuals/m^2 (Colden and Lipcius, 2015; Theuerkauf et al., 2015). Similar to reefs in previous studies, the x-reefs had greater vertical space than the other reefs tested, had a large surface area, were mostly elevated off the bottom, and offered complex environments which aided in protection of settled oysters. High oyster biomass on the shell reefs can be attributed to high densities of small oysters, as there were few large oysters (e.g., $>$ 50 mm) after one year. This may be caused by lack of space for the young spat to grow large in the shell baskets. Observational evidence during the study demonstrated that shell and granite baskets were also home to predators, such as mud crabs, that used the substrates as habitat, similar to what was seen in other studies (Bisker and Castagna, 1987; Grabowski, 2004). On the x-reef, although many oysters were small, three size cohorts were apparent, including several larger oysters ($>$ 50 mm SL) with high biomass. This same three-cohort pattern is found across the other three concrete-mix structure types and is absent from the shell and granite baskets, likely resulting from the limited room for growth that oysters have inside of densely-packed substrates in the shell and granite baskets (Lavan, 2019). The population size structure found on these reefs demonstrates the ability for artificial substrates in this area to host populations that are successful and persisting (Lipcius and Burke, 2018). In the Rappahannock River, artifical reefs have hosted oyster densities between 28 - 168 oysters/m^2 s.a.(Lipcius and Burke, 2018) compared to the 92.32 - 1,466.58 oysters/m^2 s.a. in this study. This

may be because the Rappahannock is farther up-Bay where larval supply might not be as high as in the lower York River.

For both oyster density and biomass, the protected site tended to have more success than the exposed and Andrews sites. Although there were no significant differences in sediment type among the sites, the Andrews and the exposed sites had higher water flow and likely wave energy than the protected sites. Constant exposure to a fast current and boat wakes around Gloucester Point could have led to lower oyster settlement at those two sites, as these hydrodynamic factors can lead to difficulty remaining on a structure during early stage spat settlement (Vozzo et al., 2021) and could lead to dislodgement of large oyster clumps over time. It should be noted that the impact sites for this study were located between or adjacent to many jetties that already had extant, thriving adult oyster populations. These oysters are large enough to be actively reproduce, and therefore can add additional larvae to the system. This may explain the extremely high settlement on these structures. Gloucester Point, the location of this study, is also a constriction point for the York River, causing levels of oyster population to reach historic numbers. Both the Andrews and exposed impact sites had high wave energy, but at the Andrews site, the current was moving toward the shore and breakwaters, pushing existing larvae into a cove and increasing the likelihood of settlement (Breitburg et al., 1995). Although high, these numbers are not unheard of in less harvested regions of the eastern U.S. In the 1970s, in unharvested sections of Georgia, densities were estimated to be about 14,666 oysters/m^2 (Bahr, 1974) and in South Carolina, one study found 4,400 oysters/m^2 (Dame, 1976). More recent studies in those regions still reflect those values with densities in Georgia in 2010 reaching 6,242 $\pm 670 individuals/m^2$(Manley et al., 2010). However, it should be noted that all studies with such high densities studied oyster populations in the intertidal. In this region, which is cooler than Georgia and South Carolina, the subtidal structures may have benefited oyster survival by allowing more time for feeding and less stress from desiccation (Bodenstein et al., 2021). Overall, all substrates had high enough oyster recruitment to support oyster reef communities that persisted over the one year of study.

5.2 Trends in Benthic Community Metrics

Reef substrates at the impact sites had higher density, richness, diversity, biomass, and secondary productivity than the bare-sediment control sites after a year of deployment. Reef structures provide one of the only hard substrates available in otherwise soft-sediment communities (Bertness et al., 2001). This availability of structure, along with the additional structure provided by the oysters that settled, led to high density, richness, and diversity of benthic organisms across taxonomic groups (bivalves, polychaetes, nemerteans, gastropods, crustaceans, amphipods, isopods, cnidarians, and chordates). The one metric that did not follow this trend, evenness, which was lower on reefs compared to soft-sediment controls, likely differed because amphipods, tube-building polychaetes from the Sabellidae family, and *Alitta succinea* dominated the reef structures. The soft-sediment control sites had a more even spread of organisms, including many burrowing clams, such as *Macoma balthica* and *Ameritella mitchelli*. Even with lower evenness at the impact vs. control sites, overall secondary productivity both with and without the oysters (BACI results) was extremely high at the impact sites, ranging from 345.85 to 654.46 g C/m^2/yr without oysters and 1258.59 to 2316.49 g C/m^2/yr with oysters. Including oysters, this exceeds the range of 467.3 to 853.7 g ash free dry mass (AFDM)/m^2/yr found in a previous North Carolina study also designed to test the effectiveness of artificial reefs in the local ecosystem (Wong et al., 2011). This suggests that oyster restoration using any of the substrates in this experiment would substantially increase in secondary productivity and thus food availability for higher trophic levels provided that reefs are placed in areas with similarly low productivity of bare sediments (as seen in this study), high natural oyster recruitment, and accessibility to larval supplies of species to generate similar productivity (Harding and Mann, 2001; Grabowski et al., 2005; Pfirrmann and Seitz, 2019). Biomass and secondary production can be used by higher trophic levels and lead to enhanced biomass of larger consumers within the community (Pfirrmann and Seitz, 2019).

Excluding oyster density, the granite structure had the highest macrofaunal organism density despite having significantly lower oyster density than the shell substrate, which may have been

because of reduced interstitial space for other macrofauna within the shell substrate once oysters had settled. Although interstitial space was not directly measured, from qualitative observations, the granite structure had larger spaces between the stones than the shell structure, which was tightly packed with shell. Although small interstitial spaces can serve to provide early post-settlement refuge to oysters from small predators (Nestlerode et al., 2007; Callaway, 2018), they can limit the quantity of other macrofauna since there is no room for larger organisms to settle or move through the structure. Most of the concrete-mix structures had similar macrofaunal community densities, with the exception of the diamond structure. Similar to mechanisms underlying the low oyster density on the diamond structures, this discrepancy was probably a result of sedimentation and sinking. For all structures, amphipods were found in high densities.

The overall higher densities of macrofaunal organisms at the Andrews site was driven by Caprellid amphipods that congregated en masse on the reef structures there. The structures at the Andrews and protected sites supported large amounts of algae, which created an ideal environment for amphipod families such as Caprellidae and Gammaridae (McCain, 1968; Fredette and Diaz, 1986; Murphy et al., 2021), although effects of algal biomass on amphipod abundance and biomass were not explicitly tested. Additionally, the Andrews site was downriver and partially protected on one side, which may have acted as a physical barrier for organisms or larvae that were swept into the Andrews site (Breitburg et al., 1995). They combined physical structure and increased water flow and could have led to increased macrofaunal settlement compared to the exposed and the protected sites, both of which were farther upriver and river-facing.

For diversity, the high richness on castle structures was likely the result of a combination of differing microhabitats, including the flat surfaces provided by the concrete and crushed shell and the creation of interstitial space provided by the stacking of the castles (Callaway, 2018). This internal space encouraged large oysters to grow, which attracted a large variety organisms to fill the habitat niches created by the variety of internal microhabitats and vertical complexity (Margiotta et al., 2016; Grabowski, 2004; Coen and Luckenbach, 2000). The increased surface are provided by this structure also could have led to reduced competition and facilitated increased richness (Stachowicz

and Byrnes, 2006). The granite and shell structures, although internally complex, failed to provide a consistent, flat structure for tube-building organisms, such as encrusting polychaetes, resulting in overall lower richness compared to the castle. In contrast, the diamond structures, which although concrete with embedded shell, were flat on all four sides and had no internal space, such that they did not create smaller niches to be filled. Unlike richness, evenness did not significantly differ among reef types; however, overall the reef structures had lower evenness compared to the control. Across all reef types, tube-building polychaete and amphipods dominated the community assemblages and reduced overall evenness on reefs. The high abundance and thus dominance of amphipods at the Andrews site led to lower evenness compared to the other two sites.

Although the Shannon diversity (with contributions from both richness and evenness) was significantly higher at the impact compared to control sites after a year, similar to evenness, the Shannon diversity among most reef types did not vary. One exception was that the diamonds had lower Shannon diversity than the other structures. This suggests that, for projects that focus on macrofaunal organism diversity as a measure of oyster reef success, a more nuanced approach to community measurements, such as examining richness and evenness separately, may be needed for at least the first year of monitoring a restored reef, especially as seen by the BACI analysis, richness was the primary driver of the difference in diversity between reef types. Diversity also differed by site, with the protected site having significantly higher Shannon diversity than the Andrews site. Again, the presence of algae and abundant amphipods at the Andrews site led to dominance of those species, reduced evenness, and therefore reduced Shannon diversity. As the protected site was sheltered from wave energy, it allowed multiple types of organisms to settle on the reefs and experience favorable growth conditions, and the community was not dominated by any one species. As competition leads to diversity to fill the available niches (Tilman, 2004; Stachowicz and Byrnes, 2006), it is no surprise that the protected site had higher overall Shannon diversity. The exposed site also had high diversity compared to the Andrews site. Because of the high water flow at the exposed site, the organisms were exposed to abundant food from the moving current (Palardy and Witman, 2011). This trend may not have been present at the Andrews site

because of the domination of the Andrews by macroalgae. Although this algae created habitat for amphipods, the early on-set biofouling at this site may have prohibited growth and settlement by other species.

High biomass and secondary productivity on the granite reef was largely driven by the mud crab populations that preferred the shelter and protected foraging habitat offered by the granite in their associated baskets. Mud crab species such as *Panopeus herbstii*, one of the main mud crab species collected in this study, can grow to be over 4 cm (Bisker and Castagna, 1987), and prefer structurally complex structures like riprap (Day and Lawton, 1988; Seitz et al., 2019). These large organisms have high biomass, and crustaceans have a high P/B ratio both of which are used to derive secondary production. The many large mud crabs led to granite's higher secondary productivity compared to the other five structures. Although the shell reef had biomass that was close to the c-dome and the x-reef, it also had many mud crabs, which brought its secondary productivity close to that of the granite, again, because crustaceans are weighed more heavily than other organisms in the P/B ratios (Diaz and Schaffner, 1990). Surprisingly, this structure also had the presence of large oyster toad fish *Opsanus tau*, which were found in both of the the basket structures. This could have influenced over all oyster recruitment and mesopredator populations through density- or trait-mediated effects (Grabowski, 2004).

One important factor to note that could have driven these community differences was the basket used for the shell and granite structures. These baskets were an additional barrier of protection for the macrofauna within and prevented predation of the benthic macrofauna and the oysters by higher tropic level organisms such as fish and large blue crabs that were external to the reef structure.

This study showed that both reef type and site can impact community assemblages (PERMANOVA). Most reefs differed from one another in terms of community density and biomass. All structures had densities and biomass that were higher than the diamond structure, likely because of the diamond sinking into the sediment. Community differences in the diamond and the granite reef were most likely driven by algal coverage on the diamond reef versus the granite (pers. obsv.). The flat surfaces of the diamond were quickly covered in *Gracilaria* sp. and *Ulva lactuca* by the on-

set of warmer spring temperatures. The granite reefs had higher tunicate (*Molgula manhattensis*) assemblages than the diamond because the large pockets of internal space offered by the granite offered protection for tunicates to grow without predation. In addition, the c-dome and the x-reef had similar community structure. Given the similar material composition and structural shape (tall with internal, protected space), this similarity is no surprise. These differences in community structure are important to understand how different materials impact a restored oyster reef community. Opportunistic species, like tunicates (Andrews, 1973), were dominant across most structures within the first year of reef restoration and the presence of larger, and more mobile species, such as mud crabs, can demonstrate how much a community can develop in a year.

5.3 Impact of Oysters on the Community

Live oyster densities directly correlate with benthic community density on oyster reefs with natural shell (Karp et al., 2018). Past studies also have specifically demonstrated positive relationships between mussel and oyster densities (Hadley et al., 2010; Colden and Lipcius, 2015; Karp et al., 2018). In this study, mussels were also found in greater quantities on alternative oyster reef substrates than on bare sediment. Oysters and mussels often fulfill a similar role in benthic communities (Gedan et al., 2014), as they are both ecosystem engineers that provide habitat for other organisms. Examining mussel density in comparison to oyster density can determine whether oyster restoration methods could also be beneficial to mussel restoration, and could additionally benefit communities. Live oysters on restored structures provide more surface area on which mussels can settle and the use of hard substrates, such as concrete, similarly allow for more availability of mussel settlement surfaces (Lipcius and Burke, 2006, 2018). Additionally, oyster reefs that have high oyster densities can result in a reduced water flow over reef structures, which can promote mussel settlement (Soniat et al., 2004) and provide mussels shelter from predation (Brown et al., 2011).

Similarly, this study showed an overall increase in macrofauna on oyster reef structures. As oysters form the basis of settlement for many filter feeding, sessile organisms and habitat for other,

small nektonic organisms, this was expected (Breitburg et al., 1995; Coen and Luckenbach, 2000; Grabowski and Peterson, 2007; Karp et al., 2018).

The implications of these findings show that there are many organisms that rely on natural shell and artificial oyster reefs within the York River. By restoring oyster populations in the York River, the communities that rely on oysters can also thrive. Oysters, along with the filter-feeding organisms their reefs provide shelter for, such as tunicates and mussels, can help increase water clarity (Dame, 1999; Steimle et al., 2002; Peterson et al., 2003). As reefs grow to host more organisms, they can also increase the secondary productivity of the area (Benke and Huryn, 2006). Additionally, as subtidal artificial reef structures like these grow to host more oyster cohorts, they can increase living hard substrate close to the shoreline and aid in protecting the coast from erosion (Scyphers et al., 2011; Chowdhury et al., 2019).

5.4 Implications for Restoration

As large-scale restoration projects often occur over many acres, using small structures like the one presented in this project may not be feasible due to logistics and cost. With the current restoration standards calling for oysters to cover 30 % of the target restoration area (Sustainable Fisheries, 2011), using many small individual structures may not be possible. However, the benefit of having multiple substrates is that they can often be used in conjunction with other substrates to address common issues like shell scarcity, transport logistics, and poaching prevention. Additionally, based on the goals of restoration for the area, a combination of substrates can be used to both increase oyster populations while utilizing some of the physical benefits of hard substrate such as erosion protection. For example, if it granite is more accessible and easier to deploy, it may be more effective to cover large areas of river bottom with granite while lining the intertidal with oyster castles. This would both set up 30 % the target restoration area for current macrofaunal habitat and future oyster recruitment while immediately protecting the shoreline from erosion.

There are 4 main takeaways from this study that have larger implications for oyster reef restoration in the York River.

1. The Chesapeake Bay Foundation's GIT restoration metrics (Sustainable Fisheries, 2011), "recommends that a mean density of 50 oysters/m^2 and 50 grams dry weight/m^2 containing at least two year classes, and covering at least 30% of the reef area provides a reasonable target operational goal for reef-level restoration." All of the reef structures examined in this study that didn't sink into the sediment met this goal with model-estimated mean values from 715 oysters/m^2 - 9,852 oysters/m^2. If hard substrate made of shell, granite, or a type of concrete mixed with shell is placed in the York River in a manner that prevents sinking into the sediment, a healthy oyster population and additional macrofaunal organisms will be present on the structure within a year. Therefore, alternative oyster reef substrate types are successful, viable alternatives to natural oyster shell in this system. Though previous studies have shown successful oyster recruitment on artificial substrates, (Soniat and Burton, 2005; Lipcius and Burke, 2006; Nestlerode et al., 2007; Dunn et al., 2014; La Peyre et al., 2015; Theuerkauf et al., 2015), this is the first to show the effectiveness of new concrete-mix structures compared to traditional substrates (shell, or oyster castles) and their high productivity in an area with high natural oyster recruitment.

2. The availability of natural shell may be reduced with future large-scale restoration projects in Chesapeake Bay and elsewhere (Goelz et al., 2020). The use of shell for restoration can also have drawbacks, such as sedimentation and burial, in certain ecosystems (La Peyre et al., 2015). Substrates that combine oyster shell with concrete can find logistical success in restoration projects. Additionally, concrete-mixes, which are a cheaper alternative to pure concrete, can save project managers the cost while providing the biological effectiveness of natural shell reefs (Bersoza Hernández et al., 2018). As seen by the c-domes and x-reefs, as long as the engineered concrete-mix structure has high vertical relief and interstitial space to avoid possible sedimentation, they could be a viable alternative to oyster shell reefs in this area. In a large-scale restoration project, these structures could be used intermittently in areas where poaching is common to both save money while still generating oyster recruitment.

3. The structures used in oyster reef restoration should be chosen based on long-term goals. As seen from the second part of this study, the long-term community structure does not always reflect trends in initial oyster densities, so metrics for first-year assessments should be adjusted according to the desired type of diversity (e.g., richness, Shannon diversity) or secondary productivity. Materials like granite can immediately provide hard structure on a soft-sediment bottom while promoting oyster settlement and being relatively easy to deploy on a large scale.

4. Oyster reef restoration whether with shell or alternative substrates can successfully increase initial oyster recruitment and benthic community growth compared to soft-sediment controls in the York River. More than a year of data is needed to better understand long-term impacts of artificial reef structures.

5.5 Recommendations for Future Studies

The controls were chosen to suit both the Gloucester Point sites used in this study as well as a site farther upriver at the Naval Weapons Station Yorktown, because this project was a smaller part of the larger restoration effort. In the future, controls could be selected closer to the impact sites to ensure similar environmental conditions and faunal communities. A 3-mm sieve was used for macrofaunal samples for the sake of time. In the future, a use of a smaller mesh size would give a better idea of the diversity and density of species seen at the controls and on the structures. Additionally, sample size for this project was small with only two reef types at each site-reef combination. The additive models fitted for this experiment only had 9 degrees of freedom and relatively low power. Given that there is a high chance of an interaction effect between site and reef when looking at oyster recruitment and biomass, for future studies, more replicates of reef structures would help better test the strength of this interaction effect.

6 Conclusions

Based on this study, oyster recruitment and benthic secondary productivity in the lower York River can be substantially enhanced by the deployment of alternative oyster reef structures. All of the structures tested had very high oyster recruitment and higher benthic macrofaunal densities and productivity than bare sand. The types of structures considered should be based on the predetermined metrics of restoration success for the chosen site. As all structures tested met the Chesapeake Bay Sustainable Fisheries GIT criteria for oyster restoration success, project managers and future studies could choose from a variety of successful oyster reef substrates based on goals for recruitment and secondary productivity, logistics, and cost effectiveness.

As oyster restoration projects work to increase oyster populations in and around the Chesapeake Bay based on management mandates to restore 10 Chesapeake Bay tributaries by 2025, alternative substrates can help increase oyster numbers during times when oyster shells are difficult to obtain. As shell has the potential to become scarce with declining oyster populations and large-scale restoration efforts, alternative substrates like the ones used in this study may increasingly help restore populations. They also have the added benefit of protecting coastlines and increasing the ecosystem services provided by oysters and their reef. An abundance of filter-feeders such as oysters, mussels, tunicates, and certain polychaetes, can lead to increased water quality which is often a goal of oyster restoration projects. Introducing hard substrate into soft-sediment communities can help provide habitat for macrofauna that rely on oysters, including species that are economically and biologically important to this area.

BIBLIOGRAPHY

Anderson, D.R., 2008. Model based inference in the life sciences: a primer on evidence. volume 31. Springer.

Anderson, M.J., 2001. A new method for non-parametric multivariate analysis of variance. Australian Ecology 26, 32–46.

Andrews, J.D., 1973. Effects of Tropical Storm Agnes on epifaunal invertebrates in Virginia estuaries. Chesapeake Science 14, 223–234.

Baggett, L.P., Powers, S.P., Brumbaugh, R.D., Coen, L.D., DeAngelis, B.M., Greene, J.K., Hancock, B.T., Morlock, S.M., Allen, B.L., Breitburg, D.L., et al., 2015. Guidelines for evaluating performance of oyster habitat restoration. Restoration Ecology 23, 737–745.

Bahr, L.M., 1974. Aspects of the structure and function of the intertidal oyster reef community in Georgia. University of Georgia.

Bahr, L.M., Lanier, W.P., 1981. The ecology of intertidal oyster reefs of the South Atlantic coast: a community profile. Technical Report FWS/OBS 81/15.

Beck, M.W., Brumbaugh, R.D., Airoldi, L., Carranza, A., Coen, L.D., Crawford, C., Defeo, O., Edgar, G.J., Hancock, B., Kay, M.C., et al., 2011. Oyster reefs at risk and recommendations for conservation, restoration, and management. Bioscience 61, 107–116.

Benke, A., Huryn, A., 2006. Secondary production of macroinvertebrates. In Methods in Stream Ecology, 2nd eds , 691–710.

Bersoza Hernández, A., Brumbaugh, R.D., Frederick, P., Grizzle, R., Luckenbach, M.W., Peterson, C.H., Angelini, C., 2018. Restoring the eastern oyster: how much progress has been made in 53 years? Frontiers in Ecology and the Environment 16, 463–471.

Bertness, M.D., Gaines, S.D., Hay, M.E., 2001. Marine community ecology. QH 541.5. S3. M369 2001, Sinauer Associates Sunderland, MA.

Bisker, R., Castagna, M., 1987. Predation on single spat oysters *Crassostrea virginica (Gmelin)* by blue crabs *Callinectes sapidus* Rathbun and mud crabs *Panopeus herbstii* milne-edwards. Journal of Shellfish Research 6, 37.

Blomberg, B.N., Palmer, T.A., Montagna, P.A., Pollack, J.B., 2018. Habitat assessment of a restored oyster reef in south Texas. Ecological Engineering 122, 48–61.

Bodenstein, S., Walton, W.C., Steury, T.D., 2021. Effect of farming practices on growth and mortality rates in triploid and diploid eastern oysters crassostrea virginica. Aquaculture Environment Interactions 13, 33–40.

Breitburg, D.L., Palmer, M.A., Loher, T., 1995. Larval distributions and the spatial patterns of settlement of an oyster reef fish: responses to flow and structure. Marine Ecology Progress Series 125, 45–60.

Brown, K.M., Aronhime, B., Wang, X., 2011. Predatory blue crabs induce byssal thread production in hooked mussels. Invertebrate biology 130, 43–48.

Brumbaugh, R.D., Coen, L.D., 2009. Contemporary approaches for small-scale oyster reef restoration to address substrate versus recruitment limitation: a review and comments relevant for the Olympia oyster, *Ostrea lurida* Carpenter 1864. Journal of Shellfish Research 28, 147–161.

Butler, P.A., 1954. Selective setting of oyster larvae on artificial cultch, in: Proceedings of the National Shellfisheries Association. By. National Shellfisheries Association, pp. 95–105.

Callaway, R., 2018. Interstitial space and trapped sediment drive benthic communities in artificial shell and rock reefs. Frontiers in Marine Science , 288.

Chamberlin, T.C., 1890. The method of multiple working hypotheses. Science 15, 92–96.

Chowdhury, M.S.N., Walles, B., Sharifuzzaman, S., Shahadat Hossain, M., Ysebaert, T., Smaal, A.C., 2019. Oyster breakwater reefs promote adjacent mudflat stability and salt marsh growth in a monsoon dominated subtropical coast. Scientific Reports 9, 1–12.

Coen, L., Brumbaugh, R., Bushek, D., Grizzle, R., Luckenbach, M., Posey, M., Powers, S., Tolley, S., 2007. Ecosystem services related to oyster restoration. Marine Ecology Progress Series 341, 323–343.

Coen, L.D., Humphries, A.T., 2017. Oyster-generated marine habitats: their services, enhancement, restoration and monitoring, in: Routledge handbook of ecological and environmental restoration. Routledge, pp. 274–294.

Coen, L.D., Luckenbach, M.W., 2000. Developing success criteria and goals for evaluating oyster reef restoration: ecological function or resource exploitation? Ecological engineering 15, 323–343.

Colden, A.M., Fall, K.A., Cartwright, G.M., Friedrichs, C.T., 2016. Sediment suspension and deposition across restored oyster reefs of varying orientation to flow: implications for restoration. Estuaries and Coasts 39, 1435–1448.

Colden, A.M., Latour, R.J., Lipcius, R.N., 2017. Reef height drives threshold dynamics of restored oyster reefs. Marine Ecology Progress Series 582, 1–13.

Colden, A.M., Lipcius, R.N., 2015. Lethal and sublethal effects of sediment burial on the eastern oyster *Crassostrea virginica*. Marine Ecology Progress Series 527, 105–117.

Crisp, D., 1967. Chemical factors inducing settlement in crassostrea virginica (gmelin). The Journal of Animal Ecology , 329–335.

Dame, R.F., 1976. Energy flow in an intertidal oyster population. Estuarine and Coastal Marine Science 4, 243–253.

Dame, R.F., 1999. Oyster reefs as components in estuarine nutrient cycling: Incidental or regulating. Technical Report. Oyster reef habitat restoration: a synopsis and synthesis of approaches. Edited by MW Luckenbach, R. Mann and JA Wesson. Virginia Institute of Marine Science Press.

Davenport, T.M., Seitz, R.D., Knick, K.E., Jackson, N., 2018. Living shorelines support nearshore benthic communities in upper and lower chesapeake bay. Estuaries and Coasts 41, 197–206.

Day, E., Lawton, P., 1988. Mud crab (crustacea: Brachyura: Xanthidae) substrate preference and activity. Journal of Shellfish Research 7, 421–426.

Diaz, R.J., Schaffner, L.C., 1990. The functional role of estuarine benthos. Perspectives on the Chesapeake Bay 1990, 25–56.

D'Itri, F.M., 2018. Artificial reefs: marine and freshwater applications (1st edition). CRC Press.

Dunn, R.P., Eggleston, D.B., Lindquist, N., 2014. Effects of substrate type on demographic rates of eastern oyster (*Crassostrea virginica*). Journal of Shellfish Research 33, 177–185.

Edgar, G.J., 1990. The use of the size structure of benthic macrofaunal communities to estimate faunal biomass and secondary production. Journal of Experimental Marine Biology and Ecology 137, 195–214.

Eggleston, D.B., Lipcius, R.N., Hines, A.H., 1992. Density-dependent predation by blue crabs upon infaunal clam species with contrasting distribution and abundance patterns. Marine Ecology Progress Series , 55–68.

Fan, C., Clark, K., Mclean, N., Bundy, M., 2020. The impacts of recycled concrete aggregate (rca) on epifaunal community structure and eastern oyster recruitment: Implication of using rca as bottom conditioning material for oyster restoration and aquaculture. Current Research in Environmental Sustainability 2, 100012.

Fredette, T.J., Diaz, R.J., 1986. Life history of gammarus mucronatus say (amphipoda: Gammaridae) in warm temperate estuarine habitats, York River, Virginia. Journal of Crustacean Biology 6, 57–78.

Friedrichs, C.T., 2009. York River physical oceanography and sediment transport. Journal of Coastal Research , 17–22.

Gedan, K.B., Kellogg, L., Breitburg, D.L., 2014. Accounting for multiple foundation species in oyster reef restoration benefits. Restoration ecology 22, 517–524.

George, L.M., De Santiago, K., Palmer, T.A., Beseres Pollack, J., 2015. Oyster reef restoration: effect of alternative substrates on oyster recruitment and nekton habitat use. Journal of Coastal Conservation 19, 13–22.

Gillett, D.J., Schaffner, L.C., 2009. Benthos of the York River. Journal of Coastal Research , 80–98.

Goelz, T., Vogt, B., Hartley, T., 2020. Alternative substrates used for oyster reef restoration: a review. Journal of Shellfish Research 39, 1–12.

Grabowski, J.H., 2004. Habitat complexity disrupts predator–prey interactions but not the trophic cascade on oyster reefs. Ecology 85, 995–1004.

Grabowski, J.H., Hughes, A.R., Kimbro, D.L., Dolan, M.A., 2005. How habitat setting influences restored oyster reef communities. Ecology 86, 1926–1935.

Grabowski, J.H., Peterson, C.H., 2007. Restoring oyster reefs to recover ecosystem services. Ecosystem engineers: Plants to Protists 4, 281–298.

Graham, P.M., Palmer, T.A., Beseres Pollack, J., 2017. Oyster reef restoration: substrate suitability may depend on specific restoration goals. Restoration Ecology 25, 459–470.

Hadley, N.H., Hodges, M., Wilber, D.H., Coen, L.D., 2010. Evaluating intertidal oyster reef development in south carolina using associated faunal indicators. Restoration Ecology 18, 691–701.

Harding, J.M., Mann, R.L., 2001. Oyster reefs as fish habitat: opportunistic use of restored reefs by transient fishes. Journal of Shellfish Research 20, 951.

Harwell, H.D., Posey, M.H., Alphin, T.D., 2011. Landscape aspects of oyster reefs: effects of fragmentation on habitat utilization. Journal of Experimental Marine Biology and Ecology 409, 30–41.

Haven, D.S., Morales-Alamo, R., 1966. Aspects of biodeposition by oysters and other invertebrate filter feeders 1. Limnology and Oceanography 11, 487–498.

Heinle, D., D'Elia, C., Wilson, J., Cole-Jones, M., Caplins, A., Cronin, L., 1980. Historical review of water quality and climatic data from Chesapeake Bay with emphasis on effects on enrichment. Technical Report. Chesapeake Bay Program, Environmental Protection Agency (Report No. EPA/600/3-82/083).

Héral, M., Rothschild, B.J., Goulletquer, P., 1990. Decline of oyster production in the Maryland portion of the Chesapeake Bay: Causes and perspectives, in: ICES meeting, Copenhagen (Denmark), 4-12 Oct 1990.

Hoellein, T.J., Zarnoch, C.B., Grizzle, R.E., 2015. Eastern oyster (*Crassostrea virginica*) filtration, biodeposition, and sediment nitrogen cycling at two oyster reefs with contrasting water quality in Great Bay Estuary (New Hampshire, USA). Biogeochemistry 122, 113–129.

Hueckel, G.J., Buckley, R.M., Benson, B.L., 1989. Mitigating rocky habitat loss using artificial reefs. Bulletin of Marine Science 44, 913–922.

Humphries, A.T., Ayvazian, S.G., Carey, J.C., Hancock, B.T., Grabbert, S., Cobb, D., Strobel, C.J.,

Fulweiler, R.W., 2016. Directly measured denitrification reveals oyster aquaculture and restored oyster reefs remove nitrogen at comparable high rates. Frontiers in Marine Science 3, 74.

Jud, Z.R., Layman, C.A., 2020. Changes in motile benthic faunal community structure following large-scale oyster reef restoration in a subtropical estuary. Food Webs 25, e00177.

Karp, M.A., Seitz, R.D., Fabrizio, M.C., 2018. Faunal communities on restored oyster reefs: effects of habitat complexity and environmental conditions. Marine Ecology Progress Series 590, 35–51.

Kellogg, M.L., Cornwell, J.C., Owens, M.S., Paynter, K.T., 2013. Denitrification and nutrient assimilation on a restored oyster reef. Marine Ecology Progress Series 480, 1–19.

Kellogg, M.L., Paynter, K.T., Ross, P.G., Dreyer, J.C., Turner, C., Pant, M., Birch, A., Smith, E., 2016. Integrated assessment of oyster reef ecosystem services: Macrofauna utilization of restored oyster reefs. Virginia Institute of Marine Science, William & Mary .

Kellogg, M.L., Smyth, A.R., Luckenbach, M.W., Carmichael, R.H., Brown, B.L., Cornwell, J.C., Piehler, M.F., Owens, M.S., Dalrymple, D.J., Higgins, C.B., 2014. Use of oysters to mitigate eutrophication in coastal waters. Estuarine, Coastal and Shelf Science 151, 156–168.

Koehl, M., Hadfield, M.G., 2010. Hydrodynamics of larval settlement from a larva's point of view. Integrative and Comparative Biology 50, 539–551.

La Peyre, M.K., Miller, L.S., Miller, S., Melancon, E., 2017. Comparison of oyster populations, shoreline protection service, and site characteristics at seven created fringing reefs in Louisiana: Key parameters and responses to consider, in: Living Shorelines. CRC Press, pp. 363–382.

La Peyre, M.K., Serra, K., Joyner, T.A., Humphries, A., 2015. Assessing shoreline exposure and oyster habitat suitability maximizes potential success for sustainable shoreline protection using restored oyster reefs. PeerJ 3, e1317.

Lavan, B., 2019. Examining the effect of interstitial space on eastern oysters (*Crassostrea virginica*): Applications of photogrammetry and three-dimensional modeling. JMU Scholarly Commons, Masters Thesis. 615 .

Lenth, R.V., 2022. emmeans: Estimated Marginal Means, aka Least-Squares Means. URL: `https://CRAN.R-project.org/package=emmeans`. r package version 1.7.3.

Lipcius, R., Burke, R.P., 2006. Abundance, biomass and size structure of eastern oyster and hooked mussel on a modular artificial reef in the Rappahannock River, Chesapeake Bay. Technical Report 390. Special Reports in Applied Marine Science and Ocean Engineering (SRAMSOE), Virginia Institute of Marine Science, William & Mary.

Lipcius, R.N., Burke, R.P., 2018. Successful recruitment, survival and long-term persistence of eastern oyster and hooked mussel on a subtidal, artificial restoration reef system in Chesapeake Bay. PloS One 13, e0204329.

Luckenbach, M.W., Coen, L.D., Ross Jr, P., Stephen, J.A., 2005. Oyster reef habitat restoration: relationships between oyster abundance and community development based on two studies in Virginia and South Carolina. Journal of Coastal Research , 64–78.

Luckenbach, M.W., Ross, P.G., 2003. An experimental evaluation of the effects of scale on oyster reef restoration .

Mackin, J.G., Owen, H.M., Collier, A., 1950. Preliminary note on the occurrence of a new protistan parasite, *Dermocystidium marinum* n. sp. in *Crassostrea virginica* (Gmelin). Science 111, 328–329.

Manley, J., Power, A., Walker, R., Hurley, D., Belcher, C., Richardson, J., 2010. Ecological succession on restored intertidal oyster habitat in the tidal creeks of coastal georgia. Journal of Shellfish Research 29, 917–926.

Mann, R., Powell, E.N., 2007. Why oyster restoration goals in the Chesapeake Bay are not and probably cannot be achieved. Journal of Shellfish Research 26, 905–917.

Margiotta, A.M., Shervette, V.R., Hadley, N.H., Plante, C.J., Wilber, D.H., 2016. Species-specific responses of resident crabs to vertical habitat complexity on intertidal oyster reefs. Journal of Experimental Marine Biology and Ecology 477, 7–13.

McArdle, B.H., Anderson, M.J., 2001. Fitting multivariate models to community data: a comment on distance-based redundancy analysis. Ecology 82, 290–297.

McCain, J.C., 1968. The Capreillidae (crustacea: Amphipoda) of the Western North Atlantic. Bulletin of the United States National Museum , 1–147.

Michener, W.K., Kenny, P.D., 1991. Spatial and temporal patterns of *Crassostrea virginica* (Gmelin) recruitment: relationship to scale and substratum. Journal of Experimental Marine Biology and Ecology 154, 97–121.

Molesky, T.J., 2003. Interactions between oyster reefs and adjacent sandflats: effects on microphytobenthos and sediment characteristics. Ph.D. thesis. University of North Carolina at Wilmington.

Murphy, C.E., Orth, R.J., Lefcheck, J.S., 2021. Habitat primarily structures seagrass epifaunal communities: a regional-scale assessment in the Chesapeake Bay. Estuaries and Coasts 44, 442–452.

Nestlerode, J.A., 2004. Evaluating restored oyster reefs in Chesapeake Bay: how habitat structure influences ecological function. Ph.D. thesis. William & Mary. Paper 1539616791.

Nestlerode, J.A., Luckenbach, M.W., O'Beirn, F.X., 2007. Settlement and survival of the oyster *Crassostrea virginica* on created oyster reef habitats in Chesapeake Bay. Restoration Ecology 15, 273–283.

Newell, R.I., 1988. Ecological changes in Chesapeake Bay: are they the result of overharvesting the American oyster, *Crassostrea virginica*? Understanding the estuary: advances in Chesapeake Bay research 129, 536–546.

Newell, R.I., Fisher, T.R., Holyoke, R.R., Cornwell, J.C., 2005. Influence of eastern oysters on nitrogen and phosphorus regeneration in Chesapeake Bay, USA, in: The comparative roles of suspension-feeders in ecosystems. Springer, pp. 93–120.

Palardy, J.E., Witman, J.D., 2011. Water flow drives biodiversity by mediating rarity in marine benthic communities. Ecology Letters 14, 63–68.

Peterson, C.H., Grabowski, J.H., Powers, S.P., 2003. Estimated enhancement of fish production resulting from restoring oyster reef habitat: quantitative valuation. Marine Ecology Progress Series 264, 249–264.

Pfirrmann, B.W., Seitz, R.D., 2019. Ecosystem services of restored oyster reefs in a Chesapeake Bay tributary: abundance and foraging of estuarine fishes. Marine Ecology Progress Series 628, 155–169.

Plumb, R.H., 1981. Procedures for handling and chemical analysis of sediment and water samples. Technical Report. State University of New York College at Buffalo Great Lakes Lab.

Reay, W.G., 2009. Water quality within the York River estuary. Journal of Coastal Research , 23–39.

Ridge, J.T., Rodriguez, A.B., Fodrie, F.J., 2017. Evidence of exceptional oyster-reef resilience to fluctuations in sea level. Ecology and Evolution 7, 10409–10420.

Ridge, J.T., Rodriguez, A.B., Joel Fodrie, F., Lindquist, N.L., Brodeur, M.C., Coleman, S.E., Grabowski, J.H., Theuerkauf, E.J., 2015. Maximizing oyster-reef growth supports green infrastructure with accelerating sea-level rise. Scientific Reports 5, 1–8.

Rodney, W.S., Paynter, K.T., 2006. Comparisons of macrofaunal assemblages on restored and non-restored oyster reefs in mesohaline regions of Chesapeake Bay in Maryland. Journal of Experimental Marine Biology and Ecology 335, 39–51.

Rodriguez, A.B., Fodrie, F.J., Ridge, J.T., Lindquist, N.L., Theuerkauf, E.J., Coleman, S.E., Grabowski, J.H., Brodeur, M.C., Gittman, R.K., Keller, D.A., et al., 2014. Oyster reefs can outpace sea-level rise. Nature Climate Change 4, 493–497.

Rothschild, B.J., Ault, J.S., Goulletquer, P., Héral, M., 1994. Decline of the Chesapeake Bay oyster population: a century of habitat destruction and overfishing. Marine Ecology Progress Series , 29–39.

Ruesink, J.L., Lenihan, H.S., Trimble, A.C., Heiman, K.W., Micheli, F., Byers, J.E., Kay, M.C., 2005. Introduction of non-native oysters: ecosystem effects and restoration implications. Annual Review of Ecology, Evolution, and Systematics 36, 643–689.

Rutledge, K.M., Alphin, T., Posey, M., 2018. Fish utilization of created vs. natural oyster reefs (*Crassostrea virginica*). Estuaries and Coasts 41, 2426–2432.

Schulte, D.M., 2017. History of the Virginia oyster fishery, Chesapeake Bay, USA. Frontiers in Marine Science 4, 127.

Schulte, D.M., Burke, R.P., Lipcius, R.N., 2009. Unprecedented restoration of a native oyster metapopulation. Science 325, 1124–1128.

Scyphers, S.B., Powers, S.P., Heck Jr, K.L., Byron, D., 2011. Oyster reefs as natural breakwaters mitigate shoreline loss and facilitate fisheries. PloS One 6, e22396.

Sedano, F., Navarro-Barranco, C., Guerra-García, J., Espinosa, F., 2020. Understanding the effects of coastal defence structures on marine biota: The role of substrate composition and roughness in structuring sessile, macro-and meiofaunal communities. Marine Pollution Bulletin 157, 111334.

Seitz, R.D., Aguilera, S., Wood, M.A., Lipcius, R.N., 2019. Production and vertical distribution of invertebrates on rip rap shorelines in Chesapeake Bay: A novel rocky intertidal habitat. Estuarine, Coastal and Shelf Science 228, 106357.

Shipp, R.L., 1999. The artificial reef debate: Are we asking the wrong questions? Gulf of Mexico Science 17, 6.

Soniat, T.M., Broadhurst, R.C., Haywood, E., 1991. Alternatives to clam shell as cultch for oysters and the use of gypsum for the production of cultchless oysters. Journal of Shellfish Research 10, 405–410.

Soniat, T.M., Burton, G.M., 2005. A comparison of the effectiveness of sandstone and limestone as cultch for oysters, *Crassostrea virginica*. Journal of Shellfish Research 24, 483–485.

Soniat, T.M., Finelli, C.M., Ruiz, J.T., 2004. Vertical structure and predator refuge mediate oyster reef development and community dynamics. Journal of Experimental Marine Biology and Ecology 310, 163–182.

Stachowicz, J.J., Byrnes, J.E., 2006. Species diversity, invasion success, and ecosystem functioning: disentangling the influence of resource competition, facilitation, and extrinsic factors. Marine Ecology Progress Series 311, 251–262.

Steimle, F., Foster, K., Kropp, R., Conlin, B., 2002. Benthic macrofauna productivity enhancement by an artificial reef in Delaware Bay, USA. ICES Journal of Marine Science 59, S100–S105.

Stokes, S., Wunderink, S., Lowe, M., Gereffi, G., 2012. Restoring Gulf Oyster Reefs. Technical Report. Environmental Defense Fund.

Stricklin, A.G., Peterson, M.S., Lopez, J.D., May, C.A., Mohrman, C.F., Woodrey, M.S., 2010. Do small, patchy, constructed intertidal oyster reefs reduce salt marsh erosion as well as natural reefs? Gulf and Caribbean Research 22, 21–27.

Stunz, G.W., Minello, T.J., Rozas, L.P., 2010. Relative value of oyster reef as habitat for estuarine nekton in Galveston Bay, Texas. Marine Ecology Progress Series 406, 147–159.

Sustainable Fisheries, G.I.T., 2011. Restoration Goals, Quantitative Metrics, and Assessment Protocols for Evaluating Success on Restored Oyster Reef Sanctuaries. Technical Report.

Taylor, J., Bushek, D., 2008. Intertidal oyster reefs can persist and function in a temperate North American Atlantic estuary. Marine Ecology Progress Series 361, 301–306.

Theuerkauf, S.J., Burke, R.P., Lipcius, R.N., 2015. Settlement, growth, and survival of eastern oysters on alternative reef substrates. Journal of Shellfish Research 34, 241–250.

Tilman, D., 2004. Niche tradeoffs, neutrality, and community structure: a stochastic theory of resource competition, invasion, and community assembly. Proceedings of the National Academy of Sciences 101, 10854–10861.

Underwood, A., 1992. Beyond BACI: the detection of environmental impacts on populations in the real, but variable, world. Journal of Experimental Marine Biology and Ecology 161, 145–178.

Underwood, A., Chapman, M., 2003. Power, precaution, type II error and sampling design in assessment of environmental impacts. Journal of Experimental Marine Biology and Ecology 296, 49–70.

Vozzo, M.L., Cumbo, V.R., Crosswell, J.R., Bishop, M.J., 2021. Wave energy alters biodiversity by shaping intraspecific traits of a habitat-forming species. Oikos 130, 52–65.

Wall, L.M., Walters, L.J., Grizzle, R.E., Sacks, P.E., 2005. Recreational boating activity and its impact on the recruitment and survival of the oyster *Crassostrea virginica* on intertidal reefs in Mosquito Lagoon, Florida. Journal of Shellfish Research 24, 965–973.

Wentworth, C.K., 1922. A scale of grade and class terms for clastic sediments. The Journal of Geology 30, 377–392.

Wheeler, J.D., Helfrich, K.R., Anderson, E.J., Mullineaux, L.S., 2015. Isolating the hydrodynamic triggers of the dive response in eastern oyster larvae. Limnology and Oceanography 60, 1332–1343.

Wiberg, P.L., Taube, S.R., Ferguson, A.E., Kremer, M.R., Reidenbach, M.A., 2019. Wave attenuation by oyster reefs in shallow coastal bays. Estuaries and Coasts 42, 331–347.

Wilberg, M.J., Livings, M.E., Barkman, J.S., Morris, B.T., Robinson, J.M., 2011. Overfishing, disease, habitat loss, and potential extirpation of oysters in upper Chesapeake Bay. Marine Ecology Progress Series 436, 131–144.

Wong, M.C., Peterson, C.H., Piehler, M.F., 2011. Evaluating estuarine habitats using secondary production as a proxy for food web support. Marine Ecology Progress Series 440, 11–25.

Wood, J.L., Andrews, J.D., 1962. *Haplosporidium costale* (Sporozoa) associated with a disease of Virginia oysters. Science 136, 710–711.

Supplementary Material

Tables

Table S1: Means of the reef types for the generalized linear negative binomial model m_f4 for oyster density in fall 2021 standardized to 1 m^2 of river bottom. Note that these means are derived from an emmeans analysis that was performed on m_f4. SE = standard error; df = degrees of freedom; asymp.LCL = asymptotic lower confidence level; asymp.UCL = asymptotic upper confidence level.

Reef Type	Response	SE	df	asymp.LCL	asymp.UCL
shell	16721.22	4220.08	Inf	10196.31	27421.62
granite	2668.02	676.54	Inf	1623.10	4385.64
castle	1440.98	364.30	Inf	877.94	2365.11
diamond	825.43	209.40	Inf	502.04	1357.11
c-dome	6515.85	1644.91	Inf	3972.71	10686.97
x-reef	10530.63	2656.74	Inf	6422.55	17266.37

Results are averaged over the levels of: site

Table S2: Pairwise comparisons between reef types for the generalized linear negative binomial model m_f4 for oyster density in fall 2021. All numbers are standardized to m^2 of river bottom. Note that these comparisons are derived from the emmeans for this model. SE = standard error; df = degrees of freedom.

Contrast	Ratio	SE	df	z.ratio	p.value
granite - shell	0.16	0.06	Inf	-5.13	<0.01
castle - shell	0.09	0.03	Inf	-6.86	<0.01
castle - granite	0.54	0.19	Inf	-1.72	0.52
diamond - shell	0.05	0.02	Inf	-8.41	<0.01
diamond - granite	0.31	0.11	Inf	-3.27	0.01
diamond - castle	0.57	0.21	Inf	-1.56	0.63
c-dome - shell	0.39	0.14	Inf	-2.64	0.09
c-dome - granite	2.44	0.87	Inf	2.50	0.13
c-dome - castle	4.52	1.62	Inf	4.22	<0.01
c-dome - diamond	7.89	2.83	Inf	5.77	<0.01
x-reef - shell	0.63	0.22	Inf	-1.30	0.79
x-reef - granite	3.95	1.41	Inf	3.84	<0.01
x-reef - castle	7.31	2.61	Inf	5.57	<0.01
x-reef - diamond	12.76	4.56	Inf	7.12	<0.01
x-reef - c-dome	1.62	0.58	Inf	1.35	0.76

Results are averaged over the levels of: site

Table S3: Pairwise comparisons between impact sites for the generalized linear negative binomial model m_f4 for oyster density in fall 2021. All numbers are standardized to m^2 of river bottom. Note that these comparisons are derived from the emmeans for this model. SE = standard error; df = degrees of freedom.

Contrast	Ratio	SE	df	z.ratio	p.value
exposed - andrews	0.62	0.16	Inf	-1.86	0.15
protected - andrews	1.57	0.40	Inf	1.79	0.17
protected - exposed	2.52	0.64	Inf	3.65	<0.01

Results are averaged over the levels of: reef

Table S4: Means of the reef types for the generalized linear negative binomial model m_d4 for oyster density in summer 2022 standardized to 1 m^2 of river bottom. Note that these means are derived from an emmeans analysis that was performed on m_d4. SE = standard error; df = degrees of freedom; asymp.LCL = asymptotic lower confidence level; asymp.UCL = asymptotic upper confidence level.

Reef	Response	SE	df	asymp.LCL	asymp.UCL
shell	9852.98	1154.97	Inf	7830.50	12397.84
granite	2829.89	337.47	Inf	2240.08	3575.00
castle	2219.71	260.40	Inf	1763.77	2793.52
diamond	715.72	85.99	Inf	565.56	905.75
c-dome	3202.30	376.86	Inf	2542.66	4033.07
x-reef	3816.67	447.29	Inf	3033.39	4802.20

Results are averaged over the levels of: site

Table S5: Pairwise comparisons between reefs for the generalized linear negative binomial model m_d4 for oyster density in summer 2022. All numbers are standardized to m^2 of river bottom. Note that these comparisons are derived from the emmeans for this model. SE = standard error; df = degrees of freedom.

Contrast	Ratio	SE	df	t.ratio	p.value
granite - shell	0.28	0.05	Inf	-7.46	<0.01
castle - shell	0.22	0.04	Inf	-8.99	<0.01
castle - granite	0.78	0.13	Inf	-1.45	0.70
diamond - shell	0.07	0.01	Inf	-15.62	<0.01
diamond - granite	0.25	0.04	Inf	-8.12	<0.01
diamond - castle	0.32	0.05	Inf	-6.74	<0.01
c-dome - shell	0.33	0.05	Inf	-6.77	<0.01
c-dome - granite	1.13	0.19	Inf	0.74	0.98
c-dome - castle	1.44	0.24	Inf	2.21	0.24
c-dome - diamond	4.47	0.75	Inf	8.91	<0.01
x-reef - shell	0.39	0.06	Inf	-5.72	<0.01
x-reef - granite	1.35	0.22	Inf	1.79	0.47
x-reef - castle	1.72	0.29	Inf	3.27	0.01
x-reef - diamond	5.33	0.90	Inf	9.97	<0.01
x-reef - c-dome	1.19	0.20	Inf	1.06	0.90

Results are averaged over the levels of: site

Table S6: Means of the sites for the generalized linear negative binomial model m_d4 for oyster density in summer 2022 standardized to 1 m^2 of river bottom. Note that these means are derived from an emmeans analysis that was performed on m_f4. SE = standard error; df = degrees of freedom; asymp.LCL = asymptotic lower confidence level; asymp.UCL = asymptotic upper confidence level

Reef	Response	SE	df	asymp.LCL	asymp.UCL
andrews	3246.29	270.47	Inf	2757.20	3822.13
exposed	1743.77	146.77	Inf	1478.57	2056.53
protected	4110.42	341.59	Inf	3492.59	4837.53

Results are averaged over the levels of: reef

Table S7: Pairwise comparisons between impact sites for the generalized linear negative binomial model m_d4 for oyster density in summer 2022. All numbers are standardized to m^2 of river bottom. Note that these comparisons are derived from the emmeans for this model. SE = standard error; df = degrees of freedom.

Contrast	Ratio	SE	df	z.ratio	p.value
exposed - andrews	0.54	0.06	Inf	-5.25	<0.01
protected - andrews	1.27	0.15	Inf	2.01	0.11
protected - exposed	2.36	0.28	Inf	7.25	<0.01

Results are averaged over the levels of: reef

Table S8: Means of the reef types for the generalized linear negative binomial model m_s4 for oyster density in summer 2022 standardized to 1 m^2 of surface area. Note that these means are derived from an emmeans analysis that was performed on m_s4. SE = standard error; df = degrees of freedom; asymp.LCL = asymptotic lower confidence level; asymp.UCL = asymptotic upper confidence level.

Reef	Response	SE	df	asymp.LCL	asymp.UCL
castle	1466.58	168.15	Inf	1171.42	1836.10
diamond	92.32	10.85	Inf	73.32	116.24
cdome	808.21	92.97	Inf	645.07	1012.60
xreef	1387.71	158.93	Inf	1108.69	1736.94

Results are averaged over the levels of: site

Table S9: Pairwise comparisons between reef types for the generalized linear negative binomial model m_s4 for oyster density in summer 2022. All numbers are standardized to m^2 of surface area. Note that these comparisons are derived from the emmeans for this model. SE = standard error; df = degrees of freedom.

Contrast	Ratio	SE	df	z.ratio	p.value
diamond - castle	0.06	0.01	Inf	-16.84	<0.01
cdome - castle	0.55	0.09	Inf	-3.67	<0.01
cdome - diamond	8.75	1.44	Inf	13.19	<0.01
xreef - castle	0.95	0.15	Inf	-0.34	0.99
xreef - diamond	15.03	2.47	Inf	16.51	<0.01
xreef - cdome	1.72	0.28	Inf	3.33	<0.01

Results are averaged over the levels of: site

Table S10: Means of the site for the generalized linear negative binomial model m_s4 for oyster density in summer 2022 standardized to 1 m^2 of surface area. Note that these means are derived from an emmeans analysis that was performed on m_s4. SE = standard error; df = degrees of freedom; asymp.LCL = asymptotic lower confidence level; asymp.UCL = asymptotic upper confidence level.

Reef	Response	SE	df	asymp.LCL	asymp.UCL
andrews	698.64	69.67	Inf	574.60	849.46
exposed	377.39	38.03	Inf	309.76	459.80
protected	922.59	91.73	Inf	759.24	1121.08

Results are averaged over the levels of: reef

Table S11: Pairwise comparisons between impact sites for the generalized linear negative binomial model m_s4 for oyster density in summer 2022. All numbers are standardized to m^2 of surface area. Note that these comparisons are derived from the emmeans for this model. SE = standard error; df = degrees of freedom.

Contrast	Ratio	SE	df	z.ratio	p.value
exposed - andrews	0.54	0.08	Inf	-4.34	<0.01
protected - andrews	1.32	0.19	Inf	1.97	0.12
protected - exposed	2.44	0.35	Inf	6.32	<0.01

Results are averaged over the levels of: reef

Table S12: Reef means for the linear model m_b4 for oyster biomass in summer 2022. Note that these means are derived from an emmeans analysis that was performed on m_b4.

Reef Type	mean	SE	df	lower.CL	upper.CL
shell	743.90	65.12	28	610.50	877.30
granite	280.83	65.12	28	147.44	414.23
castle	345.92	65.12	28	212.52	479.32
diamond	117.48	65.12	28	-15.92	250.88
c-dome	418.33	65.12	28	284.94	551.73
x-reef	531.75	65.12	28	398.35	665.15

Results are averaged over the levels of: site

Table S13: Site means for the linear model m_b4 for oyster density in summer 2022. Note that these means are derived from an emmeans analysis that was performed on m_b4.

Site	mean	SE	df	lower.CL	upper.CL
andrews	456.21	46.05	28	361.88	550.54
exposed	267.83	46.05	28	173.50	362.15
protected	495.07	46.05	28	400.74	589.40

Results are averaged over the levels of: reef

Table S14: Pairwise comparisons between reef types for linear model m_b4 for oyster biomass in summer 2022.

Contrast	Estimate	SE	df	t.ratio	p.value
granite - shell	-463.06	92.10	28	-5.03	<0.01
castle - shell	-397.97	92.10	28	-4.32	<0.01
castle - granite	65.09	92.10	28	0.71	0.98
diamond - shell	-626.42	92.10	28	-6.8	<0.01
diamond - granite	-163.36	92.10	28	-1.77	0.50
diamond - castle	-228.44	92.10	28	-2.48	0.16
c-dome - shell	-325.56	92.10	28	-3.54	0.02
c-dome - granite	137.50	92.10	28	1.50	0.67
c-dome - castle	72.41	92.10	28	0.79	0.97
c-dome - diamond	300.85	92.10	28	3.27	0.03
x-reef - shell	-212.15	92.10	28	-2.30	0.23
x-reef - granite	250.92	92.10	28	2.72	0.10
x-reef - castle	185.83	92.10	28	2.02	0.36
x-reef - diamond	414.27	92.10	28	4.50	<0.01
x-reef - c-dome	113.42	92.10	28	1.23	0.82

Results are averaged over the levels of: site

Table S15: Pairwise comparisons between impact sites for linear model m_b4 for oyster biomass in summer 2022.

Contrast	Estimate	SE	df	t.ratio	p.value
exposed - andrews	-188.39	65.12	28	-2.89	0.02
protected - andrews	38.86	65.12	28	0.60	0.82
protected - exposed	227.24	65.12	28	3.490	<0.01

Results are averaged over the levels of: reef

Table S16: Reef means for the linear model $m_{dw}4$ for oyster dry weight in summer 2022. Note that these means are derived from an emmeans analysis that was performed on $m_{dw}4$.

Reef Type	mean	SE	df	lower.CL	upper.CL
shell	895.03	76.30	28	738.74	1051.32
granite	348.71	76.30	28	192.41	505.00
castle	418.59	76.30	28	262.30	574.89
diamond	147.12	76.30	28	-9.18	303.49
c-dome	497.68	76.30	28	341.38	653.97
x-reef	649.76	76.30	28	493.47	806.06

Results are averaged over the levels of: site

Table S17: Pairwise comparisons between reef types for linear model $m_{dw}4$ for oyster dry weight in summer 2022.

Contrast	Estimate	SE	df	z.ratio	p.value
granite - shell	-546.32	107.90	28	-5.06	<0.01
castle - shell	-476.44	107.90	28	-4.42	<0.01
castle - granite	69.89	107.90	28	0.65	0.99
diamond - shell	-747.91	107.90	28	-6.93	<0.01
diamond - granite	-201.59	107.90	28	-1.87	0.44
diamond - castle	-271.48	107.90	28	-2.52	0.15
c-dome - shell	-397.35	107.90	28	-3.68	0.01
c-dome - granite	148.97	107.90	28	1.38	0.74
c-dome - castle	79.09	107.90	28	0.73	0.98
c-dome - diamond	350.56	107.90	28	3.25	0.03
x-reef - shell	-245.27	107.90	28	-2.27	0.24
x-reef - granite	301.06	107.90	28	2.79	0.09
x-reef - castle	231.17	107.90	28	2.14	0.30
x-reef - diamond	502.65	107.90	28	4.66	<0.01
x-reef - c-dome	152.087	107.90	28	1.41	0.72

Results are averaged over the levels of: site

Table S18: Site means for the linear model $m_{dw}4$ for oyster density in summer 2022. Note that these means are derived from an emmeans analysis that was performed on $m_{dw}4$.

Site	Mean	SE	df	lower.CL	upper.CL
andrews	553.92	53.95	28	443.41	664.44
exposed	308.09	53.95	28	197.58	418.61
protected	616.42	53.95	28	505.91	726.94

Results are averaged over the levels of: reef

Table S19: Pairwise comparisons between impact sites for linear model $m_{dw}4$ for oyster dry weight in summer 2022.

Contrast	Estimate	SE	df	t.ratio	p.value
exposed - andrews	-245.83	76.30	28	-3.22	<0.01
protected - andrews	62.50	76.30	28	0.82	0.70
protected - exposed	308.33	76.30	28	4.04	<0.01

Results are averaged over the levels of: reef

Table S20: Parameter means for univariate response variables. Note that all means are derived from an emmeans analysis that was performed on the models listed on the "Model" column for each response variable. X represents factors that were not included in that model. The transformations applied to the models used to derive the means for each row are represented under each response variable.

Response	Model	Shell	Granite	Castle	Diamond	C-dome	X-reef	Exposed	Protected	Andrews
Density	u_4	22859 ±	51696±	24098±	10168±	28672±	24961±	21933±	11788±	55676±
(Neg. Bin.)		3995	9027	4206	1776	5006	4358	2708	1457	6871
Richness	u_4	16.8 ±	19.0±	20.3±	15.0±	17.8±	19.5±	16.6±	18.0±	19.7±
(LM)		0.75	0.75	0.75	0.75	0.75	0.75	0.53	0.53	0.53
Evenness	u_4	0.69 ±	0.59±	0.61±	0.57±	0.68±	0.61±	0.66±	0.73±	0.48±
(LM)		0.05	0.05	0.05	0.05	0.05	0.05	0.04	0.04	0.04
Diversity	u_4	1.93 ±	1.73±	1.81±	1.47±	1.95±	1.80±	1.82±	2.10±	1.43±
(LM)		0.14	0.14	0.14	0.14	0.14	0.14	0.10	0.10	0.10
Biomass	u_4	188.4 ±	333.3±	140.3±	43.4±	211.4±	234.0±	142±	185±	248±
(LM)		32	32	32	32	32	32	22.6	22.6	22.6
Secondary	u_2	644.48 ±	800.70±	365.64±	97.16±	394.56±	313.71±	X	X	X
Production		3.30	3.30	3.30	3.30	3.30	3.30			
(LM*)										

* Means back-transformed from a model that used square-root transformed data.

Table S21: Pairwise comparisons between reef types for generalized negative binomial model u_4 for benthic community density at the impact sites in summer 2022. All numbers are standardized to m^2 of river bottom. Note that these comparisons are derived from the emmeans for this model. SE = standard error; df = degrees of freedom.

Contrast	Ratio	SE	df	z.ratio	p.value
granite - shell	2.26	0.56	Inf	3.30	0.01
castle - shell	1.05	0.26	Inf	0.21	1.00
castle - granite	0.47	0.12	Inf	-3.09	0.02
diamond - shell	0.44	0.11	Inf	-3.28	0.01
diamond - granite	0.20	0.05	Inf	-6.58	<0.01
diamond - castle	0.42	0.10	Inf	-3.49	0.01
c-dome - shell	1.25	0.31	Inf	0.92	0.94
c-dome - granite	0.55	0.14	Inf	-2.39	0.16
c-dome - castle	1.19	0.29	Inf	0.70	0.98
c-dome - diamond	2.82	0.70	Inf	4.20	<0.01
x-reef - shell	1.09	0.27	Inf	0.36	1.00
x-reef - granite	0.48	0.12	Inf	-2.95	0.04
x-reef - castle	1.04	0.26	Inf	0.14	1.00
x-reef - diamond	2.45	0.61	Inf	3.64	<0.01
x-reef - c-dome	0.87	0.21	Inf	-0.56	0.99

Results are averaged over the levels of: site

Table S22: Pairwise comparisons between impact sites for generalized negative binomial model u_4 for benthic community density at the impact sites in summer 2022. All numbers are standardized to m^2 of river bottom. Note that these comparisons are derived from the emmeans for this model. SE = standard error; df = degrees of freedom.

Contrast	Estimate	SE	df	t.ratio	p.value
exposed - andrews	-0.93	0.17	Inf	-5.336	<0.01
protected - andrews	-1.55	0.17	Inf	-8.890	<0.01
protected - exposed	-0.62	0.17	Inf	-3.555	<0.01

Results are averaged over the levels of: reef

Table S23: Pairwise comparisons between reef types for the linear model, u_4, for benthic community richness at the impact sites in summer 2022. Note that these comparisons are derived from the emmeans for this model. SE = standard error; df = degrees of freedom.

Contrast	Estimate	SE	df	t.ratio	p.value
granite - shell	2.17	1.05	28	2.06	0.34
castle - shell	3.50	1.05	28	3.32	0.03
castle - granite	1.33	1.05	28	1.26	0.80
diamond - shell	-1.83	1.05	28	-1.74	0.52
diamond - granite	-4.00	1.05	28	-3.79	0.01
diamond - castle	-5.33	1.05	28	-5.06	<0.01
c-dome - shell	1.00	1.05	28	0.95	0.93
c-dome - granite	-1.17	1.05	28	-1.11	0.87
c-dome - castle	-2.50	1.05	28	-2.37	0.20
c-dome - diamond	2.83	1.05	28	2.69	0.11
x-reef - shell	2.67	1.05	28	2.53	0.15
x-reef - granite	0.50	1.05	28	0.47	1.00
x-reef - castle	-0.83	1.05	28	-0.79	0.97
x-reef - diamond	4.50	1.05	28	4.27	<0.01
x-reef - c-dome	1.67	1.05	28	1.58	0.62

Results are averaged over the levels of: site

Table S24: Pairwise comparisons between impact sites for the linear model, u_4, for benthic community richness in summer 2022. Note that these comparisons are derived from the emmeans for this model. SE = standard error; df = degrees of freedom.

Contrast	Estimate	SE	df	t.ratio	p.value
exposed - andrews	-3.08	0.75	28.00	-4.14	<0.01
protected - andrews	-1.67	0.75	28.00	-2.24	0.08
protected - exposed	1.42	0.75	28.00	1.90	0.16

Results are averaged over the levels of: reef

Table S25: ANOVAs run on models u_3 and u_4 for the evenness and diversity response variables to determine significant differences between the models. u_3 includes only site as a variable and u_4 includes both site and reef as variables. Models were comparing using Chi square Test of Independence.

Response	Model	Variables	Res.Df	RSS	Df	Sum of Sq	Pr(>Chi)
Diversity	u_3	Site	33	4.3414	-5	-0.90179	0.1965
	u_4	Reef, Site	28	3.4396			
Evenness	u_3	Site	33	0.48866	-5	-0.071455	0.4413
	u_4	Reef, Site	28	0.41720			

Table S26: Pairwise comparisons between reef types for the linear model, u_4, for benthic community evenness at the impact sites in summer 2022. Note that these comparisons are derived from the emmeans for this model. SE = standard error; df = degrees of freedom.

Contrast	Estimate	SE	df	t.ratio	p.value
granite - shell	-0.10	0.07	28	-1.35	0.75
castle - shell	-0.08	0.07	28	-1.13	0.86
castle - granite	0.02	0.07	28	0.22	1.00
diamond - shell	-0.12	0.07	28	-1.74	0.52
diamond - granite	-0.03	0.07	28	-0.39	1.00
diamond - castle	-0.04	0.07	28	-0.61	0.99
c-dome - shell	-0.01	0.07	28	-0.14	1.00
c-dome - granite	0.09	0.07	28	1.21	0.83
c-dome - castle	0.07	0.07	28	0.99	0.92
c-dome - diamond	0.11	0.07	28	1.60	0.61
x-reef - shell	-0.08	0.07	28	-1.12	0.87
x-reef - granite	0.02	0.07	28	0.23	1.00
x-reef - castle	0.00	0.07	28	0.01	1.00
x-reef - diamond	0.04	0.07	28	0.62	0.99
x-reef - c-dome	-0.07	0.07	28	-0.98	0.92

Results are averaged over the levels of: site

Table S27: Pairwise comparisons between impact sites for the linear model, u_4, for benthic community evenness in summer 2022. Note that these comparisons are derived from the emmeans for this model. SE = standard error; df = degrees of freedom.

Contrast	Estimate	SE	df	t.ratio	p.value
exposed - andrews	0.17	0.05	28	3.48	<0.01
protected - andrews	0.25	0.05	28	5.03	<0.01
protected - exposed	0.08	0.05	28	1.55	0.28

Results are averaged over the levels of: reef

Table S28: Pairwise comparisons between reef types for the linear model, u_4, for benthic community diversity at the impact sites in summer 2022. Note that these comparisons are derived from the emmeans for this model. SE = standard error; df = degrees of freedom.

Contrast	Estimate	SE	df	t.ratio	p.value
granite - shell	-0.20	0.20	28	-1.00	0.91
castle - shell	-0.12	0.20	28	-0.59	0.99
castle - granite	0.08	0.20	28	0.41	1.00
diamond - shell	-0.46	0.20	28	-2.27	0.24
diamond - granite	-0.26	0.20	28	-1.27	0.80
diamond - castle	-0.34	0.20	28	-1.68	0.56
c-dome - shell	0.02	0.20	28	0.09	1.00
c-dome - granite	0.22	0.20	28	1.09	0.88
c-dome - castle	0.14	0.20	28	0.68	0.98
c-dome - diamond	0.48	0.20	28	2.36	0.20
x-reef - shell	-0.13	0.20	28	-0.66	0.98
x-reef - granite	0.07	0.20	28	0.33	1.00
x-reef - castle	-0.01	0.20	28	-0.07	1.00
x-reef - diamond	0.32	0.20	28	1.61	0.60
x-reef - c-dome	-0.15	0.20	28	-0.75	0.97

Results are averaged over the levels of: site

Table S29: Pairwise comparisons between impact sites for the linear model, u_4, for benthic community diversity in summer 2022. Note that these comparisons are derived from the emmeans for this model. SE = standard error; df = degrees of freedom.

Contrast	Estimate	SE	df	t.ratio	p.value
exposed - andrews	0.39	0.14	28	2.75	0.03
protected - andrews	0.68	0.14	28	4.73	<0.01
protected - exposed	0.28	0.14	28	1.99	0.13

Results are averaged over the levels of: reef

Table S30: Pairwise comparisons between reef types for the linear model, u_4, for benthic community biomass (g AFDW) at the impact sites in summer 2022. Note that these comparisons are derived from the emmeans for this model. SE = standard error; df = degrees of freedom.

Contrast	Estimate	SE	df	t.ratio	p.value
granite - shell	144.84	45.29	28	3.20	0.04
castle - shell	-48.17	45.29	28	-1.06	0.89
castle - granite	-193.01	45.29	28	-4.26	<0.01
diamond - shell	-145.04	45.29	28	-3.20	0.04
diamond - granite	-289.88	45.29	28	-6.40	<0.01
diamond - castle	-96.87	45.29	28	-2.14	0.30
c-dome - shell	23.01	45.29	28	0.51	1.00
c-dome - granite	-121.83	45.29	28	-2.69	0.11
c-dome - castle	71.18	45.29	28	1.57	0.62
c-dome - diamond	168.05	45.29	28	3.71	0.01
x-reef - shell	45.60	45.29	28	1.01	0.91
x-reef - granite	-99.24	45.29	28	-2.19	0.27
x-reef - castle	93.76	45.29	28	2.07	0.33
x-reef - diamond	190.64	45.29	28	4.21	<0.01
x-reef - c-dome	22.58	45.29	28	0.50	1.00

Results are averaged over the levels of: site

Table S31: Pairwise comparisons between impact sites for the linear model, u_4, for benthic community biomass (g AFDW) in summer 2022. Note that these comparisons are derived from the emmeans for this model. SE = standard error; df = degrees of freedom..

Contrast	Estimate	SE	df	t.ratio	p.value
exposed - andrews	-106.29	32.02	28	-3.32	0.01
protected - andrews	-63.65	32.02	28	-1.99	0.13
protected - exposed	42.64	32.02	28	1.33	0.39

Results are averaged over the levels of: reef

Table S32: Pairwise comparisons between reef types for linear model u_2 for benthic community secondary productivity (g C/m^2/yr) at the impact sites in summer 2022 standardized to m^2 of river bottom. Note that all numbers have been back-transformed by squaring, as this model used a square root transformation for normality.

Contrast	Estimate	SE	df	t.ratio	p.value
granite - shell	8.47	6.60	30	1.13	0.86
castle - shell	39.25	6.60	30	-2.44	0.18
castle - granite	84.18	6.60	30	-3.57	0.01
diamond - shell	241.17	6.60	30	-6.04	<0.01
diamond - granite	340.02	6.60	30	-7.18	<0.01
diamond - castle	85.84	6.60	30	-3.61	0.01
c-dome - shell	30.50	6.60	30	-2.15	0.29
c-dome - granite	71.12	6.60	30	-3.28	0.03
c-dome - castle	0.55	6.60	30	0.29	1.00
c-dome - diamond	100.13	6.60	30	3.89	0.01
x-reef - shell	58.90	6.60	30	-2.99	0.06
x-reef - granite	112.04	6.60	30	-4.12	<0.01
x-reef - castle	1.99	6.60	30	-0.55	0.99
x-reef - diamond	61.70	6.60	30	3.06	0.05
x-reef - c-dome	4.63	6.60	30	-0.84	0.96

Table S33: List of species found at the control and impact sites in 2021 and 2022.

Taxonomic Group	Species
Actiniaria	*Actiniaria*
Bivalve	*Anadara tranversa*
Bivalve	*Ameritella mitchelli*
Bivalve	*Crassostrea virginica*
Bivalve	*Gemma gemma*
Bivalve	*Geukensia demissa*
Bivalve	*Ischadium recurvum*
Bivalve	*Macoma balthica*
Bivalve	*Macoma tenta*
Bivalve	*Mercenaria mercenaria*
Bivalve	*Mulinia lateralis*
Bivalve	*Mya arenaria*
Bivalve	*Tagelus plebeius*
Chordata	*Chasmodes bosquianus*
Chordata	*Gobiesox strumosus*
Chordata	*Gobiosoma bosc*
Chordata	*Gobiosoma ginsburgi*
Chordata	*Hypsoblennius hentz*
Chordata	*Molgula manhattensis*
Chordata	*Opsanus tau*
Crustacean	*Alpheus heterochelis*
Crustacean	*Callinectus sapidus*
Crustacean	*Caprellidae*
Crustacean	*Corophiidae*
Crustacean	*Dyspanopeus sayi*
Crustacean	*Eurypanopeus depressus*
Crustacean	*Gammaridae*
Crustacean	*Hexapanopeus angustifrons*
Crustacean	*Libinia dubia*
Crustacean	*Litopenaeus setiferus*
Crustacean	*Palaemonetes pugio*
Crustacean	*Panopeus herbstii*
Crustacean	*Rhithropanopeus harrisii*
Crustacean	*Synidotea laevidorsalis*
Crustacean	*Upogenia affinis*
Crustacean	*Zaops ostreum*
Gastropoda	*Astyris lunata*
Gastropoda	*Boonea impressa*
Gastropoda	*Costoanachis avara*
Gastropoda	*Crepidula plana*
Gastropoda	*Littoraria irrorata*
Gastropoda	*Phrontis vibex*
Gastropoda	*Pyrgocythara plicosa*
Gastropoda	*Triphora nigrocincta*
Nemertea	*Nemertea*
Polychaete	*Alitta succinea*
Polychaete	*Capitellida sp.*
Polychaete	*Clymenella torquata*
Polychaete	*Drilonereis longa*
Polychaete	*Glycera dibranchiata*
Polychaete	*Glycinde solitaria*
Polychaete	*Hydroides protulicola*
Polychaete	*Leitoscoloplos sp.*
Polychaete	*Loimia medusa*
Polychaete	*Nephtys squamosa*
Polychaete	*Parasabella microphthalma*
Polychaete	*Potamilla neglecta*
Polychaete	*Sabellaria vulgaris*
Polychaete	*Spiochaetopterus oculatus*
Polychaete	*Sthenelais boa*
Spinoida	*Spionid*

Figures

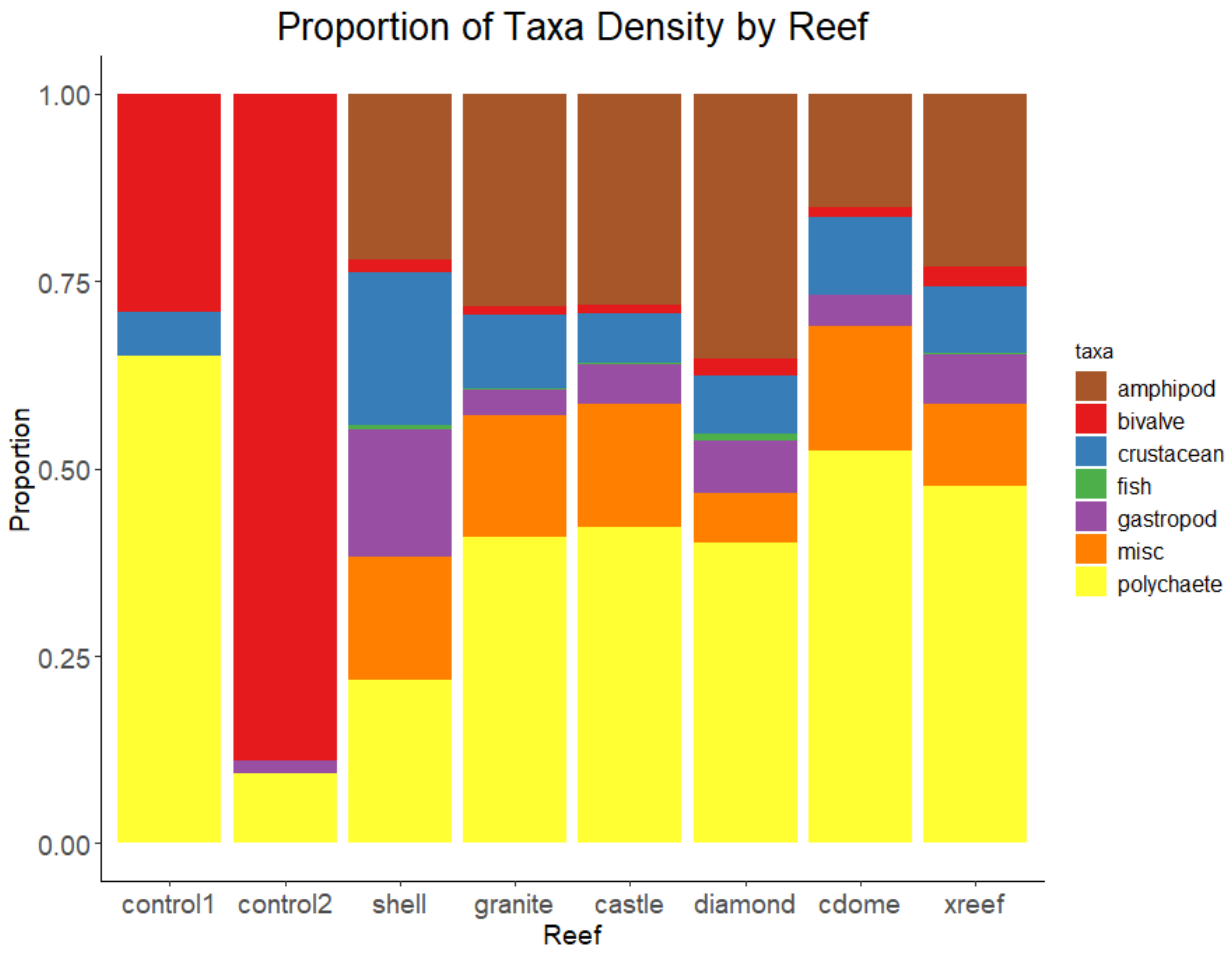

Figure S1: Proportion of density of taxa found at the on the reef structures and control sites in 2022 by taxonomic group. Crustacean refers to non-amphipod crustaceans.

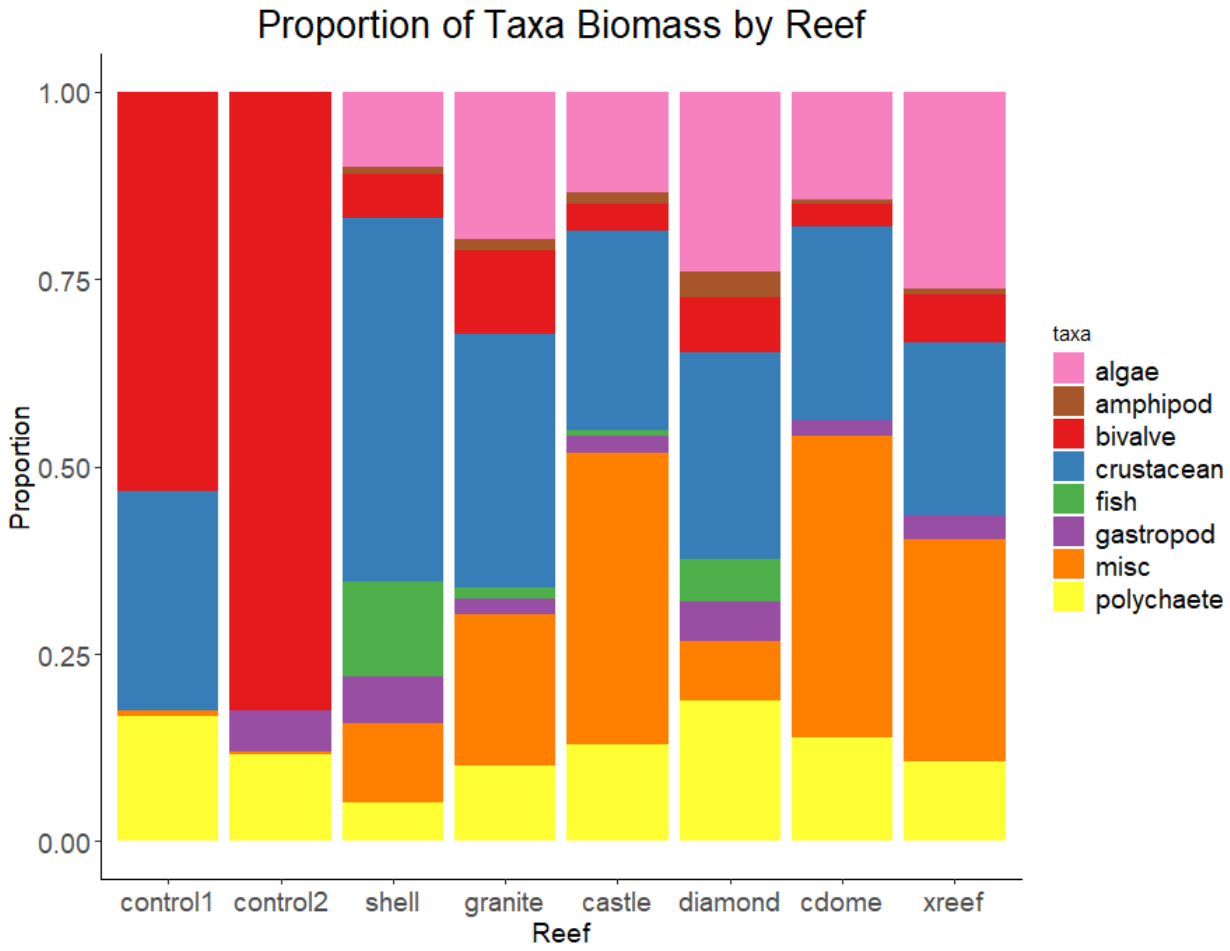

Figure S2: Proportion of biomass of taxa found at the on the reef structures and control sites in 2022 by taxonomic group. Crustacean refers to non-amphipod crustaceans.